NOTE TO USERS

This reproduction is the best copy available.

UMI®

Downloaded from SHAREOK. Persistent Handle URL: https://hdl.handle.net/11244/758

UNIVERSITY OF OKLAHOMA

GRADUATE COLLEGE

NON-OXIDATIVE CONVERSION OF METHANE IN A DC PLASMA REACTOR

A Dissertation

SUBMITTED TO THE GRADUATE FACULTY

in partial fulfillment of the requirements for the

degree of

Doctor of Philosophy

By

CHRISTOPHER L. GORDON
Norman, Oklahoma
2004

UMI Number: 3135700

INFORMATION TO USERS

The quality of this reproduction is dependent upon the quality of the copy submitted. Broken or indistinct print, colored or poor quality illustrations and photographs, print bleed-through, substandard margins, and improper alignment can adversely affect reproduction.

In the unlikely event that the author did not send a complete manuscript and there are missing pages, these will be noted. Also, if unauthorized copyright material had to be removed, a note will indicate the deletion.

UMI®

UMI Microform 3135700

Copyright 2004 by ProQuest Information and Learning Company.

All rights reserved. This microform edition is protected against unauthorized copying under Title 17, United States Code.

ProQuest Information and Learning Company
300 North Zeeb Road
P.O. Box 1346
Ann Arbor, MI 48106-1346

© Copyright by Christopher L. Gordon 2004
All Rights Reserved.

NON-OXIDATIVE CONVERSION OF METHANE IN A DC PLASMA REACTOR

A Dissertation APPROVED FOR THE SCHOOL OF CHEMICAL ENGINEERING AND MATERIALS SCIENCE

BY

Lance Lobban

Dr. Lance Lobban

Dr. Richard Mallinson

Daniel Resasco

Dr. Daniel Resasco

Dr. Dimitrios Papavassiliou

Robert White

Dr. Robert White

ACKNOWLEDGEMENTS

I would like to thank my mother, father and brother for without them none of this would be possible. Their encouragement, understanding, and love have truly been a driving force in my life. They have given me the basic life principles to make me successful in life, and I hope that in the end I have made them as proud of me as I am of all of them. I suppose those puzzles were a precursor of things to come. I would also like to thank Nana, Papa, and Mama for instilling these qualities and characteristics in my parents so they could pass them along to me.

Next, I would like to thank my advisors Dr. Lance Lobban and Dr. Richard Mallinson. It was truly an honor to have both of them as my advisors and to be able to interact with them on a day to day basis. Regardless of their schedules or workload, they both had an open-door for discussion of ideas, problems and solutions.

Dr. Mallinson and Dr. Lobban have truly provided me with what I feel is most important from a doctoral degree: the ability to critically think. They always pushed for an understanding of the cause and effect, and not just the results. I feel that my problem solving and understanding of how to interpret results and how to isolate a cause and effect is on a much higher level than before I began my degree.

In addition, I have had the great opportunity to have both as an instructor. Dr. Lobban has a tremendous passion for teaching and communicating to students, and it shows in the classroom. I feel that he is one of the premier instructors, not only in the department, but campus wide. Dr. Mallinson also posses tremendous abilities as an instructor. One of my favorite aspects of Dr. Mallinson classroom is that he brings the textbook knowledge to life. He incorporates the textbook fundamentals to the real world applications and industrial processes. I feel this provides an excellent opportunity to enhance the understanding of the material at hand.

I would like to thank Dr. Resasco for being a member of my committee. Throughout my time at OU I have had the opportunity to learn from Dr. Resasco in the classroom and the laboratory. His passion for both is obvious. Never more obvious than the time covering some difficult material and he felt by the lack of questions the class did not understand and would not move forward until he felt satisfied with the level of understanding. He has also assisted in the critical component of a successful researcher: to think outside the box.

Similarly, I would like to thank Dr. Papavassiliou and Dr. White for being a part of my doctoral committee. I appreciate their time and guidance on issues involving my research. Their specific research may not be exactly correlated, but it was nice to obtain viewpoints from different angles.

Over the time, I had the pleasure of working with many skilled graduate students within our lab. I would like to thank Phil Howard, Terrance Caldwell, and David Larkin for being a friend and colleague in the lab. In addition, I would like

thank Huy Le, Trung Pham, and Trung Huang for their assistance within the lab. Also, my friendships developed with Kent Leach and Susan Stagg-Williams within the department will always be memory of my time at OU.

The staff within the department is also crucial piece of a degree. I would like to thank Larry Isley for his assistance and instructions on the machining and building of various equipment within the lab. I would like to than Donna and Sherry within the department office, and Terri Coliver for always dropping whatever she was working on in order to provide assistance.

TABLE OF CONTENTS

ACKNOWLEDGEMENTS iv
TABLE OF CONTENTS vii
LIST OF FIGURES ix
LIST OF TABLES xii
ABSTRACT xiii
CHAPTER 1 - Background Discussion of Fuels, Energy, and Plasmas 1
1.1 Introduction to Natural Gas 1
1.1.2 Natural Gas Resources 1
1.1.2 Natural Gas to Higher Value Commodities 4
1.2 Plasma Chemistry 11
1.2.1 Background of Plasma 11
1.2.2 Description of Different Types of Plasmas 18
1.3 Past dc Corona Discharge Research 22
1.4 Theory Behind Present Research 24
1.5 Literature Cited 26
CHAPTER 2 - Experimental Procedure 30
2.1 Experimental Apparatus 30
2.1.1 Upstream Section 30
2.1.2 Reactor Section 32
2.2 Catalyst Preparation 35
2.3 Catalyst Pretreatment 38
2.4 Calibrations 39
2.5 Definitions 39
2.6 Reproducibility/Propagation of Error 41
2.7 Transmission Electron Microscopy 41
2.8 Infrared Temperature Camera 43
2.9 Literature Cited 43
CHAPTER 3 - Stability 45
3.1 Introduction 45
3.2 Experimental Procedure 47
3.3 Results and Discussion 50
3.3.1 Effect of different discharges 51
3.3.2 Role of material within dc plasma system 76
3.4 Conclusions 92
3.5 Literature Cited 93
CHAPTER 4 – Conversion of Methane to Hydrogen and Higher Hydrocarbons Using a dc Plasma Reactor 97
4.1 Introduction 97

4.2 Experimental 101
4.3 Results and Discussion 103
4.3.1 Radial Bypassing and Oxidative Experiments 103
4.3.2 Non-oxidative Studies 107
4.3.3 Environmental Impact and Hydrogen Cost Analysis 115
4.3.4 Elevated Operating Pressure 119
4.4 Conclusions 121
4.6 Literature Cited 123
CHAPTER 5 - Selective hydrogenation of acetylene to ethylene during the conversion of methane in a catalytic dc plasma reactor 125
5.1 Introduction 125
5.2 Experimental 130
5.3 Results and Discussion 134
5.3.1 In-Situ Selective Hydrogenation of Acetylene using a Pd-Y zeolite 134
5.3.2 In-Situ Selective Hydrogenation of Acetylene using a Ag-Pd-Y zeolite 139
5.3.4 Higher Methane Partial Pressures and Energy Efficiency 142
5.4 Conclusions 154
5.5 Acknowledgements 155
5.6 Literature Cited 155
CHAPTER 6 - In-Situ Selective Hydrogenation of High Concentrations of Acetylene over a Pd and Ag-Pd Y-Zeolite Catalyst in a DC Plasma Reactor 158
6.1 Introduction 158
6.2 Experimental 162
6.2.2 ICP Results 164
6.2.3 TEM 165
6.3 Results and Discussion 173
6.3.1 Selective Hydrogenation with Ag-Pd-Y zeolite 173
6.4 Conclusions 182
6.5 Literature Cited 182
CHAPTER 7 : Conclusions and Future Work 187
7.1 Conclusions 187
7.2 Future Work 190
APPENDIX A – GC Calibrations 192
APPENDIX B – Propagation of Error 200
APPENDIX C - Capacitor Derivation 207

LIST OF FIGURES

Figure 1.1: Cost of various transportation methods for various petroleum commodities.....3
Figure 1.2: Front-end de-ethanizer reactor system.....9
Figure 1.3: Probability of single ionization by electron impact.....15
Figure 1.4: The current-voltage characteristics of a DC glow discharge.....17
Figure 2.1: Catalytic dc plasma discharge system.....31
Figure 2.2: Catalytic dc Plasma Discharge Reactor.....33
Figure 2.3: Comparison of 0.025 wt% Pd-Y zeolite using two different impregnation methods.....37
Figure 2.4: Comparison of different batches of prepared NaOH Y zeolite.....42
Figure 3.1: Characterization of the different types of discharges that occur within the dc plasma system.....53
Figure 3.2: Effect of various catalysts loadings on the methane conversion and product selectivity.....55
Figure 3.3: Effect of different materials loaded into reactor on the conversion and product selectivity.....57
Figure 3.4. Effect of the reduced electric field (E/P) on the percentage of energy deposited into the inelastic group process (excitation and dissociation) of a pure methane system.....62
Figure 3.5. Effect of the reduced electric field (E/P) on the percentage of energy deposited into the inelastic group process (excitation and dissociation) of a 2/1 CH_4/O_2 system. Overlaid is the C_2 selectivity data of Larkin et al.....63
Figure 3.6. Effect of the reduced electric field (E/P) on the percentage of energy deposited into the inelastic group process (excitation and dissociation) of a 1/1/8 CH_4/H_2/He with 2% O_2 system.....66
Figure 3.7. Effect of the reduced electric field (E/P) on the percentage of energy deposited into the inelastic group process (excitation and dissociation) of a 1/1 CH_4/H_2 with 2% O_2 system.....67
Figure 3.8. Effect of the reduced electric field (E/P) on the percentage of energy deposited into the inelastic group process (excitation and dissociation) of a 2/1 CH_4/H_2 with 2% O_2 system.....68

Figure 3.9. Effect of the reduced electric field (E/P) on the energy efficiency of the dc plasma reactor. Also included is the generalization of various reactors studied and their associated E/P and efficiency.....71
Figure 3.10 Digital image of dc plasma reactor. 3mm glass bead height. 7kV, $2/1H_2/CH_4$ with 2% O_2.....73
Figure 3.11 IR image of dc plasma reactor. 3mm glass bead height. 7kV, $2/1H_2/CH_4$ with 2% O_2.....74
Figure 3.12 CH image form PLIFS study. 7kV, $2/1H_2/CH_4$ with 2% O_2.....75
Figure 3.13: Effect of temperature on acetylene conversion over a variety of zeolite catalysts.....78
Figure 3.14: Characterization of the electric field within a parallel-plate capacitor.....83
Figure 3.15: Effect of varying bed height of different dielectric materials on the breakdown voltage of the dc plasma system 85
Figure 3.16: Voltage versus temperature for different materials loaded within the reactor 87
Figure 3.17: Voltage versus temperature for different conditions within the reactor89
Figure 4.1: Methane conversion versus residence time in two different cross sectional area reactors.....105
Figure 4.2: Hydrogen selectivity and yield for the two different reactor cross sectional areas at different residence times.....108
Figure 4.3: Acetylene selectivity and yield for the two different reactor cross sectional areas at different residence times.....109
Figure 4.4: Carbon monoxide selectivity and yield for the two different reactor cross sectional areas at different residence times.....110
Figure 4.5: Methane conversion and electrical efficiency (eV/molecule of methane converted) versus methane partial pressure.....112
Figure 4.6: Comparison of methane conversion versus residence time for two different systems 114
Figure 4.7: Hydrogen selectivity and yield for the two different feed compositions at different residence times 116
Figure 4.8: Acetylene selectivity and yield for the two different feed compositions at different residence times 117
Figure 4.9: Carbon monoxide selectivity and yield for the two different feed compositions at different residence times 118
Figure 4.10: Carbon dioxide production for an oxidative and non-oxidative system, before and after water-gas shift reaction 120
Figure 4.11: Methane reaction rate versus residence time at varying total system pressure 122
Figure 5.1: Simplified flowsheet of plasma process.....131
Figure 5.2: Effect of different Pd loadings on methane conversion and hydrocarbon selectivity 135
Figure 5.3: Effect of oxygen on methane conversion and hydrocarbon selectivity.137

Figure 5.4: Effect of addition and removal of carbon monoxide on methane conversion and hydrocarbon selectivity 138
Figure 5.5: Effect of temperature on methane conversion and hydrocarbon selectivity 140
Figure 5.6: Effect of metal loading on C_2 selectivity 141
Figure 5.7: Effect of residence time on methane conversion, power consumption, and overall C_2 selectivity 143
Figure 5.8: Effect of feed composition on methane conversion, power consumption, and overall C2 selectivity 144
Figure 5.9: Effect of higher methane partial pressures on conversion, selectivity and energy efficiency 146
Figure 5.10: Oscilloscope output of the dc plasma discharge voltage during a stable streamer discharge 147
Figure 5.11: Effect of electrical consumption on profit. Hydrogen selectivity, 75%; ethylene selectivity 153
Figure 6.1: TEM image of NaOH Y zeolite.....167
Figure 6.2: TEM image of 1.0 wt % Pd-Y zeolite.....169
Figure 6.3: TEM image of 0.05 wt% Pd-Y zeolite.....171
Figure 6.4: TEM image of 0.025 wt% Ag- 0.025 wt% Pd Y zeolite 172
Figure 6.5: Effect of Ag loading on methane conversion and ethylene and ethane selectivity 175
Figure 6.6: Effect of temperature on methane conversion and acetylene hydrogenation.....177
Figure 6.7: Effect of temperature on ethylene selectivity and ethane selectivity...178
Figure 6.8: Effect of temperature on acetylene conversion at elevated acetylene concentrations 180
Figure 6.9: Effect of temperature on ethylene production at high acetylene concentrations and acetylene conversion 181

LIST OF TABLES

Table 1.1: Ionization of different gases.....16
Table 3.1 Dielectric constants of various materials 81
Table 4.1: Variance of CO_2 co-production with different hydrocarbon feedstocks100
Table 5.1: Ethylene Feedstocks in the U.S.A.....127
Table 5.2 Energy Cost of Plasma Process 149
Table 5.3 Product values 151
Table 5.4 Economic Potential 152
Table 6.1 ICP Results 166
Table 6.2 Catalyst particle size and dispersion 170

ABSTRACT

The interest in natural gas utilization has increased tremendously over the last decade. Natural gas is being looked at as an energy source, as well as a basis for the production of many chemicals. New technologies are needed for smaller scale, remote and niche applications to utilize natural gas resources that will not be suitable for large-scale production of distillate products via synthesis gas. Low temperature plasma reactors have been shown to be an effective method for the conversion of methane, and under some conditions have low power consumption. The advantage of low temperature processing is the reduction of the energy requirements and therefore the cost. Cold plasmas have energetic electrons that exist at high temperatures while the bulk gas temperature remains relatively low (~65C). This allows for reactions that would not normally occur at these low temperatures, and removes the necessity to pre-heat feed streams.

The dc plasma system utilizes a particle bed to assist in the stabilization of the discharge. Without the bed present, the breakdown voltage is much higher (10.5 kV versus 6.5 kV). In addition, without the bed present the discharge typically transforms from the stable streamer discharge to an arc discharge within 30 minutes. The material in the bed behaves similar to a dielectric barrier. A dielectric material may become polarized in an electric field, which reduces the overall electric field and

in return the potential voltage difference. By reducing the voltage, the power input is reduced which lowers the temperature within the reactor. This in return reduces the tendency to form carbon. Carbon deposition on the walls and in the reactor bed result in a smaller effective gap between the electrodes, which causes the streamer discharge to convert to an arc discharge.

The reduced electric field plays an important role in the conversion and selectivity of the system. The reduced electric field (E/P) is a function of the breakdown voltage, pressure, and gas gap. The lower the reduced field, the lower the average electron energy and the higher the fraction of energy going into methane excitation versus methane dissociation. The excitation of methane only requires around .2 eV, while the dissociation of methane requires near 10 eV. The excitation of methane via vibrational excitation is responsible for the high conversions and high selectivity toward acetylene. The excited molecules may proceed down a reaction path similar to a pyrolysis process resulting in acetylene production.

The feed reactants for this study consist of methane, hydrogen, and oxygen. For the dc plasma reactor using NaOH treated Y zeolite, the primary products are acetylene, hydrogen, and carbon monoxide. The relative amounts of the products depend on the feed concentrations. For an oxidative system of 4/1 CH_4/O_2, the primary products are carbon monoxide and hydrogen with some acetylene. Even under the oxidative conditions very little carbon dioxide or water is produced. This indicates that very little combustion occurs. However, for a non-oxidative system of 2/1 CH_4/H_2 and 2% O_2, the primary products are acetylene, hydrogen, and small

amounts of carbon monoxide from the small concentrations of oxygen. The selectivities are nearly independent of conversion and residence time. The primary reason for not operating at longer residence times is that the throughput of methane is reduced while maintaining the same power input, effectively decreasing the energy efficiency.

For the non-oxidative system, acetylene yields as high as 50% were obtained. However, acetylene is not the most desirable product. Ethylene production is much more favorable as it is the highest hydrocarbon commodity produced worldwide. Ethylene can be produced by the in-situ selective hydrogenation of the acetylene to ethylene. A supported palladium catalyst is commonly used in industry for the selective hydrogenation of small amounts of acetylene in the purification of ethylene produced in crackers. The addition of palladium to the NaOH treated Y zeolite maintains the same methane conversion (20-60%), but allows for the selective hydrogenation of the acetylene to ethylene. The catalyst is most selective around 45°C, where it produces an ethylene to ethane ratio of about 4 to 1 with no acetylene. The addition of silver to the Pd-Y zeolite allows for an increase in the ethylene to ethane ratio from 4 to at least 7, and as high as 11. In addition, the addition of silver expands and shifts the temperature operating range. Ethylene yields as high as 30% and hydrogen yields as high as 40% have been obtained without attempting to optimize these yields; and it is expected, based on preliminary results, that higher yields can be obtained.

TEM imaging and oxidative reactions were used to determine the particle size and dispersion of metal on the Pd and Ag-Pd catalysts. An extremely high dispersion was obtained for the catalysts. The high dispersion allows for a more selective hydrogenation of the acetylene to ethylene.

CHAPTER 1 - Background Discussion of Fuels, Energy, and Plasmas

1.1 Introduction to Natural Gas

1.1.2 Natural Gas Resources

Natural gas is an important part of the present and future energy and chemical markets of the world. Political issues, resource limitations, and environmental concerns are just some of the factors that have led to the vast and progressive research in natural gas utilization.

Recoverable natural gas resources in the United States have been estimated at 1100 trillion cubic feet (TCF). The current consumption in the United States is 23 TCF/year, and is projected to grow to 35 TCF/year by 2025 [1]; which would project the natural gas that is recoverable by current technologies to last a minimum of 50 years. An advantage of natural gas is that it is a very clean energy source. The

combustion of methane, the primary component of natural gas, results in less carbon dioxide production than combustion of any other hydrocarbon. Currently, power generation and industrial uses are the two primary markets for natural gas.

Power generation is an expanding market for natural gas, as 95% of the power generation units being built are natural gas driven. New technologies for natural gas fired power generation units have increased the overall efficiency of plants, and natural gas efficiencies are far greater than that of coal fired power generation units.

The vast majority of natural gas reserves are in remote locations, and are termed "stranded gas". Stranded gas refers to gas that lacks means of transportation to market. A disadvantage of natural gas is that it is just that, a gas. Being in the gas state makes transportation and delivery much harder and more expensive. In order for gas to be transported, it must be either compressed to an extremely high pressure so that it may be transported via a pipeline or it must be compressed and refrigerated until its state is change to liquefied natural gas (LNG) such that tankers can transport it. Figure 1.1 shows how the cost of transportation for various methods such as oil tanker, oil pipeline, LNG tanker, and NG pipeline are affected by transportation distance. The base cost of a gas pipeline is almost three times that of an oil pipeline, and the disparity only increases as the distance required to get the product to market increases. This is due to the large number of costly pumping stations that are required for the natural gas. Similarly, the base cost of LNG transportation is much higher than that of oil transported via tanker. However, the additional cost due to transporting long distance is independent of LNG or oil. This is due to the cost

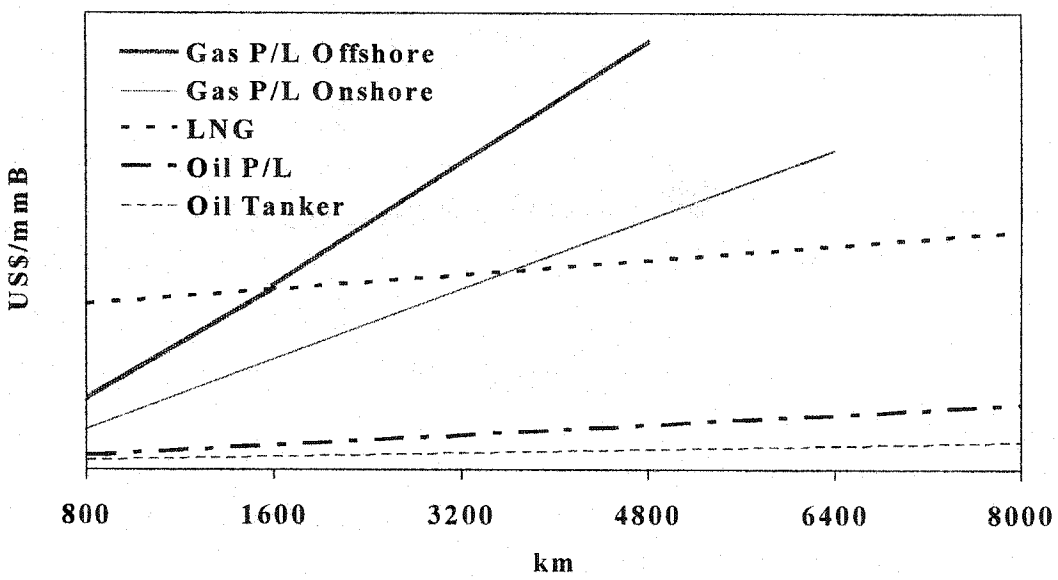

Figure 1.1 Cost of various transportation methods for various petroleum commodities.

associated with building the LNG production plant and the investment in cryogenic tankers, but once in the liquid form it varies very little from oil in its transportation requirements.

1.1.2 Natural Gas to Higher Value Commodities

1.1.2.1 Natural Gas to Syngas

Another alternative to transporting natural gas is to convert the commodity gas on location to a more valuable resource such as a liquid that would be easier to transport, or to a more valuable chemical. Methane is the primary building block, or chemical feedstock for many processes. Methane can be used as a source of hydrogen and carbon monoxide (known as synthesis gas), which is the primary feedstock for a variety of chemicals in the petroleum industry. In addition, methane may be upgraded via chain building to higher hydrocarbons.

In the years to come, hydrogen is expected to play an increasingly important role as a source of energy. The demand in hydrogen will increase dramatically as it becomes an energy source for space heating, electrical power generation, and as a transportation fuel [2]. Hydrogen also may be stored as a gas or liquid, and may be transported by means of a pipeline [3]. Methane is an excellent source of hydrogen with its 4:1 hydrogen to carbon ratio. Approximately 50% of all hydrogen produced worldwide comes from methane. The primary means of hydrogen production is through the catalytic steam reforming of methane, accounting for 40% of hydrogen

production. Steam reforming of methane is also the "greenest" form of hydrocarbon-based hydrogen production based on the amount of carbon dioxide produced. Steam reforming results in four hydrogen molecules for every carbon dioxide produced, while the partial oxidation of coal results in a ratio of 1:1.

The production of hydrogen from steam reforming results from the following two reversible steps:

$$CH_4 + H_2O \leftrightarrow CO + 3H_2, \qquad \Delta H_{298} = 206 \text{ kJ mol}^{-1}$$

$$CO + H_2O \leftrightarrow CO_2 + H_2, \qquad \Delta H_{298} = -41 \text{ kJ mol}^{-1}$$

With the overall reaction as:

$$CH_4 + 2H_2O \leftrightarrow CO_2 + 4H_2, \qquad \Delta H_{298} = 165 \text{ kJ mol}^{-1}$$

The manufacturing of methanol and ammonia, and a variety of other petroleum processes requires large quantities of hydrogen as a feedstock. Production of synthesis gas (hydrogen and carbon monoxide) constitutes approximately 60% of the overall cost of the production of methanol. Thus, it is desired to develop a process that would allow for a more economical or straightforward process for the production of syngas. It is believed that the one-step conversion of methane to hydrogen and other chemicals via a dc plasma reactor might be a solution.

1.1.2.2 Natural Gas to Hydrocarbons

Methane is also the building block for higher hydrocarbons. One of those higher hydrocarbon groups is C_2's, which consist of ethane, ethylene, and acetylene. Ethane is primarily used for the production of ethylene. Ethane is either recovered from associated natural gas or stripped from product streams to be converted to ethylene. Although both ethylene and acetylene can be used as a feedstock, the inherent safety concerns associated with acetylene make it much less desirable.

Ethylene is another chemical that is in high demand and production within the petroleum industry. Ethylene is highly reactive, due to its double bond, allowing it to be converted to a wide variety of products by oxidative, addition, and polymerization reactions. Ethylene is the largest-volume petrochemical produced worldwide [4]. Ethylene is primarily a chemical building block, used to produce plastics and high polymers. Ethylene became an important intermediate in the petroleum industry around 1940 when industry started separating it from industry waste streams. Thus, ethylene has essentially replaced acetylene in chemical processes.

Pyrolysis, also known as steam cracking, is the primary process for the production of ethylene, and is responsible for over 97% of the ethylene worldwide [4]. Pyrolysis is defined as the thermal decomposition of hydrocarbon molecules when exposed to high temperatures. Pyrolysis of hydrocarbons to ethylene is almost exclusively performed in fired tubular reactors. Reactor design and technological advances have allowed for an increase in plant sizes from 70,000 metric tons per year in 1950 to 150,000 tons per year in 1970 and above 450,000 tons per year today [5].

The pyrolysis process is highly endothermic. The hydrocarbon stream has to be heated then mixed with steam, and further heated to around 500°C. At that point, it enters the reactor where it is heated to the operating temperature of around 800°C. The saturated hydrocarbons are cracked into primarily ethylene. The product stream is cooled upon exit of the reactor to prevent further reactions or degradation of the desired product. This highly endothermic process is very energy intensive. The steam cracking of ethane, it requires long residence times and high temperatures to get to the desired conversion and selectivity. The reaction typically operates near 60% conversion of the ethane, and an ethylene selectivity of 85%. The burning of the undesired byproducts drives the endothermic reaction. The byproducts from combustion can account for up to 10% of the original ethane being converted to undesired greenhouse gases, carbon dioxide and nitrogen oxides. Likewise, heavier feedstocks also have their own disadvantages. The higher feedstocks result in a wider range of products, resulting in less selectivity to the desired ethylene. This wider variety of products also results in a higher capital cost, as the equipment size is considerably larger.

Ethylene is the feedstock for many industrial processes. However, when ethylene is produced there are many byproducts associated with it. The manufacturing of polymer grade ethylene requires the elimination of small amounts of acetylene and diolefins through the process of selective hydrogenation [6]. Many different processes have been developed over the years, and are listed below[7]:

1.) Solvent Extraction

2.) Cracked Gas Train or Raw Gas Catalytic Hydrogenation Reactors

3.) Backend Catalytic Hydrogenation Reactors

4.) Front-End Selective Catalytic Hydrogenation reactors

The solvent extraction process uses a solvent, typically dimethyl formamide, to selectively adsorb the acetylene which is it is later sold as a product. The raw gas catalytic hydrogenation process treats the cracked gas effluent with a nickel catalyst to selectively hydrogenate the acetylene. This process is typically used where the hydrogenation unit precedes the caustic tower, as a nickel catalyst can handle sulfur while the palladium based catalysts have a low sulfur tolerance.

The last two processes deal with the placement of the hydrogenation unit that would utilize a palladium catalyst for the selective hydrogenation of the acetylene. For the backend unit, the C_2 rich stream that contains the acetylene is mixed in stoichiometric proportions with hydrogen, and sometimes with carbon monoxide. The hydrogenation unit is located downstream of the demethanizer and before the de-ethanizer. In the front-end selective catalytic hydrogenation processes, the reactor precedes the demethanizer. Thus, the feed to the hydrogenation unit contains an excess amount of hydrogen, typically 10 to 35 mol percent. Figure 1.2 shows a front-end de-ethanizer reactor system.

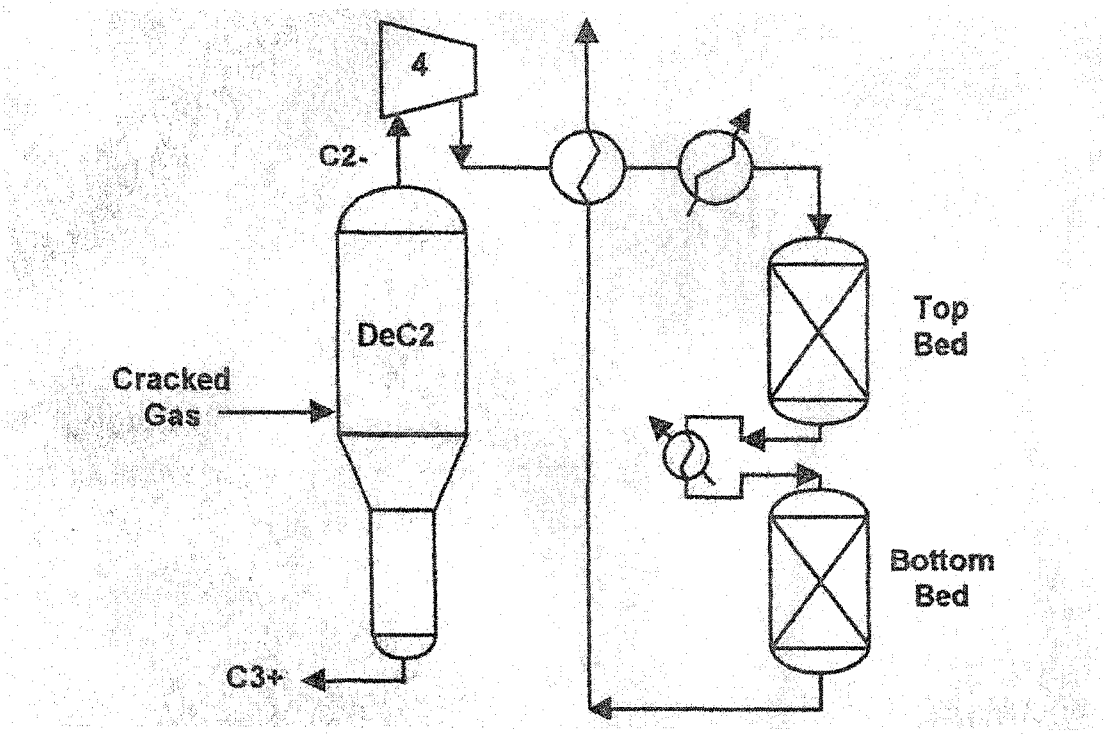

Figure 1.2 Front-end de-ethanizer reactor system. Depicting the location of the (dual bed in series) hydrogenation unit. (Tiedtke, et al. 2001)

The process of selective hydrogenation has advanced over the years and has led to a very developed catalyst that provides high ethylene selectivities with a reduction in the over hydrogenation to ethane, as well as catalysts that are more tolerant to poisons and feed condition variances. The main mechanism that controls the hydrogenation activity of the catalysts is the availability of the palladium sites, while the selectivity of the catalyst is dependent on the preferential adsorption of the reactant. Literature shows that the strength of adsorption on palladium based on heat of adsorption follows [7]:

CO > acetylene >> conjugated diolefins >= alkyl acetylene > diolefins >> olefins

In general, the rate of hydrogenation and selectivity is greatly dependent on preventing ethylene from staying on the surface. Acetylene is adsorbed stronger on the surface than ethylene, thus when it is adsorbed it is hydrogenated to ethylene. As long as there is sufficient concentrations of acetylene the ethylene will be displaced before it is over hydrogenated to ethane. The intrinsic rate of ethylene hydrogenation is twice that of acetylene hydrogenation, so if the ethylene is not removed from the surface it will quickly be hydrogenated to ethane. This becomes an important factor as the conversion of acetylene approaches 100%. Since carbon monoxide also strongly adsorbs on palladium, addition of CO is very effective in controlling the selective hydrogenation of acetylene to ethylene. Carbon monoxide prevents ethylene from adsorbing on the catalyst as the acetylene concentration becomes low. However, since CO competes with acetylene for adsorption sites, the overall activity of the catalyst is reduced. There are many poisons that also affect the overall

performance of the catalyst. Poisons such as hydrogen sulfide or carbonyl sulfide may block palladium sites, or poisons such as arsenic and mercury may form alloys with the palladium, thus reducing the adsorption strength of acetylene.

1.2 Plasma Chemistry

1.2.1 Background of Plasma

Langmuir was the first to study the phenomenon known as plasma, as well as the first to use the term "plasma" to describe an ionized gas. A plasma is defined as an ionized gas that is generated by combustion, flames, or electrical discharges. Plasma chemistry can be grouped into two main categories:

1.) volume chemistry, which is associated with an industrial application: ozone generation

2.) surface plasma chemistry, which is associated with etching, deposition, and surface modifications that are commonly used in the electronics industry.

The focus of this dissertation is on volume chemistry, which in its most basic form consists of electrodes and the discharge volume in which the reaction occurs [8].

Plasma can be considered the fourth state of matter. The particles within a plasma (non-electrons) exist at temperatures as high as 10^4 to 10^5 K. In comparison, a regular gas temperature exists as high as 20000K and liquids and solids are below 5000K. A plasma can also be characterized as a quasi-neutral gas of charged and neutral particles [9].

For a neutral gas, the behavior of the particles is described by the kinetic theory of gases. The motion of a neutral particle has no external forces acting upon it, thus it travels in a straight line until it collides with another particle or the boundary of the container. The cross section for collision (σ), mean free path (λ), and average velocity (v) of the molecules are defined as:

$$\sigma = \pi * r^2 \qquad \text{Equation 1.1}$$

$$\lambda = \frac{1}{\sigma * n} \qquad \text{Equation 1.2}$$

$$v = \left(\frac{\kappa * T}{M} \right)^{1/2} \qquad \text{Equation 1.3}$$

For charged particles in a plasma, the particle moves along a path which closely follows that of the electric field. The Debeye length, λ_D, is the dimensional size of the small volumes to which the local concentrations of charges in a plasma are confined. In order for a plasma to be stable, it is necessary for the dimension of the "system" to be much larger than that of the Debeye length. Outside these concentrated volumes of charge, the density of electrons is nearly equal to that of the density of ions resulting in an electrically neutral plasma. Thus, the plasma is considered a quasi-neutral gas.

A plasma is achieved when sufficient energy is added to atoms of a gas causing ionization and production of ions and electrons from the formation of the ions. Plasmas are generally thought of as gas discharges, since they are generally created by passing an electrical discharge through the gas. Even though plasma are generally created by electrical discharges in gases, a plasma may also be created in a

solid or liquid when sufficient energy is supplied to cause ionization or vaporization. Electrons are primarily responsible for the transfer of energy from the electric field to the gas. Ionization by electron impact is probably the most important process in the breakdown of gases [10].

The ionization of gas depends on the electrons energy and its ability to transfer energy to a molecule. Electrons moving at a slow rate will not have the energy necessary to produce ionization. Naturally occurring radioactivity and cosmic rays produce small amounts of free electrons in a gas. Free electrons can also be produced by field emission or photoionization [9]. As a voltage is applied to a gas in a discharge reactor, the electrons are accelerated via the electric field resulting in an increase in kinetic energy. Electrons and ions are both accelerated by the electric field, but electrons are the lightest so they are accelerated the easiest. If the electron energy is still too low to produce ionization, the electrons will lose energy during collisions with other atoms and molecules within the gas. Since the mass of the target is sufficiently large compared to the light electron, only a very small fraction of the energy of the electron is lost to the collision target; thus, these collisions are considered elastic. The collision target may be excited by this collision which may allow ionization by collision with another low energy electron. However, if the electric field is strong enough to produce electrons with sufficient energy to cause ionization the collisions will be inelastic. Inelastic collisions result in a large transfer of energy. Upon ionization, the electrons produced by the ionization are accelerated in the existing electric field where they impact another target molecule resulting in

ionization. This series of events is termed electron multiplication. On the other hand, electrons with extremely high energy are extremely poor at ionization. Each gas has an optimum electron energy level that will have the highest probability of ionization. This ionization curve can be seen in Figure 1.3. Table 1.1 shows a comparison of various ionization potentials of different gases.

The changes that take place within a gas as a function of applied voltage are dependent on discharge current. This dependence is described as the I-V characteristic of a discharge, and can be seen in Figure 1.4 for a typical DC glow discharge. The low current flow that exists when the applied voltage is low is from the collection of free electrons present in the gas. When the voltage is increased (which is accompanied by an increase in the electric field), gas ionization occurs creating more charged particles and the current increases steadily. This stage is known as the Townsend discharge. Once the applied voltage reaches a threshold known as the breakdown voltage, an avalanche results from three simultaneous processes:

1.) Ions that are accelerated by the high electric field strike the cathode resulting in a release of secondary electrons. These secondary electrons collide with neutral species forming more ions.

2.) These new ions are accelerated to the cathode where they collide producing more electrons and thus new ions.

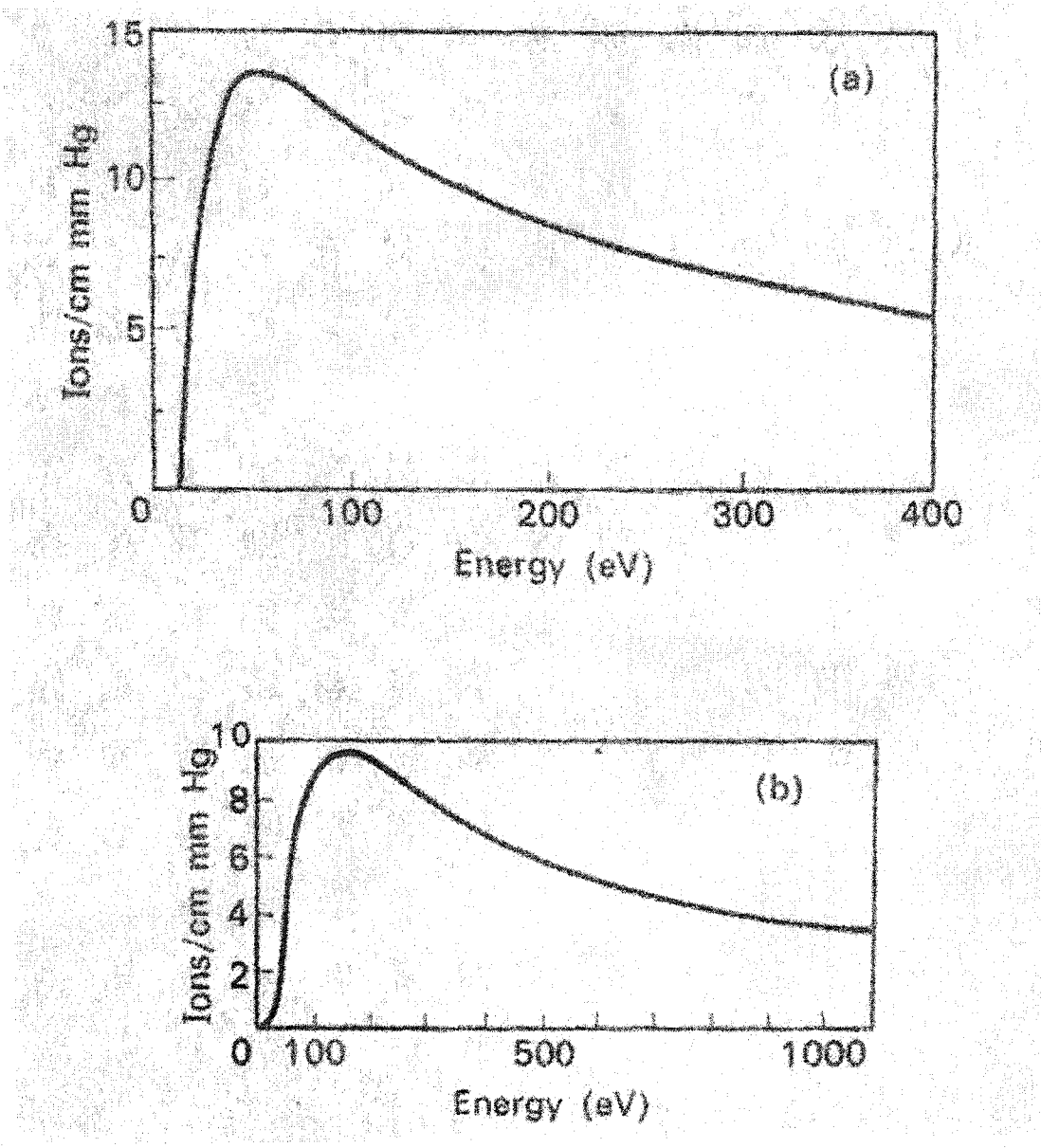

Figure 1.3 Probability of single ionization by electron impact: (a) in Hg vapor, (b) in air (Abdullah, M., et al. 1970)

Table 1.1 Ionization of different gases

Neutral	Ion	Ionization Potential
Ar	Ar^+	15.8
H	H^+	13.6
He	He^+	24.6
CH_4	CH_4^+	13
O	O^+	13.6

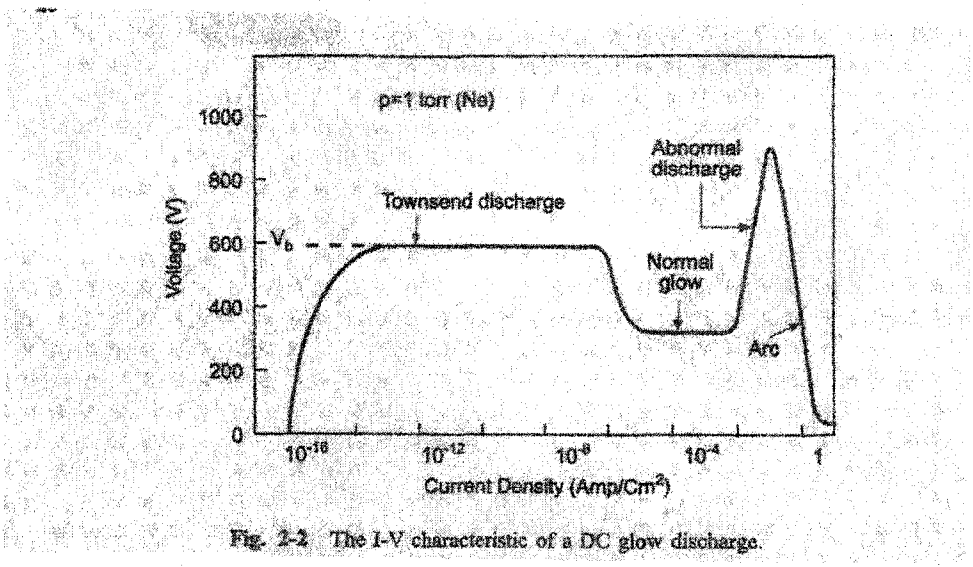

Fig. 2-2 The I-V characteristic of a DC glow discharge.

Figure 1.4 The current-voltage characteristics of a DC glow discharge. (Grill. 1993)

3.) Some electrons are removed from the process by collision with walls and ions back to a neutral state.

Steady-state within the discharge is reached when the rate of formation of ions is equivalent to the rate of recombination of electrons with the ions. At this steady-state operation the discharge is self-sustaining, and is called a glow discharge. The formation of the glow discharge is accompanied by a voltage drop and a sharp rise in current flow. The visual glow of the discharge is due to the decay of electronically excited species. The number of ions that must impinge on the cathode is far greater than the number of electrons that are emitted as secondary electrons. Thus, each secondary electron is responsible for ionizing 10-20 ions. Once the breakdown voltage is reached, if the power is increased further the voltage and current will increase. At this point, the further increase in power results in a heating of the cathode, and an arc discharge is formed.

1.2.2 Description of Different Types of Plasmas

Volume plasma chemistry can also be categorized into non-equilibrium plasmas and equilibrium plasmas. A non-equilibrium plasma is also commonly referred to as a cold plasma because the temperature of the electrons and kinetic energy of the electrons are much higher than that of the bulk molecules. Thus, the overall temperature of the plasma is very low. In an equilibrium plasma, the energy of electrons and gas molecules are nearly equal is a result of a very high temperature.

There are many types of non-equilibrium plasmas. The five most common types of non-equilibrium discharges are:

1.) Radio frequency discharge (RF)

2.) Microwave discharge

3.) Glow discharge

4.) Silent discharge

5.) Corona discharge

Radio frequency discharges are commonly used for spectroscopic instrumentation. Typical frequencies for RF discharges are around 2-60MHz. Since the wavelength of RF frequencies is larger than the dimension of the reactors, the plasma can be created outside of the discharge volume. This limits the eroding of the electrodes and contamination of the discharge volume with the sputtered metal from the electrode. Thus, RF discharge is commonly used in the semiconductor industry where a tediously clean environment is essential.

Microwave discharges operate in the 0.3-10 GHz range. The wavelength of the electric field is close to the dimensions of the vessel. Thus, it is necessary to produce them in a waveguide structure or resonant cavity. These are very much a non-equilibrium system since only the lightest of the electrons can follow the oscillations of the extreme high frequencies. A common frequency is 2.45 GHz, which is also used in microwave ovens. Reactors can be up to 4 m long, and operate at low pressures up to atmospheric pressure.

A glow discharge is typically a low pressure (less than 10 mbar), and high electric field system. The high energy of the accelerated electrons allows for easy excitation of the gas molecules. This excitation creates a glow, hence the name glow discharge. These discharges are commonly used in florescent lightening. However, due to the low pressures and low mass throughputs, these reactors are not commonly used in industry applications.

Silent electric discharge allows for high mass throughput and operation at atmospheric pressures, both useful for industrial processes. A unique feature of a silent discharge is that one of the electrodes is covered with a dielectric material. Thus, silent discharges are also known as dielectric barrier discharges, or DBD. The dielectric barrier plays the most important role in the creation of the discharge. The dielectric limits the amount of charge transported by a single microdischarge, as well as distributes the microdischarges through the entire electrode area. Once ionization of gas molecules has occurred, the dielectric allows for a location for the charges to accumulate. This accumulation creates a field that in return reduces the field in the gap, which then interrupts the current flow. [8] The reduced field that occurs at breakdown within a dielectric barrier discharge reactor corresponds to electron energies of 1-10 eV, which is an optimum level the excitation of many gases.

The most common industrial plasma discharge reactor is the ozone generator. An ozone generator is a member of the silent discharge reactor group. In addition, it has been found that DBD reactors are capable of producing valuable chemicals. Many reactors have been utilized within our research group for the production of

valuable products from methane. The direct conversion of methane to higher hydrocarbons[11] and organic oxygenates [12]has been investigated. The primary problem with these systems is the relatively high energy requirements. Though the mass flow rates are substantial, these reactors have high power requirements that resulting in a low energy efficiency.

The last type of cold plasma is the corona discharge. The corona discharge is the specific plasma system specifically related to this dissertation. The glow discharge previously described operates at low electric fields and low pressure. Conversely, the corona discharge operates at higher electric fields and pressures. A corona discharge is relatively low power, high electric field discharge that can operate around atmospheric pressures. At higher pressures and fields, the discharge has a tendency to become unstable resulting in a high-current arc discharge. The use of inhomogeneous electrodes allows for stable operation. An example of an inhomogeneous discharge would be a configuration that has a point as one electrode and a plate as another electrode. The configuration of the electrodes and the orientation of the applied field results in two distinct discharges, a positive corona and a negative corona.

For a positive corona, the discharge goes through several stages: burst pulse, streamer, glow, and spark discharge. As the voltage is increased, the pulse discharge will change to the streamer discharge, which represents a typical corona phenomenon. As the voltage is increased, the streamer discharge will result in a glow corona

discharge around the point of the tip. A further increase in voltage results in a spark or arc discharge across the gap.

In a negative corona, the initial voltage results in a Trichel pulse corona. The total current from the electrode is fairly constant, but the discharge is composed of many individual pulses. These individual pulses are electron avalanches which trigger successive avalanches at nearby locations. This discharge is relatively noisy, and may lead to spark formation. If the voltage is too high a spark discharge will occur bridging the gap.

1.3 Past dc Corona Discharge Research

A lot of research and effort has focused on the use of a dc plasma system for the conversion of methane to more valuable chemicals. Much of the past research focused on the use of partial oxidation conditions for the conversion of methane.

Liu et al. [13] compared the conversion of methane under high oxygen concentrations for a dc and ac plasma system. The results showed the highest methane conversion, 10.6%, at the highest oxygen concentration tested, 4:1 methane to oxygen. However, the experiments were performed with a feed of 75% helium, and at an elevated temperature of 650°C or higher. Though the power consumption was not reported, the low conversion and low partial pressure of methane inevitably results in an extremely low energy efficiency, eV/molecule of methane converted. In addition, the helium is less than desirable as it is impractical as a feedstock for an

industrial process. The ac plasma system was also capable of sustaining the discharge and higher C_2 selectivities, as compared to the dc plasma system.

Continued research looked for the enhancement of the dc plasma system by the addition of a catalyst to the reaction zone [14]. The combination of a catalyst bed and plasma operation allowed for a higher methane conversion than was seen independently or even combined at the lower temperatures for the oxidative coupling of methane. It was believed the OH groups were easily charged, especially at low temperatures, leading to a mechanism that enhanced the formation of methyl radicals. The results also show an increase of methane conversion with an increase of the oxygen partial pressure. Though the catalyst increased the methane conversion, it adversely affected the C_2 selectivity. The C_2 selectivity was highest with corona alone, and decreased with increasing temperature. High levels of oxygen and low throughputs of methane were major boundaries to overcome for an industrial process.

Liu et al[15] studied the effect of metal oxide catalysts within the dc plasma reactor. Sr-La_2O_3/$La(OH)_3$, Li/MgO and CaO/NaOH were studied. These catalysts in combination with the dc plasma showed a dramatic improvement in methane conversion and product selectivity over catalyst or dc plasma alone. The improvement was generally far more than the combination of the individual two methods. Thus, the catalyst played a very important role in the reaction. They speculated that the improvement was from the OH groups present on the catalyst surface.

The initial results of the improvement of the dc plasma system by a catalytic material led to a study of an extensive range of catalysts. [16] Several zeolite catalysts have been tested within the system. NaY, NaOH treated Y, HY, NaX, NaA, 5A, and Na-ZSM-5 were studied. NH_4Y zeolite was treated with NaOH to yield NaOH treated Y zeolite. The purpose of the NaOH treatment was to reduce the Si/Al ratio by dissolving some of the Si within the parent catalyst resulting in an increase in the catalyst's basicity and polarity. It was determined that the ability to obtain and maintain streamer discharge were as follows:

NaY & NaOH treated Y > HY > NaX > NaA > Linde Type 5A > Na-ZSM-5.

The last two catalysts, 5A and Na-ZSM-5, had the smallest operating temperature range and shortest stability duration. It was believed that the temperature range in which there was a stable discharge was directly related to the dehydration temperature range. NaOH treated Y zeolite had a dehydration temperature range of 25-135°C, while Na-ZSM-5 only had a dehydration temperature range from 25-50°C. Consequently, Na-ZSM-5 was only stable at temperatures under 50°C, and stable for short periods of time at that. This data suggested that OH groups in the catalyst play a large role in the stability of the dc plasma discharge.

1.4 Theory Behind Present Research

The direct conversion of methane to more valuable products using various reactor and experimental conditions has been previously investigated within our research group. The purpose of this dissertation work was to develop a process that

improves the results from the former research, as well as develop a further understanding of the reactor system. It was known that the dc plasma system was effective for the conversion of methane at atmospheric temperature and pressure. This is a benefit of the system, and an important factor for industrial practicality. As discussed, most processes for the conversion of methane to valuable products require an intensive thermal energy input in order to drive the process. For all practical purposes, the only energy input within the dc system is from the power supply. In addition, the operation at atmospheric pressure reduces the expensive cost of equipment associated with elevated pressures, and the energy required to drive compressors.

Chapter 2 will describe the experimental apparatus and procedure. The reactor design is similar to that described by Liu [15] and Marafee [14]. In addition, the calibration and calculations need to interpret the raw data are defined within the chapter.

Previous research focused on the operation and stability of the reactor system. It was thought that the catalyst played a significant role within the reactor system but the exact nature of the role was unknown. Chapter 3 of the dissertation describes the present understanding of the catalyst's role within the system.

In order to try to develop a process that would be economically feasible for industrial practice, many conditions were investigated. Chapter 4 will describe the results of these studies. Methane conversion, product selectivity and yield, and power

requirements are all important factors to consider when optimizing the reactor conditions.

Optimization of the stability of the reactor and the product stream, the product yields and methane conversion were significant. However, the main product was acetylene which is not the most desired chemical commodity. Chapter 5 investigates the use of a metal loaded catalyst for the selective hydrogenation of the acetylene to ethylene. Ethylene is the more desirable product, as it is the largest produced hydrocarbon chemical in the United States. It was determined that the loading of metal within the catalyst played a huge role in the selectivity distribution from the plasma system. In addition, the metal loading allowed higher partial pressure of methane that result in stable operation.

Chapter 6 involves the characterization of the metal loaded catalyst and the unique features of the hydrogenation catalyst.

The dissertation concludes with a summary of the state of the dc plasma system. In addition, some thoughts and suggestions on future experiments that may lead to a better understanding of the process, as well as a process that is more suited for an industrial application.

1.5 Literature Cited

1. Energy, O.o.F., *Natural Gas Fundamentals from Resource to Market*, . 2003, Department of Energy.

2. Balasubramanian, B., A. Lopez Ortiz, S. Kaytakoglu and D.P. Harrison, *Hydrogen from methane in a single-step process.* Chemical Engineering Science, 1999. **54**: p. 3543-3552.

3. Armor, J.N., *The multiple roles for catalysis in the production of hydrogen.* Applied Catalysis A: General, 1999. **176**: p. 159-176.

4. Gerhartz, W., *Ullman's Encyclopedia of Industrial Chemistry.* Vol. A10. 1987, Weinheim: VCH. 45.

5. Crynes, B.L., L.F. Tan and L.F. Albright, *Cracking, Thermal*, in *Encyclopedia of Physical Science and Technology.* 1992, Academic Press. p. 605-622.

6. Goetz, J., M.A. Volpe, A.M. Sica, C.E. Gigola and R. Touroude, *Low loaded palladium on an alpha-alumina catalysts: Characterization by chemisorption, electron microscopy, and photoelectron spectroscopy.* Journal of Catalysis, 1995(153): p. 86-93.

7. Tiedtke, D.B., T.T. Cheung, J. Leger, S.A. Zisman, J.J. Bergmeister and G.A. Delzer, *Chemicals influencing the activity of palladium-based catalysts for the selective hydrogenation of acetylene to ethylene in acetylene converters.* Ethylene Producers Conference, 2001.

8. Eliasson, B. and U. Kogelschatz, *Nonequilibrium volume plasma chemical processing.* IEEE Transactions on Plasma Science, 1991. **19**(6): p. 1063-1077.

9. Grill, A., *Cold Plasma in Materials Fabrication*, ed. W. Perkins. 1994, New York: IEEE.

10. Abdullah, M. and E. Kuffel, *High-voltage Engineering.* Applied Electricity and Electronics, ed. P. Hammond. Vol. 1. 1970, Oxford: Pergamon Press`.

11. Thanyachotpaiboon, K., T.A. Caldwell, S. Chavadej, L.L. L. L. Lobban and R.G. Mallinson, *Non-oxidative conversion of methane to higher hydrocarbons in low temperature plasmas.* AIChE Journal, 1998. **44**: p. 2252.

12. Larkin, D.W., L.L. Lobban and R.G. Mallinson, *Product selectivity control and organic oxygenate pathways from partial oxidation of methane in a silent electric discharge reactor.* Industrial Engineering & Chemical Research, 2001(40): p. 5496.

13. Liu, C.-J., A. Marafee, B.J. Hill, G. Xu, R.G. Mallinson and L.L. Lobban, *Oxidative coupling of methane with ac and dc corona discharge.* Industrial & Engineering Chemistry Research, 1996. **35**(10): p. 3295-3301.

14. Marafee, A., C.-J. Liu, G. Xu, R.G. Mallinson and L.L. Lobban, *An experimental study on the oxidative coupling of methane in a direct current corona discharge reactor over Sr/La2O3 catalyst.* Industrial & Engineering Chemistry Research, 1997. **36**: p. 632-637.

15. Liu, C.-J., A. Marafee, R.G. Mallinson and L.L. Lobban, *Methane Conversion to higher hydrocarbons in a corona discharge over metal oxide catalysts with OH groups.* Applied Catalysis A: General, 1997. **164**: p. 21-33.

16. Liu, C.-J., R.G. Mallinson and L.L. Lobban, *Comparative investigations on plasma catalytic methane conversion to higher hydrocarbons over zeolites.* Applied Catalysis A: General, 1999. **178**: p. 17-27.

CHAPTER 2 - Experimental Procedure

2.1 Experimental Apparatus

The dc plasma apparatus is depicted in Figure 2.1. The process can be broken down into three basic units:

(a) the upstream feed preparation portion

(b) the reactor section (reactor, power supply, and temperature control)

(c) the downstream portion for analysis of the effluent gas stream.

2.1.1 Upstream Section

A Porter Mass Flow Controller Series 100 is used for each individual gas, and Porter Control Module CM4 is used to control up to four mass flow controllers. Each flow controller is standardized for a particular gas and total flowrate. A conversion

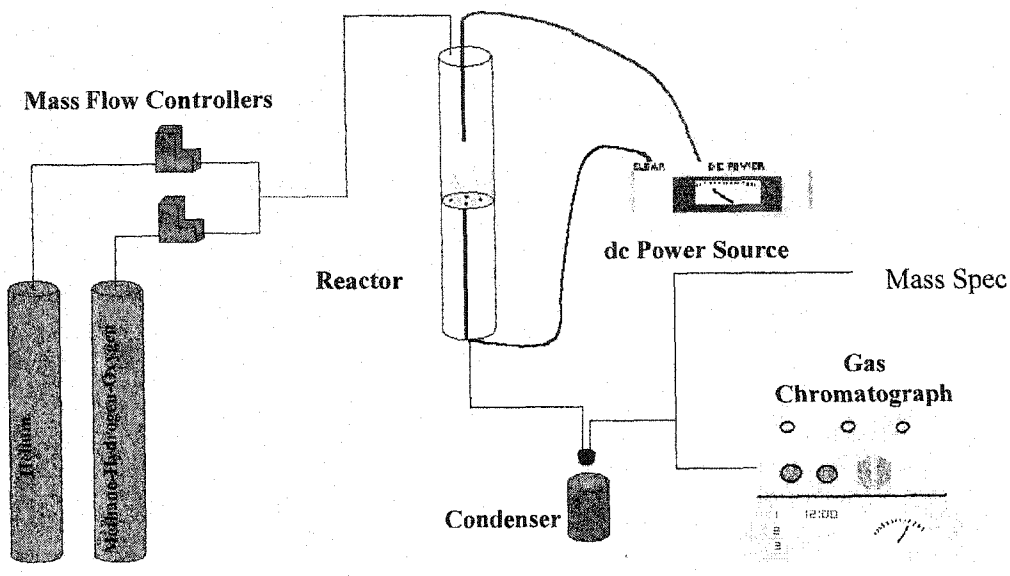

Figure 2.1 Catalytic dc plasma discharge system

chart can be used to estimate the correct setting for various other gases and flowrates. However, these conversions are best when used to estimate an initial setting in which to adjust for more accurate flowrate. Each gas flowrate is measured individually in order to achieve the desired composition and flowrate resulting in the final total flowrate. A bubble flowmeter is used in order to measure the flowrate. The flowrate needs to maintain the desired flowrate over a 45-minute period before proceeding to the next gas.

2.1.2 Reactor Section

The configuration of the reactor can be seen in Figure 2.2. The system has been described previously [1, 2]. The electrodes are configured in a point to plane geometry. The reactor tube is a quartz tube. The typical reactor has a 7mm inside diameter and a 9 mm outside diameter, although a few experiments used of a 4.5 mm ID and 10 mm OD quartz tube. The top electrode is a stainless steel 1/16-inch rod that is placed concentrically within the reactor. The bottom electrode is a 3mm stainless steel plug with 5 holes drilled through it to allow for the gas to flow through. The plug is attached to 1/16 inch rod that allows for external connection to the dc power source.

The dc power source is a Bertan Model 210-50R. The power source consists of three major connections. One of the connections is the chassis ground which is connected directly to the universal ground of the laboratory electrical system. The other two connections consist of the positive and negative leads that are attached to

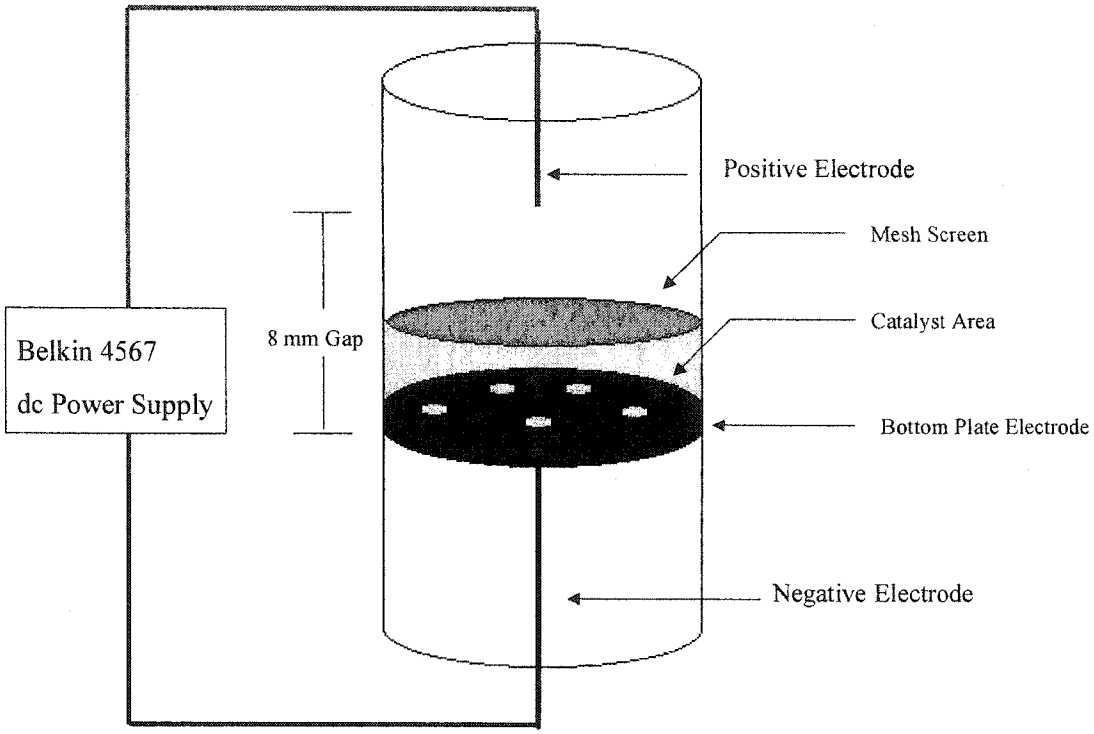

Figure 2.2 Catalytic dc Plasma Discharge Reactor

the reactor system. The top electrode is the positive electrode, while the bottom electrode is the negative electrode.

A ceramic furnace and a Watlow Series 965 are used to control the reactor temperature. The furnace is eight inches in height, which allows for a sufficient region above and below the reaction zone for uniform heating. If allowed to operate adiabatically, the reactor will operate near 65°C. If a higher temperature is desired, the furnace can be used to heat the reactor as high as 750°C. However, if a cooler operation temperature is desired, a low flow of air is passed over the quartz tube. This air flow is provided by the laboratory air system. Feed gas enters the top of the quart tube, flows through the plasma region (between the electrodes) and the catalyst bed, and exits the bottom of the tube. Upon exiting the reactor, the effluent gas flows to the analysis equipment.

2.1.3 Downstream Section

A Carle Series 400 AGC gas chromatograph and a MKS quadrupole mass spectrometer are used for quantitative analysis. The Carle GC has four analysis columns that allows for a wide variety of detection. The first detecting portion of the GC is a hydrogen transfer system (HTS), which consists of a palladium tube with nitrogen as the carrier gas. The palladium tube has a unique feature that allows for hydrogen molecules to permeate from the sample to the carrier gas, where the nitrogen picks it up. Nitrogen carrier gas is used for the HTS system, as the ionization is distinguishable from that of hydrogen. In addition, the Carle GC has

three columns: Hayesep, molecular sieve 13X, and molecular sieve 5X. These three columns allow for the detection of: C_2's, carbon monoxide; oxygen, nitrogen, methane, carbon monoxide; and higher hydrocarbons respectively.

The mass spectrometer uses a MKS quadropole residual gas analyzer, while the bulk chamber and vacuum pumps are from a preexisting Balzar's unit. The data is transferred and analyzed using the PPT software package by MKS. The closed system pressure is 10^{-7} torr, while the operating pressure is desired to be around 10^{-5} torr. The two order of magnitude difference allows for a quantitative difference between the background noise and the detectable components. The gas is drawn through a capillary tube to the sampling chamber which is at a reduced pressure, and then the sample is further drawn into the main chamber.

2.2 Catalyst Preparation

It is necessary to prepare the NaOH Y zeolite from the parent NH_4 Y zeolite. The preparation and characterization of the NaOH treated Y zeolite has been discussed elsewhere[3, 4]. The NH_4 Y zeolite is supplied by Aldrich Chemical (stock #41700, lot #J22J29). The supplied pellets are soaked in a 1 M NaOH solution for 8 hours. Approximately 30 grams of the pellets are slowly added to 400 mL of the solution in order to minimize excessive heat of reaction. After soaking, the pellets are rinsed and drained repeatedly with deoinozed water until the mixture returns to a pH of 7. The resulting pellets are drained and heated overnight at 100°C in air. The pellets are subsequently calcined in a furnace at 500°C for 2 hours. The pellets are

then granulated with a mortar and pestle which creates a wide distribution of particle sizes. A sieve system is then used to collect particles in the 60-80 mesh size. These size particles are then used in experiments and undergo an individual pretreatment before each experiment, to be described.

The palladium and silver-palladium loaded NaOH Y catalyst are prepared from the existing NaOH Y zeolite catalyst. The preparation of the Pd-Y zeolite via chemical vapor deposition used in the initial experiments studying the effect of palladium metal on the selective hydrogenation of acetylene also has been described previously [5]. Palladium was added using chemical vapor deposition according to the following procedure. The NaOH Y zeolite was calcined at 400°C, and then mixed with the appropriate amount of palladium acetylacetonate to achieve the desired Pd loading (ranging from 0.025 to 1%). The mixture was then heated slowly under vacuum to a temperature of 130°C to disperse the palladium throughout the NaOH Y zeolite. This Pd on NaOH Y zeolite will henceforth be referred to as Pd-Y zeolite. The Pd-Y zeolite was then calcined for the final time to a temperature of 350°C.

Subsequent preparations of Pd-Y and Ag-Pd-Y catalysts used the incipient wetness technique [6]. Figure 2.3 shows that at the low loadings of metal used, there were no distinguishable differences in the performance of the catalyst when comparing chemical vapor deposition and incipient wetness.

The point of incipient wetness of the Y zeolite was found by adding water to a known amount of catalyst until the catalyst was unable to adsorb any additional

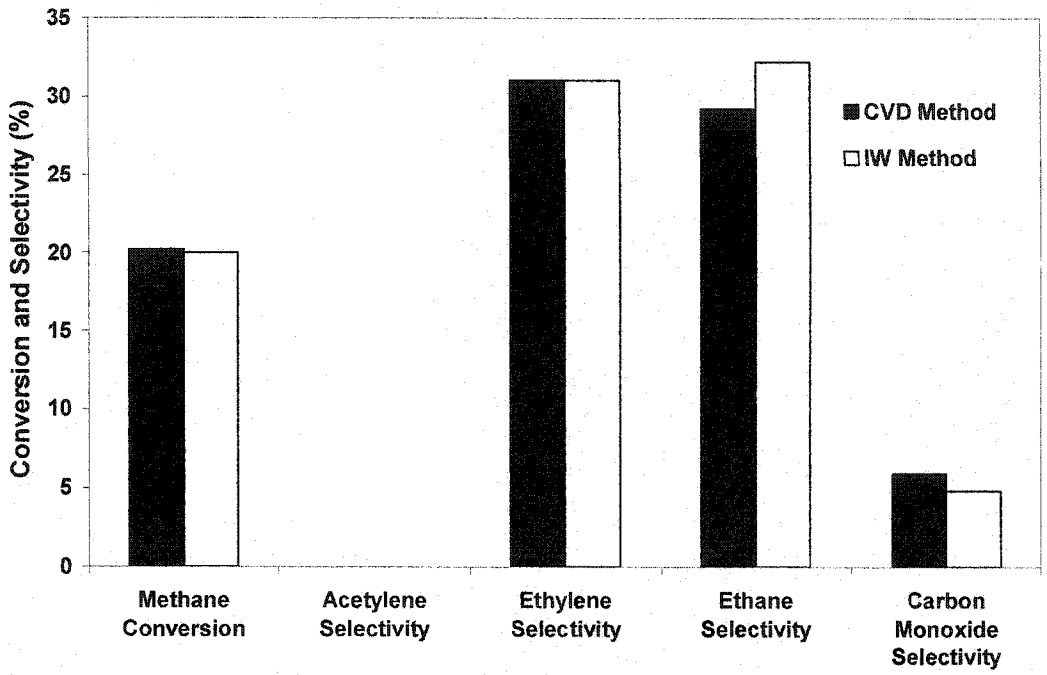

Figure 2.3 Comparison of 0.025 wt% Pd-Y zeolite using two different impregnation methods: Chemical vapor deposition (CVD) and Incipient wetness (IW). 2/1 H_2/CH_4 with 2% O_2, 10 kV, 0 psig, 40°C.

water. A solution of tetraaminepalladium (II) nitrate was made such that for the amount of catalyst to be prepared, the amount of solution used for incipient wetness would provide the desired metal loading on the catalyst, 0.025 wt% Pd-Y zeolite. The catalyst was then dried for 8 hours in a 110°C oven to remove the water. The catalyst was then subsequently calcined in air for a total of 6 hours. The catalyst was heated to 350°C over the first two hours, and then left at 350°C for the remaining 4 hours. In addition, the catalyst was reduced in hydrogen flow at 350°C prior to each experiment.

The silver-palladium Y zeolite was prepared in a similar manner using the incipient wetness technique. The silver was added to the 0.025 wt% Pd-Y zeolite using silver nitrate. The point of incipient wetness of the catalyst was assumed to be the same as determined previously. The catalyst was dried and calcined in the same manner as the 0.025 wt% Pd-Y zeolite. Loadings of 0.01 wt% Ag, 0.025 wt% Ag, and 0.100 wt% Ag on 0.025 wt% Pd-Y zeolite were prepared.

2.3 Catalyst Pretreatment

Before each experiment, the catalyst was pretreated in order to remove impurities from the catalyst surface. For the parent NaOH Y-zeolite, the catalyst was pretreated in helium to remove any adsorbed water. The catalyst was loaded into the reactor, and allowed to sit in a helium flow of 30 sccm for 2 hours at 250°C. For the metal loaded catalyst, the catalyst was reduced in hydrogen to remove any oxygen

from the surface of the metal and to ensure that the metal is completely reduced. The catalyst is slowly ramped to 350°C at a rate of 3°C/min in a hydrogen flow of 30 sccm, and then the temperature of 350°C is maintained for an additional 2 hours.

2.4 Calibrations

On average the gas chromatographs undergo a full gas calibration twice a year. In addition, complete recalibrations are performed any time the units have any types of repairs or reconditioning. An set of calibrations can be seen in Appendix A. In addition, the calibrations are always referenced to previous experiments for continuity from experiment to experiment. The calibration mixture is prepared very similar to the procedure described for the experimental feeds. A precise calculation of the mixture composition is necessary; however, it is not necessary to have a specific mixture, but a very well defined mixture. Typically, three gases are calibrated per mixture, with the compositions being varied four to five times in order to produce an accurate calibration line. Calibrations were performed over the typical compositions seen during the experiments. For example, if carbon monoxide is usually produced in the 3% to 10% range, it is better to have a calibration that covers 1% to 20% rather than one that covers 1% to 80%.

2.5 Definitions

Two basic assumptions in the calculations are:

a) Ideal gas law is applicable

b) Feed and exit conditions are at ambient temperature and pressure.

The definitions of conversion, selectivity, and yield for the system are as follows:

1)

$$CH_4\ Conversion = \left[\frac{(molar\ flow\ of\ CH_4\ in\ feed) - (molar\ flow\ of\ CH_4\ in\ effluent)}{molar\ flow\ of\ CH_4\ in\ feed}\right] \times 100\%$$

2)

$$O_2\ Conversion = \left[\frac{(molar\ flow\ of\ O_2\ in\ feed) - (molar\ flow\ of\ O_2\ in\ effluent)}{molar\ flow\ of\ O_2\ in\ feed}\right] \times 100\%$$

3)

$$H_2\ Conversion = \left[\frac{(molar\ flow\ of\ H_2\ in\ feed) - (molar\ flow\ of\ H_2\ in\ effluent)}{molar\ flow\ of\ H_2\ in\ feed}\right] \times 100\%$$

Note: In almost all cases, hydrogen is produced from methane, resulting in a net production of hydrogen. Thus if the value of equation 3 is negative then there was a net creation of hydrogen from the reaction.

4)

$$C_2H_6\ Selectivity = 2 \times \left[\frac{(moles\ of\ C_2H_6\ in\ effluent) - (moles\ of\ C_2H_6\ in\ feed)}{moles\ of\ CH_4\ converted}\right] \times 100\%$$

5)

$$C_2H_4\ Selectivity = 2 \times \left[\frac{(moles\ of\ C_2H_4\ in\ effluent) - (moles\ of\ C_2H_4\ in\ feed)}{moles\ of\ CH_4\ converted}\right] \times 100\%$$

6)

$$C_2H_2\ Selectivity = 2 \times \left[\frac{(moles\ of\ C_2H_2\ in\ effluent) - (moles\ of\ C_2H_2\ in\ feed)}{moles\ of\ CH_4\ converted}\right] \times 100\%$$

7)

$$H_2\ Selectivity = 0.5 \times \left[\frac{(moles\ of\ H_2\ in\ effluent) - (moles\ of\ H_2\ in\ feed)}{moles\ of\ CH_4\ converted}\right] \times 100\%$$

8)

$$CO\ Selectivity = \left[\frac{(moles\ of\ CO\ in\ effluent) - (moles\ of\ CO\ in\ feed)}{moles\ of\ CH_4\ converted}\right] \times 100\%$$

9)

$$C_2\ Yield = \left(\frac{CH_4\ Conversion}{100}\right) \times \sum(C_2H_6, C_2H_4, C_2H_2\ selectivities)$$

10)

$$H_2\ Yield = \left(\frac{CH_4\ Conversion}{100}\right) \times H_2\ Selectivity$$

11)

$$CO\ Yield = \left(\frac{CH_4\ Conversion}{100}\right) \times CO\ Selectivity$$

2.6 Reproducibility/Propagation of Error

The dc plasma system has excellent reproducibility of results when operating under a stable streamer discharge. Figure 2.4 shows both the reproducibility of the prepared NaOH Y zeolite and of the dc plasma system. The catalysts and experiments were prepared and performed years apart and still show no statistically different results. The error propagation analysis of the results has been performed and can be seen in Appendix B.

2.7 Transmission Electron Microscopy

A transmission electron microscope was utilized in order to determine the particle size and distribution of the various prepared catalysts. It is necessary to prepare transmission grids containing the sample for the microscope. The grids were prepared by grinding the sample catalyst into as fine as powder as possible using a mortar and pestle. Next, a dilute solution of the powder and ethanol was prepared. The mixture is sonicated in an ultra-sonic bath to help disperse the particles. It is important that the solid concentration be low so that the solid does not form a thick

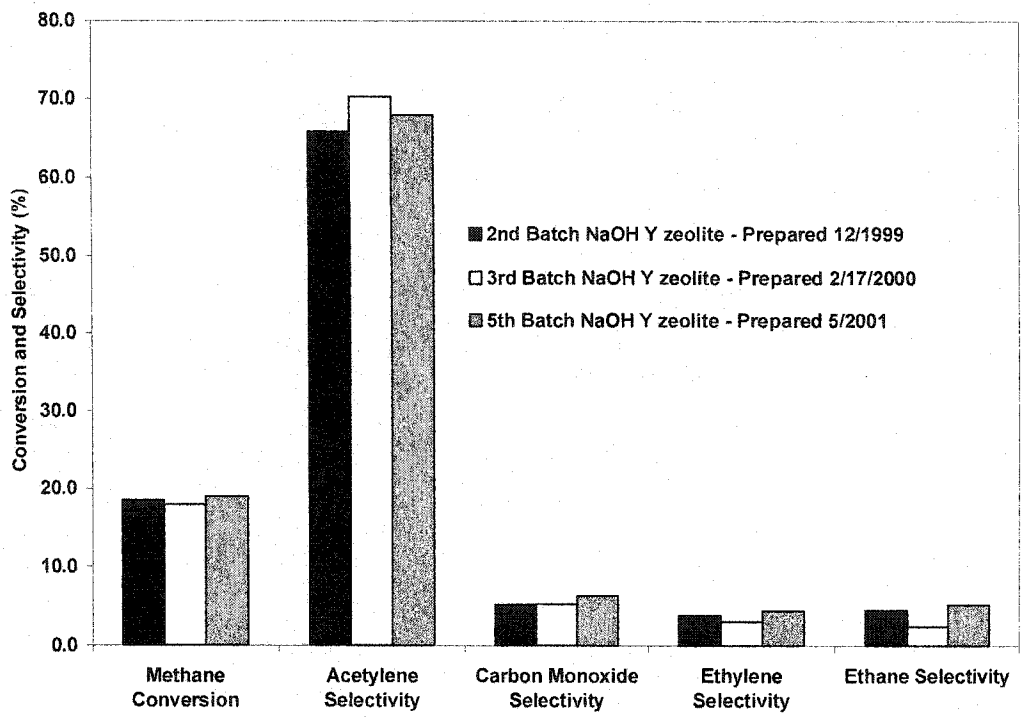

Figure 2.4 Comparison of different batches of prepared NaOH Y zeolite. 2/1 H_2/CH_4 with 2% O_2, 10 kV, 0 psig, 25°C

layer on the grid. A drop of the solution is placed on the grid and the ethanol is allowed to evaporate. The resulting grid is ready for analysis by TEM. The TEM used was a JEOL 2000-FX.

2.8 Infrared Temperature Camera

An IR Thermal Imaging and Measurement System model 600 by Inframetrics, Inc was used to monitor the reaction temperature. For these experiments, an IR-transparent sapphire tube was substituted for the quartz tube. A six inch long sapphire tube with an I.D. of 8 mm and O.D. of 10 mm was obtained from Saint-Gobain Crystals & Detectors. The emittance of the camera was adjusted by calibrating with a thermal mass of known temperature. The menu allows for the variance of the emittance from 0 to 1. The emittance of our system was determined to be 0.53. Once the camera is focused, the output of the camera can be monitored on a display. The temperature of point, line, or area can be displayed. It is important to keep the camera reservoir filled with liquid nitrogen so that the readings and operation of the camera are accurate.

2.9 Literature Cited

1. Liu, C.J., R.G. Mallinson and L.L. Lobban, *Nonoxidative methane conversion to acetylene over zeolite in a low temperature plasma.* Journal of catalysis, 1998. **179**: p. 326-334.

2. Gordon, C.L., L.L. Lobban and R.G. Mallinson, *The production of hydrogen from methane using tubular plasma reactors*, in *Advances in hydrogen energy*, C. Gregoire-Padro, Editor. 2000, Kulmer.

3. Liu, C.-J., A. Marafee, B.J. Hill, G. Xu, R.G. Mallinson and L.L. Lobban, *Oxidative coupling of methane with ac and dc corona discharge.* Industrial & Engineering Chemistry Research, 1996. **35**(10): p. 3295-3301.

4. Marafee, A., C.-J. Liu, G. Xu, R.G. Mallinson and L.L. Lobban, *An experimental study on the oxidative coupling of methane in a direct current corona discharge reactor over Sr/La2O3 catalyst.* Industrial & Engineering Chemistry Research, 1997. **36**: p. 632-637.

5. Gordon, C.L., L.L. Lobban and R.G. Mallinson, *Selective hydrogenation of acetylene to ethylene during the conversion of methane in a catalytic dc plasma reactor*, in *Natural Gas Conversion VI*, J.J. Spivey, E. Iglesia, and T.H. Fleisch, Editors. 2001, Elsevier Science: Amsterdam. p. 271-276.

6. Gordon, C.L., L.L. Lobban and R.G. Mallinson, *Ethylene production using a Pd and Ag-Pd Y-zeolite catalyst in a dc plasma reactor.* Catalysts Today, 2002. in progress.

CHAPTER 3 - Stability

3.1 Introduction

It is thought that methane will play an important role in the energy and chemical industries of the future. Methane is the "greenest" carbon based source of energy. The conversion of methane via steam reforming can result in four molecules of hydrogen for every molecule of carbon dioxide produced (including the water gas shift reaction). However, typical methane conversion processes require an intensive energy input to drive the endothermic reaction.

Plasma reactors have shown to be an effective method for the conversion of methane. Acetylene and carbon black have been produced via an arc discharge for many years. The primary drawbacks to these reactors is the high energy input and

"low–value" heat that leaves the process, as well as the excessive carbon formation. It is desired to have a process with less thermal waste, as well as production of products with a greater end-value.

Cold plasmas have shown to be capable of converting methane to a variety of different products. Cold plasmas are characterized by energetic electrons that exist at high temperatures while the bulk gas temperature remains low (less than 100°C) Thanyachotpaiboon [1] et al. showed that an ac dielectric barrier discharge is capable of converting pure methane directly to higher hydrocarbons, such as ethane, ethylene, propane, and butane. Larkin [2] et al. have shown that an ac dielectric barrier discharge is capable of the partial oxidation of methane to organic oxygenates. However, the energy efficiency of the dielectric barrier discharge reactors used in those cases have hindered their progress.

The ac tubular reactor and dc tubular reactor have significantly better energy efficiency, as well as high selectivities toward desired products. The dc plasma system has been shown to be an effective process for the conversion of methane to acetylene. The dc plasma system operates around 65°C which reduces the amount of heat that is wasted as unrecoverable energy. In addition, the primary product is acetylene and not other undesired products, such as carbon dioxide and water. The initial studies of the process used helium and oxygen to help stabilize the process. Helium is impractical as a feedstock in industrial applications. In addition, it is desired to operate without oxygen because oxygen is expensive to generate and its conversion results in the production of less desired products: carbon dioxide, carbon

monoxide, and water. Unfortunately, with oxygen removed, the tendency to form carbon increases. Carbon is an undesired by-product and carbon deposits have been found to destabilize the dc plasma system.

It has been known that the creation and stabilization of the streamer discharge is a key component of the dc plasma system. Liu [3] et al. found that the presence of a metal oxide catalyst enhanced the conversion and selectivity within the plasma system. It was hypothesized that the OH groups within the metal oxide catalyst played an important part in the mechanism of conversion and selectivity. In addition, the effect of various zeolites was studied within the dc plasma system. It was thought that the zeolites, contain numerous hydroxyl sites, would lead to the enhancement of the plasma. However, it was concluded that only certain zeolites, basic catalysts, were effective in sustaining the discharge under those conditions.

Understanding the role of the material as it helps create the discharge and stabilize the discharge is a crucial piece in the development of the dc plasma discharge. In general, the desired results occurred while there was a presence of both a material and streamer discharge. Likewise, the arc discharge and the absence of a material resulted in low conversion and low product selectivities. It is therefore desirable to determine what role, if any, the material and/or the type of discharge had on the dc plasma system.

3.2 Experimental Procedure

The experimental apparatus is similar to the system that has been described previously [4]. The feed gases consisted of a combination of methane, oxygen, hydrogen, and helium. Helium was only used in initial experiments and for characterization studies of the catalyst. The feed gas flowrates were controlled by Porter mass flow controllers, model 201. The feed gases flowed axially down the reactor tube. The reactor is a quartz tube with a 9.0 mm O.D. and an I.D. of either 4.5 mm or 7.0 mm. The configuration of the reactor can be seen in Figure 2.2.

The reactor's electrode configuration consists of a point to plane geometry, meaning that the top electrode is a wire point electrode and the bottom electrode is a flat perforated plate that also serves as a support for the catalyst. The top electrode is positioned concentrically within the reactor, and the gap between its tip and the plate is 8.0 mm and both are made of steel.

The catalyst or material is loaded from the top onto the flat plate electrode. A stainless steel wire cloth is placed between the electrode and catalyst in order to prevent the catalyst from falling through the holes on the electrode plate. Another stainless steel wire cloth is placed on top of the catalyst in order to prevent the movement of the catalyst. Due to the electrostatic nature of the zeolites and the plasma itself, this top screen is necessary to keep the catalyst bed uniform. The preparation and characterization of these zeolites has been discussed elsewhere [5, 6]. The glass beads were obtained from Aldrich in bead sizes varying in mesh size from 20 to 200. Plexiglas shavings were made from sheets of Plexiglas, and chopped and crushed in the laboratory. The shavings were not sifted, and the resulting material

ranged from fine .2mm particles to almost 1 mm shavings. The dc corona discharge is created using a high voltage power supply (Model 210-50R, Bertan Associates Inc.).

As mentioned before, this system operates at low temperatures. A furnace around the reactor is used to heat the system to the desired temperature. The temperature is measured by an Omega K-type thermocouple that is attached to the outside of the reactor near the catalyst bed. The temperature measured on the outside has been calibrated against the internal temperature of the reactor, and has been discussed elsewhere [5, 6]. However, when the desired operating temperature is below 373 K it is necessary to use cooling air to control the temperature since the plasma itself does heat the gas to some extent. The system pressure is varied between 0.1 and 0.3 kPa, depending on the experiment. The pressure is controlled using a GO back pressure regulator.

In some experiments, it was desired to measure the temperature inside the reactor tube. For these experiments an infrared camera was used. An IR Thermal Imaging and Measurement System model 600 by Inframetrics, Inc was used to monitor the temperature. For these experiments, an IR-transparent sapphire tube was substituted for the quartz tube. A six inch long sapphire tube with an I.D. of 8 mm and O.D. of 10 mm was obtained from Saint-Gobain Crystals & Detectors. The emittance of the camera was adjusted by calibrating with a thermal mass of known temperature within the sapphire tube. The menu allows for the variance of the

emittance from 0 to 1. The emittance of our system was determined to be 0.53. Once the camera is focused, the output of the camera can be monitored on a display.

In some cases it was necessary to look solely at the behavior of the catalyst. To study the catalyst-only effects (without plasma present), two reactors were used in series. The first reactor was used to create a "typical" product distribution using the normal plasma method. The effluent from the first reactor was then used as the feed stream for the second reactor. The second reactor was operated without plasma at a temperature controlled using the furnace. This allowed for more precise control and understanding of the catalytic effects.

The product gases are passed through a dry ice/acetone bath that allows for any condensable organic liquids to be separated from the product gases. It should be noted that the dc system produced no measurable liquids, including water. The effluent gases can be analyzed on-line by either a gas chromatograph or a mass spectrometer. The gas chromatograph is a CARLE series 400 AGC (EG&G) gas chromatograph equipped with a hydrogen transfer system to separate the hydrogen; a HayeSep column to separate carbon dioxide, ethane, ethylene, and acetylene; and a molecular sieve column to separate oxygen, nitrogen, methane, and carbon monoxide. A thermal conductivity detector (TCD) was used to quantify the separated products. Also, a MKS mass spectrometer is used for on-line analysis of the products and for temperature programmed oxidation of carbon deposited on the catalyst.

3.3 Results and Discussion

The dc plasma system has shown to be an effective process for the conversion of methane to acetylene, hydrogen, and carbon monoxide [4]. However, the current research has shown that it is necessary to sustain a stable streamer discharge for high methane conversion and product selectivities. In addition, the system also requires certain conditions to reduce carbon formation that leads to a change in the type of discharge from the streamer discharge to an arc discharge. Thus, a stable and successful experiment has at least two necessary conditions:

1.) creation of a stable streamer discharge

2.) minimal carbon formation (excessive carbon formation destabilizes the desired streamer discharge and leads to an arc discharge)

3.3.1 Effect of different discharges

Description of the three different types of discharges seen in the dc plasma system are illustrated in Figure 3.1. The process is considered stable if either an "active streamer" or "streamer" discharge is present. An "arc" discharge is considered unstable. The terms stable and unstable discharges also describe differences in the chemistry that are observed. A stable discharge (either active streamer or streamer) results in a significantly higher methane conversion, as well as a high selectivity to acetylene, hydrogen, and carbon monoxide. On the other hand, an unstable discharge has been found to result in low methane conversion and the predominant product is ethane.

In this system, it has been found that results were substantially enhanced by the presence of solid particles exhibiting long term stable operation at high conversion with primarily acetylene as a product [3]. Early studies [7] speculated that

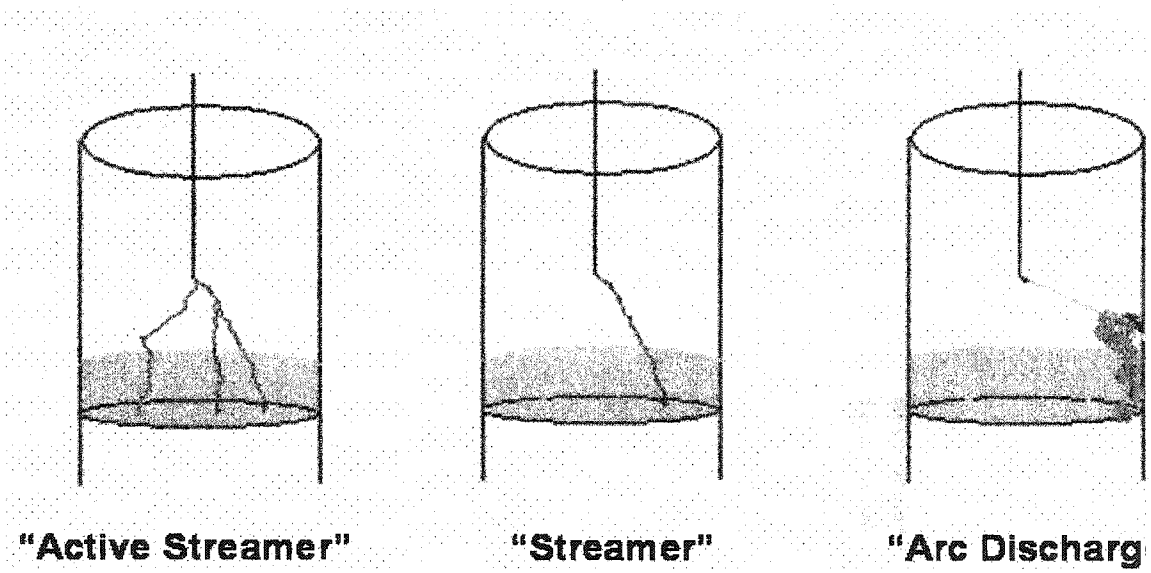

Figure 3.1 Characterization of the different types of discharges that occur within the dc plasma system.

a catalyst (with active sites available for some type of surface chemistry) within the discharge was necessary for both the creation of the streamer discharge and high conversion of the methane and product selectivities. The exact role of the material was unknown, but it was speculated that acidic catalysts led to excess carbon formation. In addition, basic catalysts with OH groups were thought to enhance the breakdown discharge. Further experiments showed that in the absence of a catalyst the discharge was unstable. Carbon deposits formed rapidly and an arc discharge appeared leading to low conversion and ethane as the primary product.

Figure 3.2 shows the effect of different catalysts loadings on the reactor chemistry. Without a catalyst charged into the reactor, the methane conversion is low and the major C_2 product is ethane. However, with catalyst present, the conversion increases dramatically and the major C_2 product becomes acetylene. The hydrogen selectivity also increases. In addition to the presence of the catalyst, a major difference in the experiments was the type of discharge present. With catalyst loaded into the system, the discharge is established near 6.5 kV and remains stable as long as certain feed requirements are met (to be discussed later). The system without catalyst requires a much higher voltage to create a breakdown, and the subsequent discharge is a streamer discharge which changes to an arc discharge typically within 15 minutes. The "no catalyst" results of Figure 3.2 were measured after the arc discharge occurred. It is unclear whether the "streamer discharges" or the catalyst was responsible for the desired results of high conversion and selectivity.

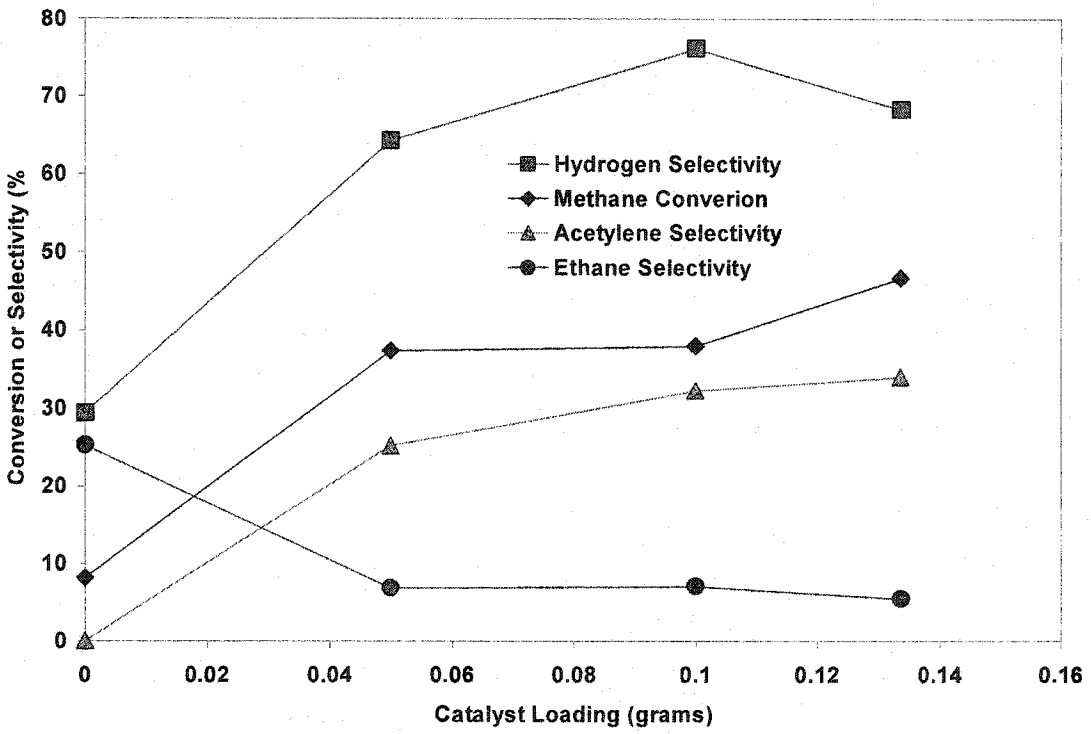

Figure 3.2 Effect of various catalysts loadings on the methane conversion and product selectivity. 2/1 H_2/CH_4 with 2% O2, NaY zeolite, 25°C, 0 psig.

In most cases, the discharge in the empty reactor quickly transforms from the streamer discharge to the arc discharge within 15 minutes because of excess carbon formation on the reactor walls. On occasion, the streamer discharge may persist for an extended period of time, 30-45 minutes. Thus, it was possible to obtain a GC sample in the short time before the carbon formation led to the arc discharge. The results indicate that there is no qualitative difference between the chemistry that occurs with and without catalyst while stable streamer discharges are present. In addition, several experiments were performed with "inert" materials, such as Plexiglas, Teflon, and glass beads. All these materials were capable of producing stable streamer discharges for extended periods of time (minimum 3 hours) and were also effective in producing the desired high methane conversion and selectivities. Figure 3.3 shows the results of various materials within the dc plasma system, all under stable streamer operation.

Thus, it is apparently not necessary to have a material with catalytic activity present in order to achieve a stable streamer discharge or high methane conversion and product selectivities. This indicates it is the type of discharge that is occurring that results in the different methane conversions and product selectivities. What is different between the two discharges that results in such discrepancies in the effluent stream?

The normal streamer discharge spans the entire gap between the top and bottom electrode. However, the arc discharge originates at the tip electrode, and typically terminates where carbon is deposited on the reactor wall. The deposited

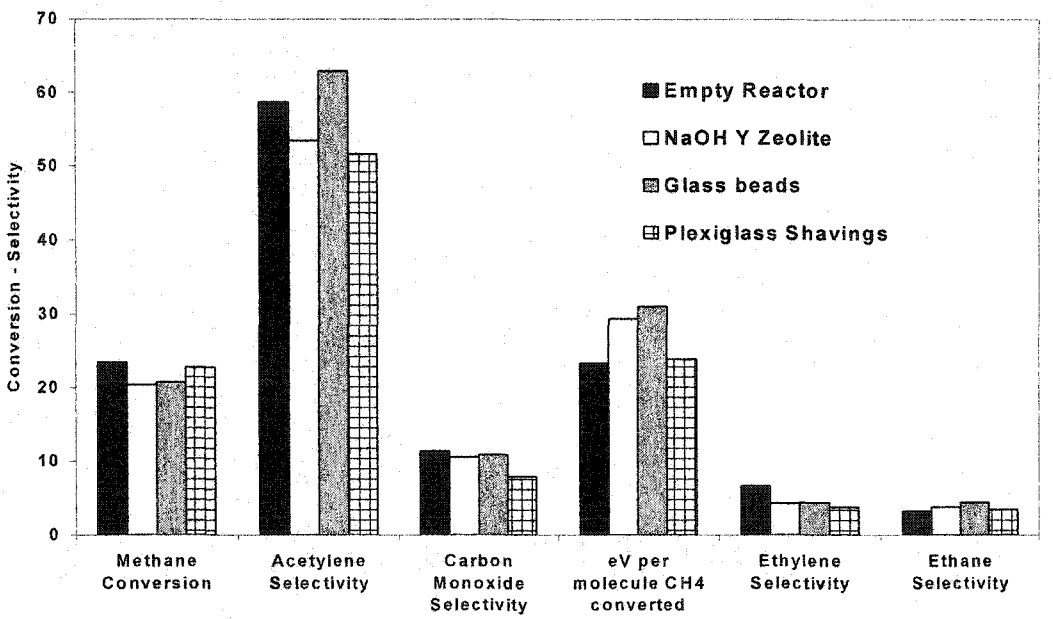

Figure 3.3. Effect of different materials in the reactor on the conversion and product selectivity with a stable discharge. 2/1 H_2/CH_4 with 2% oxygen, 32 sccm, 0 psig, 3mm bed height if applicable. The empty reactor stability is short lived (15 minutes or less).

carbon then provides a conductive path to the bottom electrode. Thus, the "gap length" of the arc discharge is considerably shorter, with a length of nominally 4 mm as compared to 8 mm with the normal streamer discharge. The electric field within the two systems is different due to the different gap lengths. The energy of the electrons is determined by two parameters:

1.) the total field they are subjected to (normally the applied field)

2.) interaction with other particles.

The equation that describes the above is the Boltzman equation, which can be written as [8-10]:

$$\frac{\partial f}{\partial t} + v \bullet \frac{\partial f}{\partial x} + a \bullet \frac{\partial f}{\partial v} = \left.\frac{\partial f}{\partial t}\right|_c \qquad \text{Equation 3.1}$$

The Boltzman equation describes the change in the electron energy distribution function (EEDF) f(x,v,t) as a function of space (x), velocity (v), and time (t) due to collisions with particles. The Boltzman equation solves for the electron energy distribution of the system. The electron energy distribution function may then be used to calculate the reaction rate of the various processes (such as excitation, dissociation, and ionization). In order to determine the reaction rate coefficients, two items must be known:

1.) electron energy distribution function (EEDF)

2.) cross section for the various processes

Once the cross section is known as a function of energy, it along with the EEDF may be used to solve for the reaction rate coefficients by the following equation[8, 11, 12].

$$r = < v\sigma >_f = \int_0^\infty v \bullet \sigma \bullet f(\varepsilon) d\varepsilon \qquad \text{Equation 3.2}$$

By following this basic procedure, Bolsig software can solve for the reaction rates of processes within the system [13]. The software uses a database of cross sectional areas for the various gases. The reaction rates can then be normalized by multiplying the reaction rate by the energy requirement for each reaction. The total energy may then be summed and normalized to provide an energy distribution of the amount of energy directed toward different processes as a function of reduced electric field.

The reduced electric field is dependent on the breakdown voltage, gas gap, and pressure of the system; and the reduced electric field has units of volts/cm/torr, given in Equation 3.3.

$$E/P = \frac{breakdown\ voltage}{electrode\ gap * system\ pressure} \qquad \text{Equation 3.3}$$

Larkin et al. [2] showed that the product selectivities were heavily dependent on the reduced electric field (E/P) of the ac dielectric barrier discharge reactor.

The reduced electric field plays an important role in the average electron energy, as well as the amount of energy that is deposited into the various collision processes. For the range of reduced electric fields encountered in the lab (E/P = 5 to 70), over 95% of the energy is in the form of the inelastic group process. Thus, the processes of elastic collisions (no transfer of energy), ionization (increases with E/P,

though still small in highest E/P), and attachment may be ignored. Within the inelastic group processes the excitation and dissociation are the two major processes that consume the energy.

Larkin et al. found that the ac dielectric barrier discharge produced organic oxygenates at high values of E/P (25-40 volt/cm/torr), while the system favored C_2 production at low E/P (less than 25). The organic oxygenates were associated with large fractions of the energy input into the system being directed toward the dissociation of oxygen. On the other hand, ethane and acetylene production were associated with the increase in the amount of energy that goes into methane and oxygen excitation at lower reduced fields, respectively. Further analysis of the work, coupled with information from a planar ac dielectric barrier discharge reactor, and results from the dc plasma system showed that the C_2 production may be better explained through the excitation and dissociation of methane alone.

Figures 3.4-3.8 show how the reduced electric field affects the percentage of energy that is input into the various inelastic methane processes and how the selectivity varies with E/P. Figure 3.4 shows the methane group processes for a pure methane system. Figure 3.5 describes the group processes of a 2/1 CH_4/O_2 system and the selectivity data of Larkin et al. in an ac cylindrical DBD reactor. Figure 3.6, 3.7, and 3.8 depict the inelastic methane processes and selectivity data of the dc plasma reactor in a 1/1/8 CH_4/H_2/He and 2% O_2 feed, 1/1 H_2/CH_4 with 2% O_2 feed, and a 2/1 H_2/CH_4 with 2% O_2 feed, respectively.

The ac planar DBD reactor used by Thanyachotpaiboon et al. [1] consisted of a pure methane feed. In addition, the small gas gaps between the electrodes and high breakdown voltages of the system resulted in a operating range of 45-75 volts/cm/torr for the reduced electric field. The primary products of the system were alkanes, with very little production of olefins. Ethane was the primary alkane product with some production of propane and butane. Figure 3.4 shows that the reduced electric field dictates how the energy that is input is directed in a pure methane system. Most of the energy (70%) is deposited into methane dissociation, which suggests that methane dissociation could be primarily responsible for the formation of ethane. This reactor configuration also extremely inefficient as far as energy requirements, because it requires high power and long residence times (up to 1-2 minutes). Equation 3.4 and 3.5 depict the mechanism for the production of ethane.

$$CH_4 + e \rightarrow CH_3 + H \qquad \text{Equation 3.4}$$

$$2CH_3 \rightarrow C_2H_6 \qquad \text{Equation 3.5}$$

Unlike the ac planar system, the ac cylindrical system used by Larkin et al. produced both ethane and acetylene. However, there were two major differences of the ac cylindrical system as compared to the ac planar system. The cylindrical system used high partial pressures of oxygen (2/1 CH_4/O_2), and in general operated at lower reduced fields. Figure 3.5 shows the selectivity data obtained by Larkin and the fraction of energy that is directed toward methane excitation and dissociation processes for various reduced electric fields. Even at the lowest E/P, the summation of the C_2 selectivity was still relatively low (26% total C_2). This low percentage was

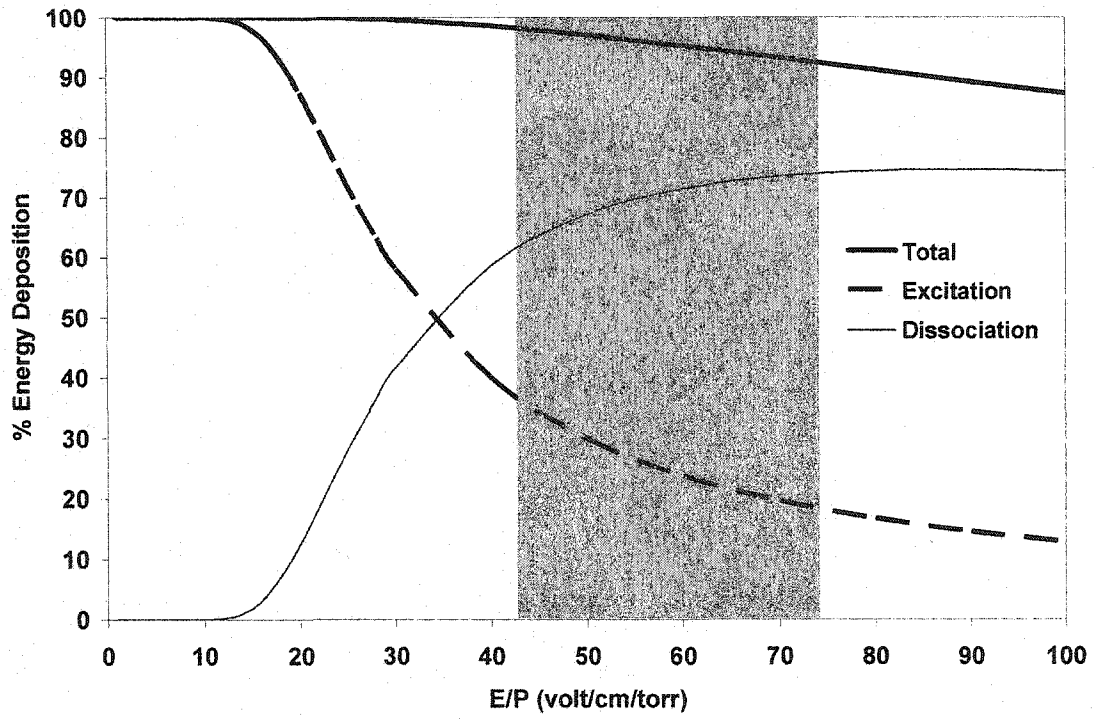

Figure 3.4. Effect of the reduced electric field (E/P) on the percentage of energy deposited into the inelastic group process (excitation and dissociation) of a pure methane system.

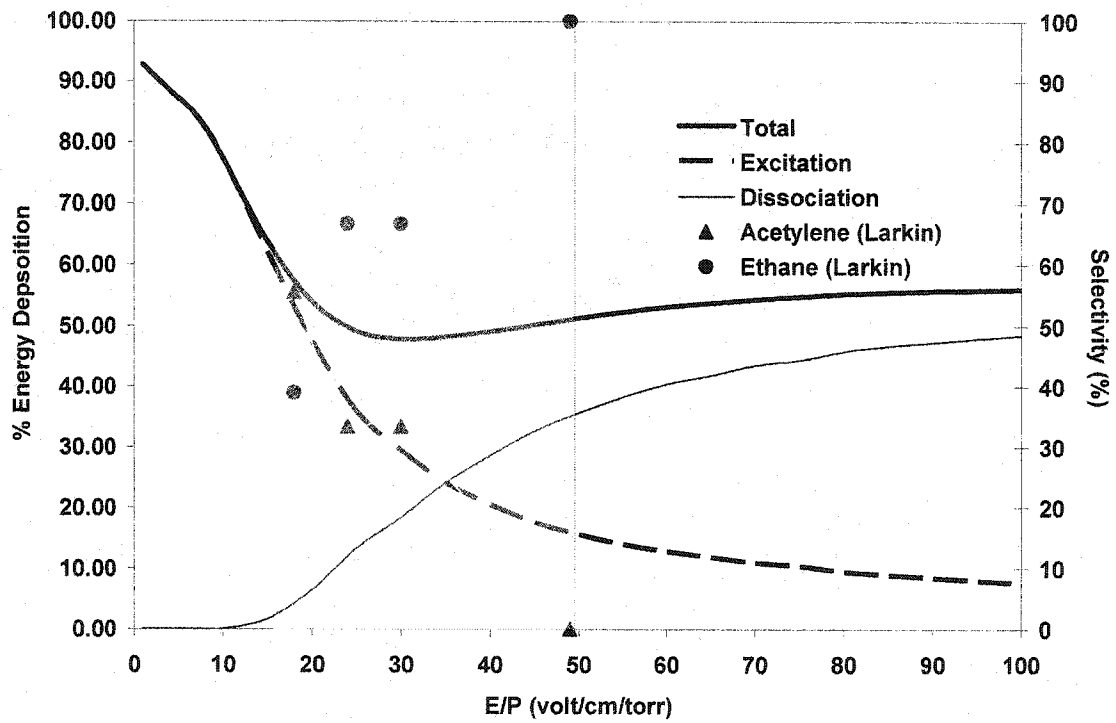

Figure 3.5. Effect of the reduced electric field (E/P) on the percentage of energy deposited into the inelastic group process (excitation and dissociation) of a 2/1 CH_4/O_2 system. Overlaid is the C_2 selectivity data of Larkin et al.

presumably due to the large amount of oxygen available for the production of CO_x in addition to the organic oxygenates, though the oxygenate production was dropping rapidly with decreasing E/P. Thus, the selectivity data presented in Figure 3.5 is normalized to the total C_2 production.

Ethane was the only C_2 produced at an E/P of 49 volts/cm/torr, which was the highest value E/P where C_2's were detected. As the E/P decreased, the acetylene selectivity increased while the ethane selectivity decreased. Larkin et al. associated the decrease in ethane production with the decrease in the amount of energy that is directed toward methane dissociation as the E/P is reduced. It is believed that this is the correct reaction pathway for the production of ethane as it directly compares to the ethane production found in the ac planar reactor which produces alkanes at high E/P's. The acetylene production was associated with the increase in oxygen excitation which increases over the same range that the acetylene selectivity increases. A leading factor of this theory was that the ac planar system, which had no oxygen excitation (no oxygen in the system), produced very little acetylene. However, this does not help to explain why the major C_2 product within the dc plasma system is acetylene.

The dc plasma system uses small concentrations of oxygen ($2/1 H_2/CH_4$ with 2% O_2), but it is highly unlikely that the 2% oxygen could contribute to yields of acetylene upwards of 50%. Therefore, it is likely that another process is responsible for the increased production of acetylene as the E/P is reduced for both the ac cylindrical reactor and the dc plasma reactor. The fraction of energy deposited into

oxygen excitation increases as the E/P is decreased; however, the fraction of energy directed toward the excitation of methane increases over the same range. It is believed that the mechanism of acetylene production and high conversion is through the excitation of the methane, because varying the oxygen concentration on the feed (from 0.5 to 5% oxygen) does not result in an increased methane conversion.

Figures 3.6, 3.7, and 3.8 show the effect of the E/P on the amount of energy that goes into the inelastic methane processes, as well as the acetylene and ethane selectivity data from the dc plasma system for a 1/1/8 CH_4/H_2/He and 2% O_2 feed, 1/1 H_2/CH_4 with 2% O_2 feed, and a 2/1 H_2/CH_4 with 2% O_2 feed, respectively. The E/P was adjusted in two different ways; by varying the gap height and by changing the operating pressure of the system. The three feed conditions vary significantly yet all three follow the same trend. As the E/P is reduced, the acetylene selectivity increases as the fraction of energy directed to methane excitation increases. Conversely, as the E/P is reduced, the selectivity toward ethane decreases since the energy directed toward methane dissociation also decreases. The lowest E/P yielded a product distribution that is almost entirely acetylene, while the highest E/P resulted in an ethane dominated product. This data correlates very well with the 'ethane only' production seen in the ac planar system and the C_2 trends seen in the ac cylindrical system.

A mechanism for the production of ethane through the dissociation of methane can be seen in Equation 3.2 and 3.3. However, the production of acetylene through the excitation of methane is more complicated. The excitation of methane

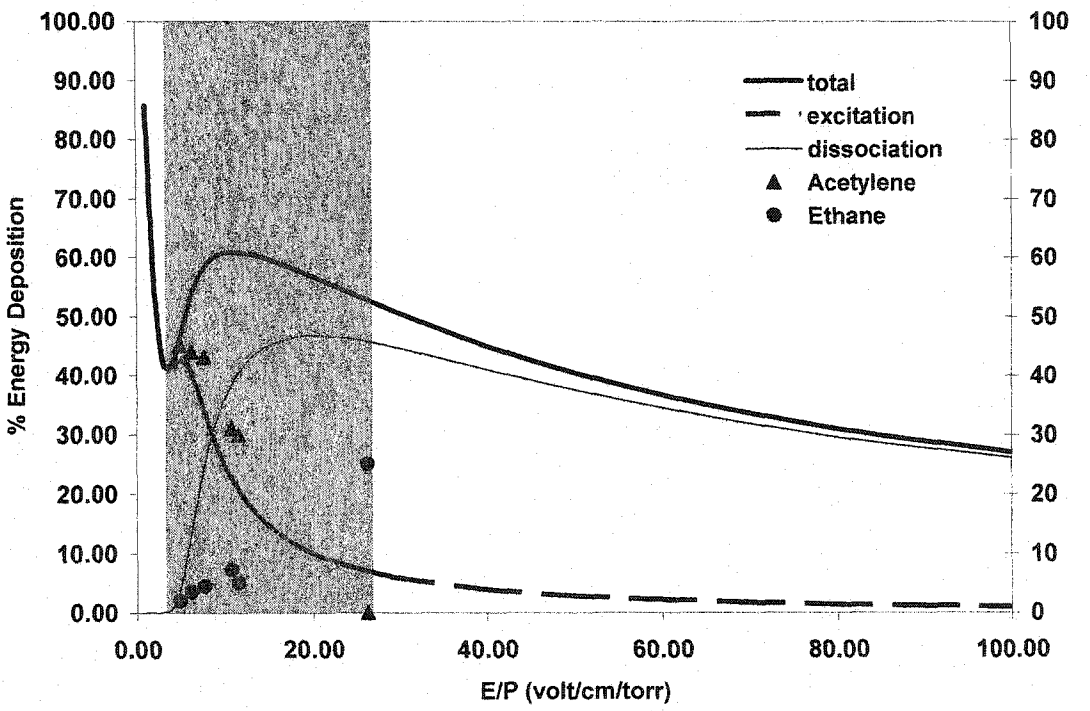

Figure 3.6. Effect of the reduced electric field (E/P) on the percentage of energy deposited into the inelastic group process (excitation and dissociation) of a 1/1/8 CH_4/H_2/He with 2% O_2 system. Overlaid is the C_2 selectivity data of dc plasma system.

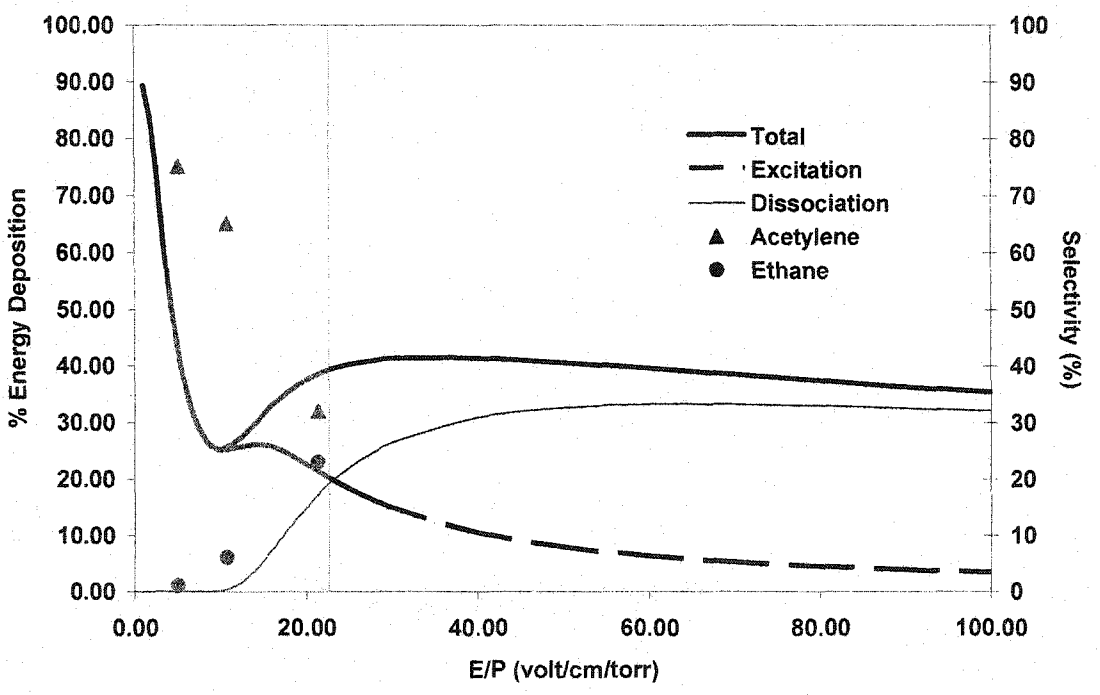

Figure 3.7. Effect of the reduced electric field (E/P) on the percentage of energy deposited into the inelastic group process (excitation and dissociation) of a 1/1 CH_4/H_2 with 2% O_2 system. Overlaid is the C_2 selectivity data of dc plasma system.

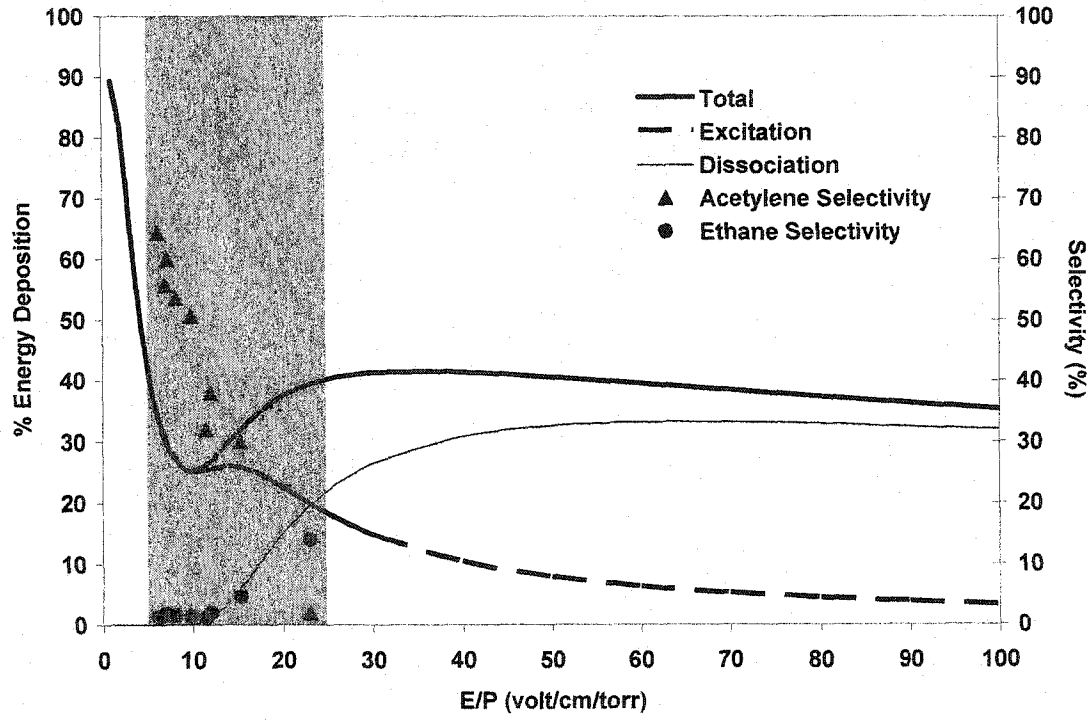

Figure 3.8. Effect of the reduced electric field (E/P) on the percentage of energy deposited into the inelastic group process (excitation and dissociation) of a 2/1 CH_4/H_2 with 2% O_2 system. Overlaid is the C_2 selectivity data of dc plasma system.

corresponds to the two levels of vibration and transitional excitation which require energies of 0.16 and 0.36 eV, respectively. It is believed that the excitation of the methane molecules allows them to overcome the activation energy to proceed to subsequent reactions. When an electron collides with a gas molecule it excites the molecule to a higher energy level and the electron loses the corresponding amount of energy [8]. The excited molecule can then initiate some reactions due to its higher internal energy. So, a reaction that may typically only occur at very high temperatures, may be initiated by an excitation collision.

The energy transferred to the methane molecule by the inelastic collision with the electron leads to the excitation of the methane molecule. This excitation of the methane molecule raises its energy to a level that may allow it to undergo other reaction pathways. Then the reaction may follow a pathway somewhat similar to the pyrolytic conversion of methane to acetylene. The energy required to drive the reactions would proceed through the excitation of the molecules by the low-level energy electrons.

The methane conversion and selectivity toward acetylene is higher at lower values of the reduced electric field where the majority of the energy is input into the system via numerous low energy electrons. On the other hand, at higher reduced fields the majority of the energy goes into electrons that have much larger electron energies, while the methane conversion is much lower and ethane is the predominate product. It is believed that these numerous excitations lead to the higher conversion of methane, as well as the subsequent reactions that lead to the formation of

acetylene. And the higher energy electrons associated with the higher reduced field are less efficient in the conversion of methane. For each molecule there is an optimum electron energy for the ionization of the species. If the electron energy is too high, there is less probability that the electron will result in the ionization of the molecule. It is hypothesized that this same theory applies to the excitation of a molecule. That is, the electrons have sufficient energy to excite the methane, but are not as efficient as the lower energy level electrons.

The methane conversion and efficiency of the system seem to also be directly related to the reduced electric field. In general the lower the reduced field the higher the methane conversion, as well as the efficiency of the system. Figure 3.9 shows the effect of reduced electric field on the dc plasma system. In addition, Figure 3.9 shows the results for the various reactors studied in the laboratory and their corresponding reduced field and efficiency. Of the four different reactors studied within the laboratory, there is a good correlation between the reduced electric field and the overall energy efficiency for the system regardless of how the electric field was achieved (geometry, pressure, power production (ac or dc).

The volume occupied by the visual aspect of the discharge is small compared to the total volume between the electrodes. Experimentally, it is known that the effective volume of the discharge is much greater than that of the immediate streamer discharge. Results show that the conversion is much higher than would be expected if bypassing of the discharge occurred in the outer volume of the reactor [4].

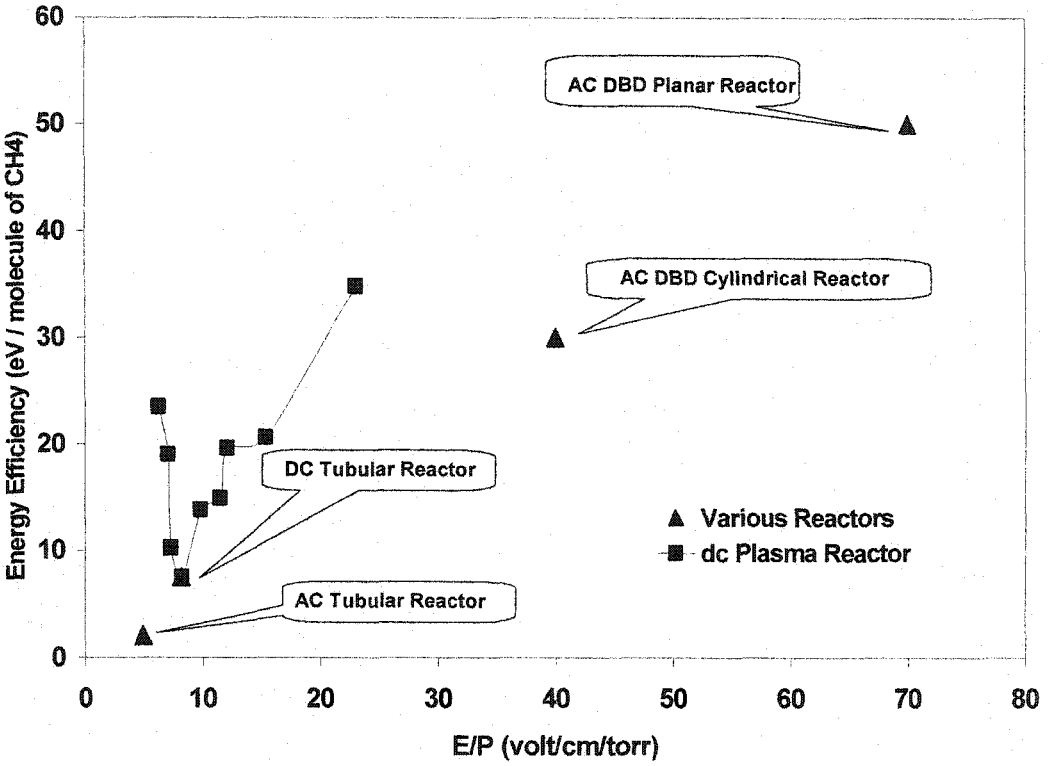

Figure 3.9. Effect of the reduced electric field (E/P) on the energy efficiency of the dc plasma reactor. Also included is the generalization of various reactors studied and their associated E/P and efficiency.

The volume of the discharge was expanded by increasing the I.D. of the reactor tube. If the discharge were only effective in transferring energy in the immediate volume of the visual discharge, then there would be no further increase in conversion associated with expanding the reactor diameter. However, the larger I.D. saw a dramatic increase in conversion at longer residence time. Thus, the added volume was not solely a bypassing zone, and is affected by the discharge zone. This can be further qualified by the use of an infrared temperature scans and planar laser induced fluorescence (PLIF) imagery.

An infrared camera was used to map the temperature profile of the discharge zone. The studies showed that the zone of higher temperature was much greater than that of just the visual zone. Figure 3.10 shows a digital image of the discharge and how the streamer only occupies a small percentage, < 5%, of the reaction zone. In comparison, Figure 3.11 shows the temperature map from the IR camera. It shows that the thermal increase is uniform throughout the reaction zone [14]. The entire reaction zone is within 10°C.

In addition, a study of the CH excitation of the system using PLIFS showed that the discharge expands wider than the visual zone. A intensified charge coupled device (ICCD) camera was then used to take an image of the fluorescence. The ICCD camera is fitted with an array of bandpass filters that allow the transmission of only the wavelengths of interest. This cuts down on background interference in the images and increases the signal to noise ration. Figure 3.12 is an image taken by a high-speed camera using a filter that captures the CH excitation within the system.

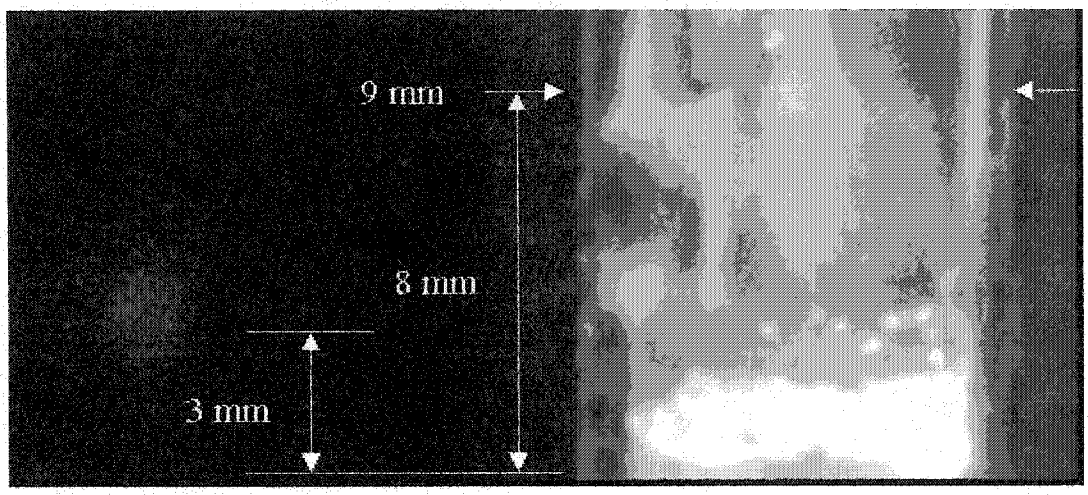

Figure 3.10 Digital image of dc plasma reactor. 3mm glass bead height. 7kV, $2/1H_2/CH_4$ with 2% O_2

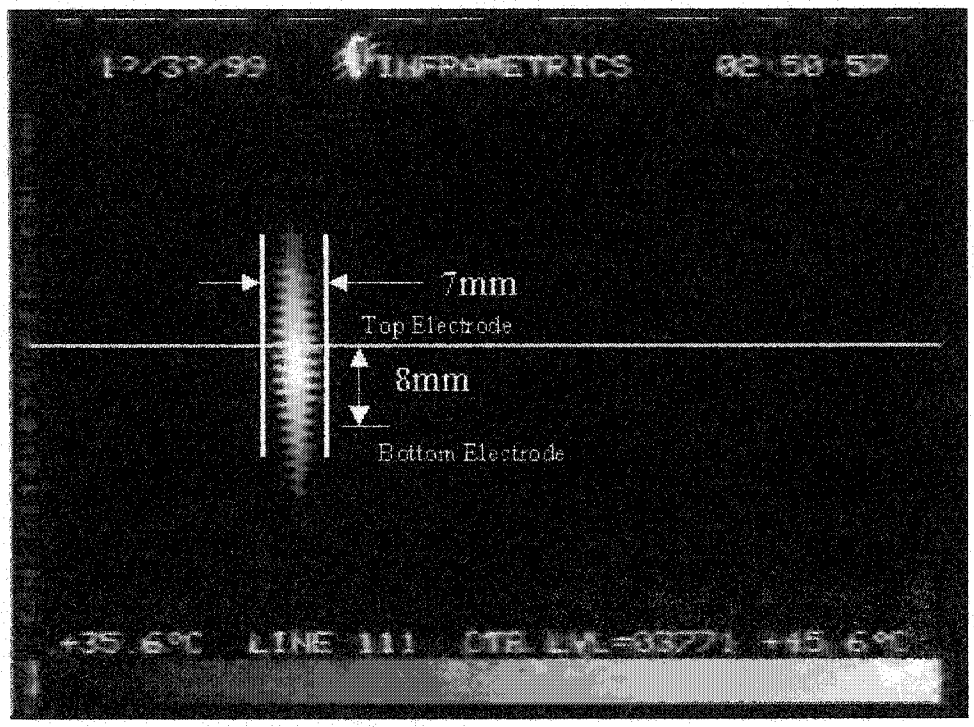

Figure 3.11 IR image of dc plasma reactor. 3mm glass bead height. 7kV, $2/1H_2/CH_4$ with 2% O_2

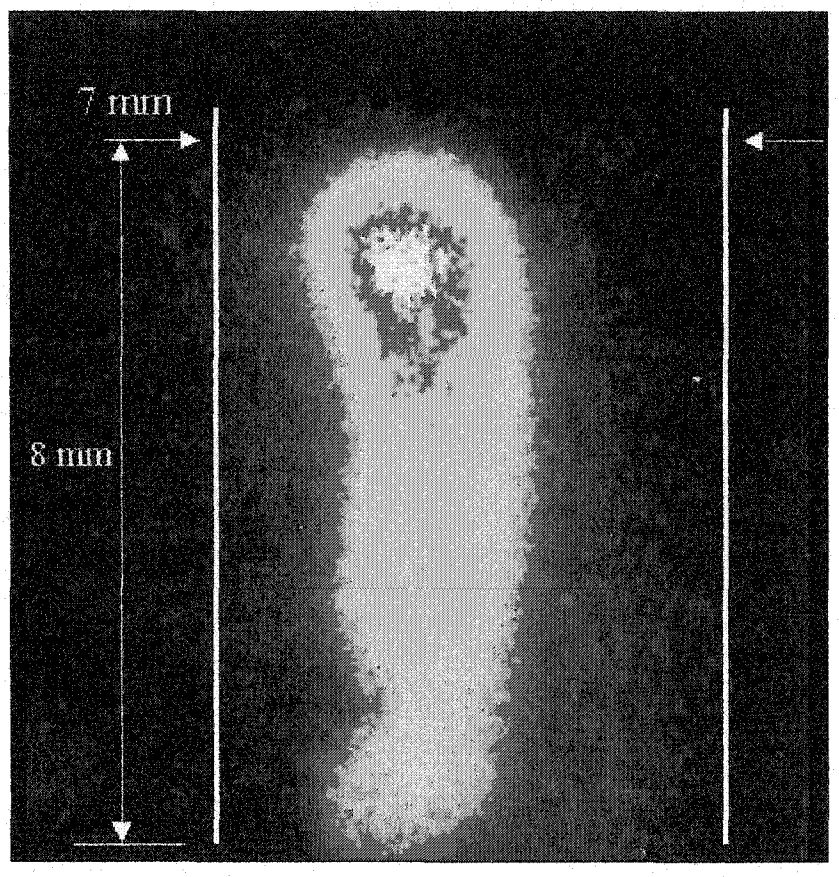

Figure 3.12 CH image form PLIFS study. 7kV, $2/1H_2/CH_4$ with 2% O_2

3.3.2 Role of material within dc plasma system

The presence of an inert material or even no material helped to clarify that active sites (or surface species) on a catalyst surface are not required for successful plasma operation and to achieve a stable streamer discharge or high methane conversion and product selectivities. Previous experiments in which the number of active sites and surface area of the catalyst were altered also showed no variation in the methane conversion or selectivity. This supports the conclusion that the catalyst has little to no catalytic role in the conversion or product selectivity. However, it doesn't help to explain why some materials [7] cause rapid destabilization of the plasma or why any material was needed to help establish the stable streamer discharge.

Previous research had shown that certain materials were ineffective for stable streamer discharge[7] under partial oxidation conditions. It was believed that a basic catalyst with a high concentration of OH groups was necessary within the plasma system. The non-acidic catalyst was thought to reduce the tendency of carbon formation, and the OH groups assisted in radical production to stabilize the streamer discharge. Recent research has shown that the catalyst can play a significant role in carbon formation. Four catalysts were studied with varying results.

NH_4Y, HY, NaY, and the commonly used (in this research) NaOH Y zeolite were studied to understand their ability to stabilize the plasma system, and their effect on carbon formation within the reactor system. NH_4Y and HY zeolite were used as they are known acidic catalysts, and NaY was used as a non-acidic catalyst for a

comparison to the prepared NaOH Y zeolite and the acidic NH_4 and HY. Results showed the NaY and NaOH Y zeolite behave similarly in the stabilization of the streamer discharge and the reaction chemistry. The HY zeolite, although acidic, performed similarly to the NaY and NaOH Y zeolite. On the other hand, NH_4Y was unsuccessful in maintaining a stable streamer discharge. Thus, there is a mechanism that allows both acidic and basic catalysts to stabilize the discharge, while at the same time causing different results between two acidic catalysts. The tendency to cause carbon formation was studied for each catalyst in order to determine the cause for the observed different behaviors.

The catalysts' abilities to crack acetylene to carbon or other products was studied at different temperatures. A feed stream containing methane, hydrogen, and acetylene was actually generated as a product stream from a plasma reactor system in series upstream. The catalysts were tested in a thermal only situation, i.e. no plasma. Each catalyst showed the ability to hydrogenate the acetylene to ethylene, even without the presence of a metal commonly used for hydrogenation [15]. Each catalyst also had the propensity to form excessive carbon during the conversion of acetylene. However, the temperature at which acetylene conversion and carbon formation occurred differed among the various catalysts. Figure 3.13 shows the effect of temperature on acetylene conversion.

The results show that NH_4 Y zeolite, the only catalyst incapable of maintaining a stable streamer discharge, has the lowest temperature at which acetylene conversion occurs. Acetylene conversion was achieved as low as 120°C on

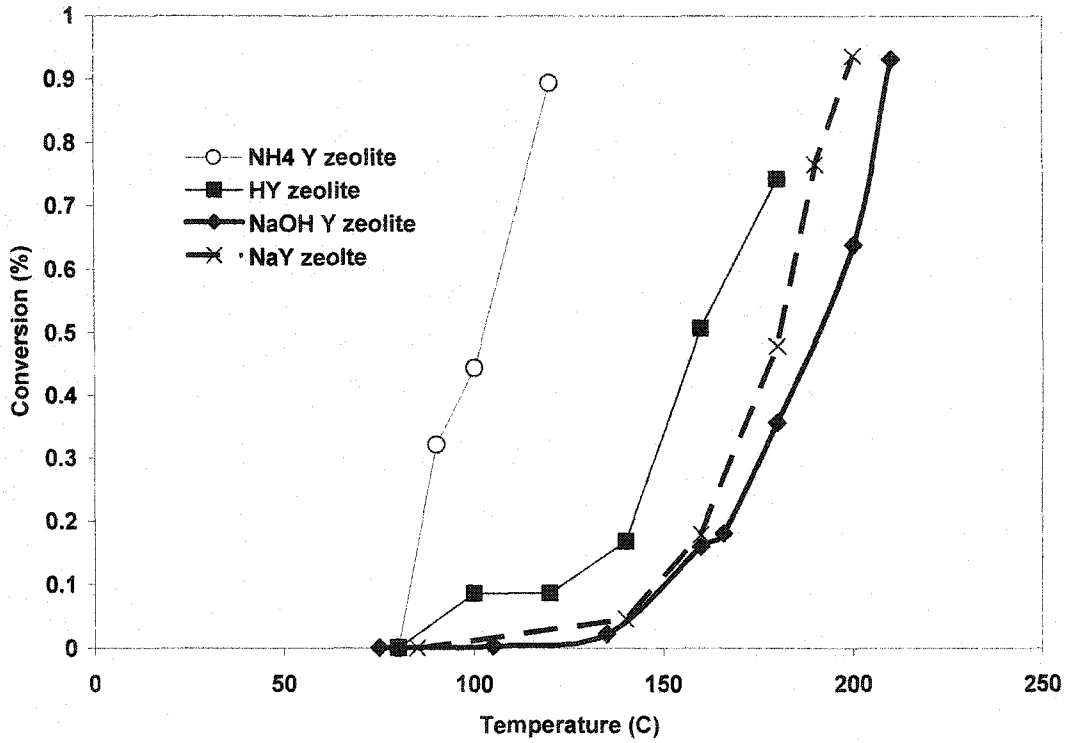

Figure 3.13. Effect of temperature on the conversion of acetylene of various catalyst.

the NH4 Y zeolite. This temperature is close to the operating temperature within the plasma. In comparison, the catalysts that yielded stable discharge systems (HY, NaY, and NaOH Y zeolite) required higher temperatures for the onset of thermal acetylene conversion; 160°C, 200°C, 200°C respectively. The NH_4 Y zeolite also produced significant amounts of carbon during the short time of stable operation in the streamer discharge. It is this carbon that is believed to be responsible for the transformation of the stable streamer discharge to the arc discharge. The formed carbon creates a conductive path that attracts the plasma discharge. This path essentially reduces the gap distance resulting in a short gap for the same applied voltage. The discharge transforms from the streamer discharge to the arc discharge. This allows for the power that is applied to the system to pass through the reactor without performing the necessary chemistry. In addition, the arc discharge is a thermal discharge that in return leads to even more carbon formation.

The destabilization of the discharge by some acidic catalysts still does not explain why the reactor behaves different with and without a material present. It was found that the presence of a material, whether it be zeolite, glass beads, or Plexiglas, allows for a significant reduction in the applied voltage that is necessary for breakdown (5-7 kV), as compared to an empty reactor (10 kV). Similarly, the voltage required to maintain the discharge is much higher when no material is present (13 kV versus 7-10 kV). The variation in the voltage between the two systems may be explained by considering the materials role as a dielectric.

Dielectric pellets have the ability to enhance a plasma discharge. When an external high voltage is applied across a gap containing dielectric pellets, the pellets become polarized and an intense electric field is formed around each pellet contact point [8, 16, 17]. In addition, the intense electric field associated with each pellet may reduce the voltage required for operation[18].

The dc plasma system before breakdown can be thought of as a capacitant system. The two electrodes have an applied potential difference between the two surfaces. The voltage difference between the two plates can be expressed in terms of the work done (force * distance) on a positive test charge (q) when it moves from the positive to negative electrode, equation 3.6 [19].

$$V = \frac{Work\ done}{charge} = \frac{F * d}{q} \qquad \text{Equation 3.6}$$

The electric field of a system is defined as the force acting on a positive charge divided by the magnitude of the charge. Thus, the electric field of a system and how it relates to the voltage can be expressed as Equation 3.7 and 3.8, respectively.

$$E = \frac{Force}{magnitude\ of\ charge} = \frac{F}{q} \qquad \text{Equation 3.7}$$

$$V = Electric\ field * distance = E * d \qquad \text{Equation 3.8}$$

The electric field, and resulting voltage, of a system can be altered by the presence of a dielectric material within the system. A dielectric material is a substance that is a poor conductor of electricity (i.e. insulator), but also an efficient supporter of electric fields. Generally, most dielectrics are solids. However, gases and liquids can also serve as dielectrics. Table 3.1 lists several dielectric materials

Table 3.1 Dielectric constants of various materials. (West, 1974)

Material	Dielectric Constant
Air	**1.00**
Plexiglas	**3.4**
Glass Beads	**5**
Water	**80.4**

and their associated dielectric constant value [20]. The dielectric constant, k, is the dimensionless factor by which the capacitance of the system increases when the dielectric material completely fills the space between the two electrodes, Equation 3.9.

$$C = \kappa * C_o \qquad \text{Equation 3.9}$$

In addition, a dielectric material placed within the system will lower the voltage between the two plates, Equation 3.10.

$$V = \frac{V_o}{\kappa} \quad or \quad \kappa = \frac{V_o}{V} \qquad \text{Equation 3.10}$$

When a dielectric material is placed between charged plates, the polarization of the dielectric produces an electric field that opposes the field that is created by the charge on the electrodes. A schematic of the electric field effect is depicted in Figure 3.14. The overall electric field is reduced by a factor of 1/κ, Equation 3.11.

$$E_{effective} = E - E_{polarization} = \frac{\sigma}{\kappa * \varepsilon} = \frac{1}{\kappa} * \frac{V}{d} \qquad \text{Equation 3.11}$$

Similarly, if the gap is not completely filled with a dielectric material, then the system should be analyzed as two capacitors in series (the air gap which is a dielectric itself and the dielectric material). The effective dielectric constant can be calculated for a system containing dielectric that does not completely fill the gap. The effective dielectric constant is defined in equation 3.12 (derivation Appendix C).

$$\kappa_{eq} = \left[\frac{(x+y)\kappa_2}{x\kappa_2 + y} \right] \qquad \text{Equation 3.12}$$

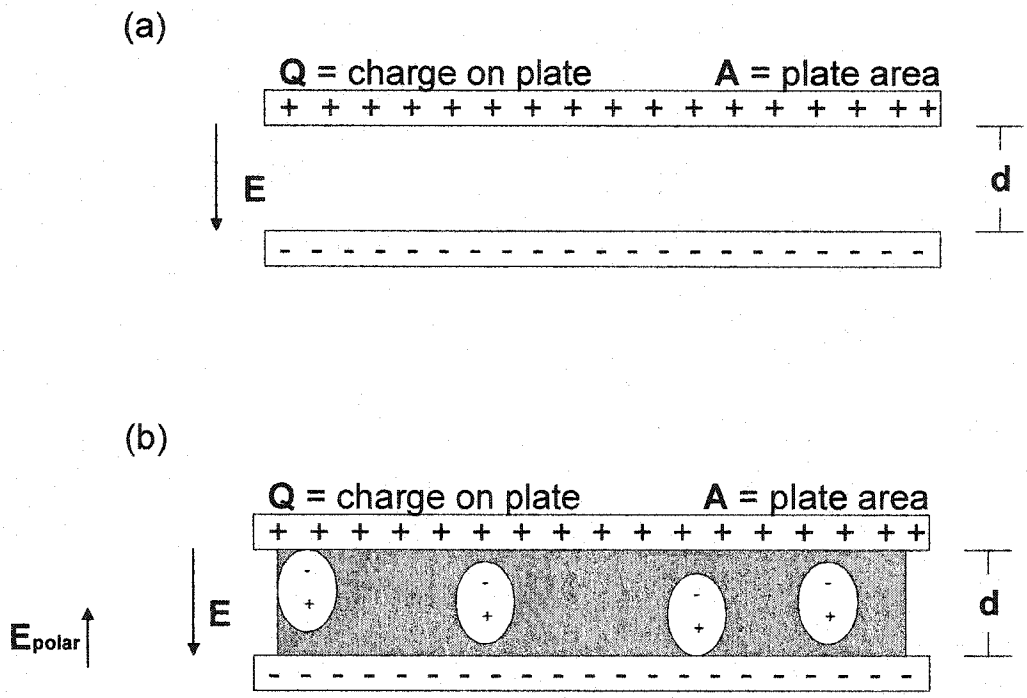

Figure 3.14 Characterization of the electric field within a parallel-plate capacitor. (a) without a dielectric material, (b) with a dielectric material filling the gap.

When this effective dielectric constant is applied to the voltage of the system (Equation 3.5), the resulting effect of the dielectric material on the system may be calculated (k_{cal} = 1.44) and compared to experimental data (k_{exp} = 1.50, from Equation 3.10 and Figure 3.15) for a bed height of 2 mm.

The effect of various materials on the observed breakdown voltage of this system was studied. The breakdown voltage of the system was noted for various materials, including Teflon, glass beads, and Plexiglas. Figure 3.15 shows how the breakdown voltage is dependent upon the various materials and bed heights. The results show that there is an immediate effect upon the addition of a material within the system. The voltage decreased to 6.5 to 7 kV for catalysts, glass beads, and Teflon when a 2-3mm bed of material was placed on the bottom electrode. However, as the bed height was increased, the breakdown voltage slowly increased to near the breakdown voltage of the empty system.

The use of a material within a system is known to assist in the stabilization of the streamer discharge, and lowers the breakdown voltage of the system by reducing the effective electric field, but the exact reason for the stabilization is thought to be associated with the temperatures corresponding with the required voltages. In order to accurately monitor the effect of voltage on the system, an IR camera was used to measure the temperature within the dc plasma system. In order to do so, an IR-transparent sapphire tube was used in place of the usual quartz tube.

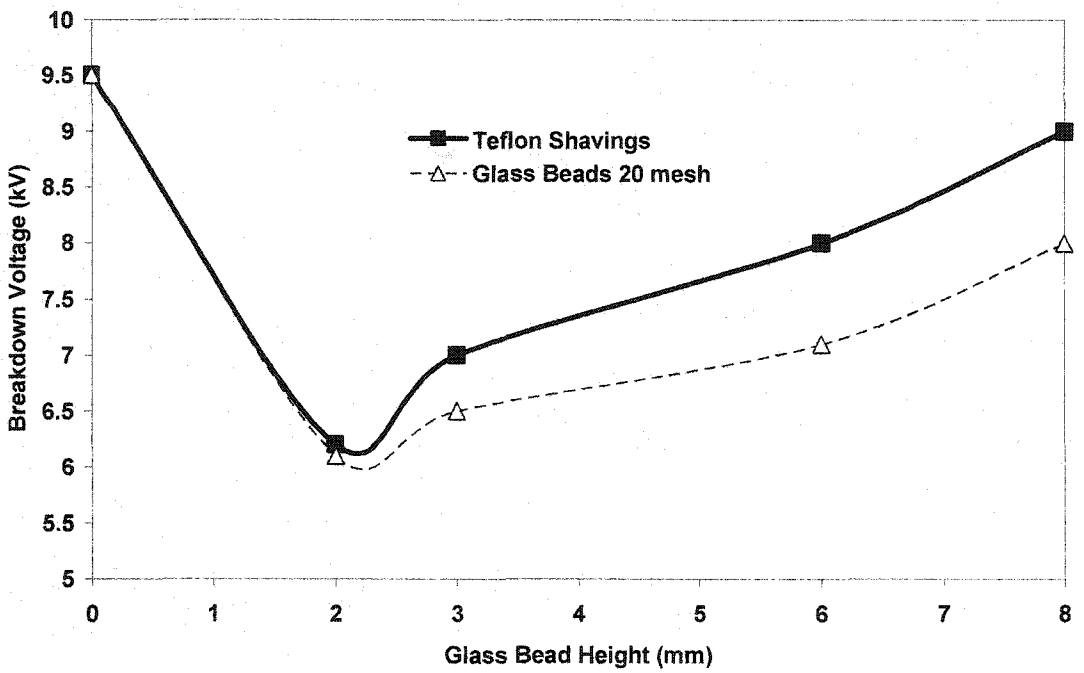

Figure 3.15 Effect of varying bed height of different dielectric materials on the breakdown voltage of the dc plasma system. 2/1 H_2/CH_4 with 2% O_2, 8mm electrode gap, 0 psig.

The first set of experiments performed for thermal comparison were the empty reactor and the 3mm bed depth catalyst experiments. These were performed at their "normal" operating voltage. It is necessary to operate the empty reactor at 13kV because breakdown does not occur until approximately 10 kV, and an "active streamer" discharge occurs at 13 kV. However, when the reactor is filled with catalyst at a bed depth of 3 mm, the breakdown discharge is around 6.5kV, and obtains an "active streamer" discharge at 7 kV. The voltage for the catalyst experiment is set at 10 kV, a "typical" experimental condition. This data set, Figure 3.16, showed that the empty reactor operated at about 15°C higher than that of the catalyst loaded reactor (for both the top and bottom electrode). Next, an experiment was performed with a glass bead depth of 3 mm (the glass beads have a diameter of about 0.5-1mm). Again, this system was operated at 10 kV because it behaves very similar in nature to that of the catalyst loaded system. These temperatures were similar to those of the catalyst-loaded conditions, Figure 3.13. Next, it was necessary to try to determine if the higher voltage necessary to obtain "active streamer" in the empty reactor was the cause of the discrepancy in temperature, or if the material had an effect.

The reactor was again loaded with 3 mm catalyst, but the voltage was varied. Each time the voltage was varied the system was allowed to come into a thermal equilibrium for about 30 minutes. The temperature was monitored and was considered stable if the temperature was constant over a 10-minute period. Figure

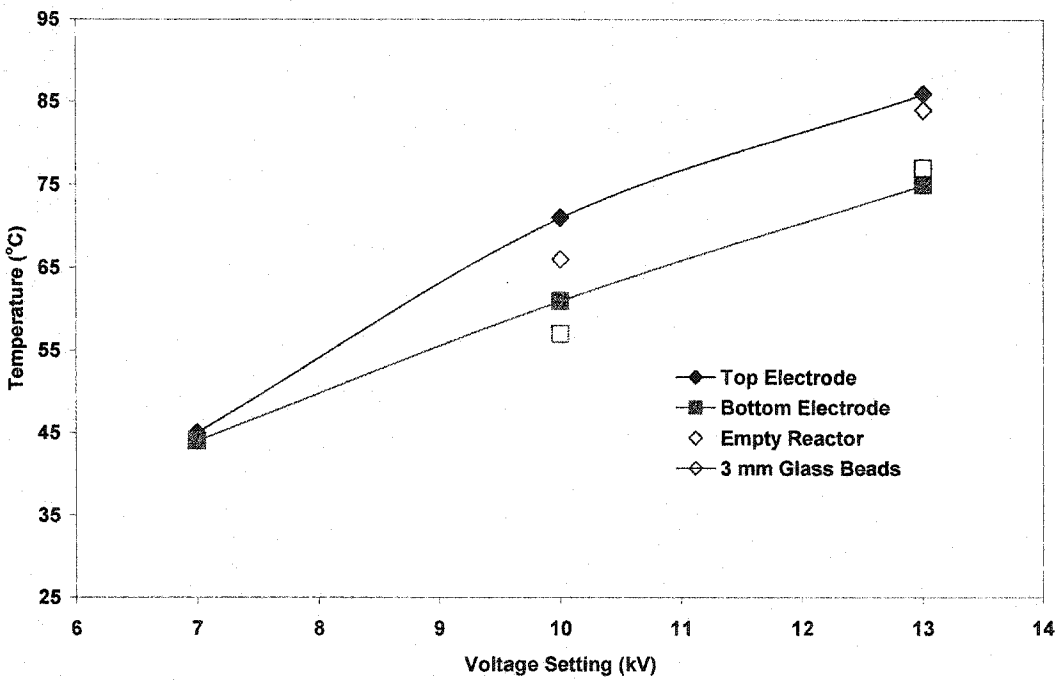

Figure 3.16 Voltage versus temperature for different materials loaded within the reactor. 2/1 H_2/CH_4 with 2% O_2, 8mm electrode gap, 0 psig.

3.16 shows the effect of applied voltage on the temperature of the top and bottom electrode. The 7 kV case was used because it was a typical experimental condition for all experiments prior to our studies involving pressure. The voltage was increased at that time because it was necessary to operate at 10 kV to obtain streamer discharges when dealing with 2 and 3 bar. The 7 kV case showed that the temperature is quite low in comparison to the higher power experiments. However, the 13 kV experiment showed that the temperature of the catalyst system is extremely close to that of an empty reactor. Therefore, this data indicates that the temperature is more a function of the applied voltage than that of the material (or lack of) within the reactor. Using the catalyst experiments as a baseline, it did not matter if a different material was used (glass beads substituted for Y zeolite) or if the material was removed as in the case of the empty reactor. In addition, it is important to note the effect of different discharges. In our system, several different discharges occur. Figure 3.1 depicts the different discharges that are encountered in the dc plasma system.

All the experiments described above were operated during an "active streamer" discharge. These active discharges look similar to many streamers occurring at one time with much movement throughout the system. The IR camera shows that there is also a distinct difference in the temperature of the above three discharges. Figure 3.17 shows how the temperature within the reactor varies with the type of discharge. During one of the experiments with the 3 mm catalyst loading, the discharge changed from the moving "active streamers" to the single "streamer"

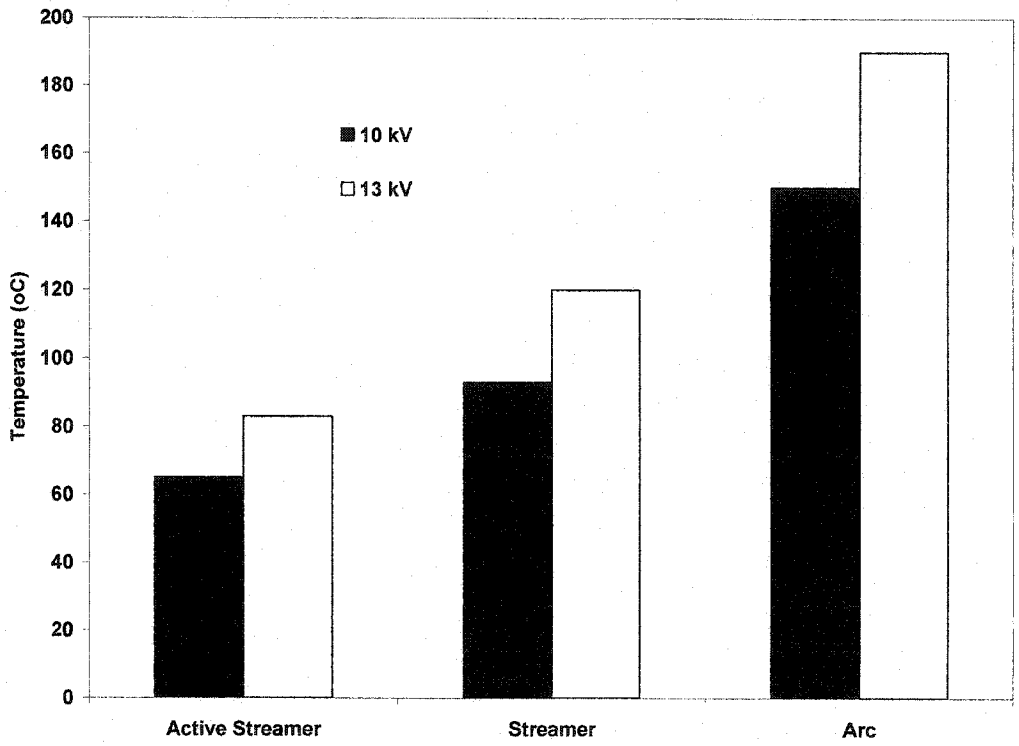

Figure 3.17 Voltage versus temperature for different conditions within the reactor. 2/1 H_2/CH_4 with 2% O_2, 8mm electrode gap, 0 psig.

discharge that does not have the active streamer movement associated with it. During this time, the temperature within the reactor increased from 65 to 90°C. Carbon deposition began to occur at the point on the reactor wall closest to the streamer discharge.

The applied voltage was further increased on this single streamer discharge. This resulted in a subsequent increase of the temperature within the reactor from 90°C to 120°C. While the discharge never changed to an arc discharge, the carbon formation continued. Previous experiments have shown that an arc discharge will result in a soot-type carbon formation throughout the reaction zone.

It is the formation of carbon that is believed to lead to the destabilization of the dc plasma discharge. Significant effort was put forth to find a set of feed conditions that allow for stable discharge operation. When the dc plasma system is operated with the NaOH Y zeolite, the following two feed conditions were found necessary to achieve stable streamer discharge:

1.) An oxygen concentration of at least 2% of the total feed.

2.) The hydrogen/methane feed ratio greater than 1 ($H_2/CH_4 > 1$)

If either of these feed conditions were not met, the reaction caused carbon formation on the walls of the reactor which resulted in a transformation of the streamer discharge to an arc discharge. The reason for these requirements are now discussed.

It is believed that the carbon formation is produced through the dehydrogenation of acetylene, as in Equation 3.13.

$$C_2H_2 \leftrightarrow 2C + H_2 \qquad \text{Equation 3.13}$$

Oxygen, if present, scavenges carbon through the oxidation of the carbon to form carbon monoxide, equation 3.14.

$$2C + O_2 \leftrightarrow 2CO \qquad \text{Equation 3.14}$$

If the first reaction (Equation 3.13) is reversible, then the hydrogen present has a two-fold effect. The hydrogen will suppress the forward reaction, as well as allow for the reverse reaction to occur. Even though hydrogen is produced during the main reaction, the hydrogen concentration must be over 50% to allow for stable operation. Without the presence of hydrogen the forward reaction dominates and carbon is formed. The carbon scavenging oxidation probably occurs while the carbon is still "afloat" in the gas phase. Once deposited on the wall the carbon is difficult to oxidize, even at elevated temperatures. During one TPO experiment, even temperatures as high as 750°C were not sufficient to remove this carbon.

However, it was found that the addition of palladium and silver-palladium to the Y zeolite changed the feed condition requirements necessary for stable discharge operation. The addition of a hydrogenation-capable metal to the catalyst allowed for much higher partial pressures of methane in the feed system. A stable streamer discharge was obtained at methane fractions as high as 98% in the feed as long as the remainder was oxygen. Carbon formation may be prevented under these conditions by removal of acetylene. The Pd and Ag-Pd catalyst have the ability to convert 100% of the acetylene formed in the gas phase to ethylene and ethane. By converting the acetylene, the precursor for the formation of coke has been removed from the system. Even though carbon can still deposit on the walls of the reactor in the gas phase

section of the reactor, the catalyst reduces the partial pressure of acetylene in the lower third of the reactor reducing the carbon formation. Thus, even if there is conductive carbon on the reactor walls in the gas phase section of the reactor, there is not a complete conductive path to the other electrode. This may be sufficient to prevent an arc discharge from forming and producing an unstable high temperature discharge.

3.4 Conclusions

The dc plasma is effective for the conversion of methane to products such as acetylene and hydrogen. The stable operation of the plasma requires establishing a streamer discharge and the prevention of carbon formation. The streamer discharge, at low E/P, provides numerous low-energy electrons that are capable of exciting methane and reacting to acetylene. During the unstable arc discharge (at high E/P) most of the energy is in higher energy electrons that lead to the dissociation of methane to form ethane.

The arc discharge is a result of the electrode gap being reduced by excessive carbon formation on the reactor walls. In order to reduce carbon formation, a material may be used to lower the electric field within the reactor, which in return reduces the operating temperature of the plasma. Higher applied voltages result in heating of the gas that leads to the decomposition of the acetylene to carbon.

3.5 Literature Cited

1. Thanyachotpaiboon, K., T.A. Caldwell, S. Chavadej, L.L. L. L. Lobban, and R.G. Mallinson, *Non-oxidative conversion of methane to higher hydrocarbons in low temperature plasmas.* AIChE Journal, 1998. **44**: p. 2252.

2. Larkin, D.W., L.L. Lobban, and R.G. Mallinson, *Product selectivity control and organic oxygenate pathways from partial oxidation of methane in a silent electric discharge reactor.* Industrial Engineering & Chemical Research, 2001(40): p. 5496.

3. Liu, C.-J., A. Marafee, R.G. Mallinson, and L.L. Lobban, *Methane Conversion to higher hydrocarbons in a corona discharge over metal oxide catalysts with OH groups.* Applied Catalysis A: General, 1997. **164**: p. 21-33.

4. Gordon, C.L., L.L. Lobban, and R.G. Mallinson, *The production of hydrogen from methane using tubular plasma reactors*, in *Advances in hydrogen energy*, C. Gregoire-Padro, Editor. 2000, Kulmer.

5. Liu, C.-J., A. Marafee, B.J. Hill, G. Xu, R.G. Mallinson, and L.L. Lobban, *Oxidative coupling of methane with ac and dc corona discharge.* Industrial & Engineering Chemistry Research, 1996. **35**(10): p. 3295-3301.

6. Marafee, A., C.-J. Liu, G. Xu, R.G. Mallinson, and L.L. Lobban, *An experimental study on the oxidative coupling of methane in a direct current corona discharge reactor over Sr/La2O3 catalyst.* Industrial & Engineering Chemistry Research, 1997. **36**: p. 632-637.

7. Liu, C.-J., R.G. Mallinson, and L.L. Lobban, *Comparative investigations on plasma catalytic methane conversion to higher hydrocarbons over zeolites.* Applied Catalysis A: General, 1999. **178**: p. 17-27.

8. Eliasson, B. and U. Kogelschatz, *Nonequilibrium volume plasma chemical processing.* IEEE Transactions on Plasma Science, 1991. **19**(6): p. 1063-1077.

9. Bera, K., B. Farouk, and P. Vitello, *Inductively coupled radio frequency methane plasma simulation.* Journal of Physics, D: Applied Physics, 2001. **34**: p. 1479-1490.

10. Morgan, W.L. and B.M. Penetrante, *Elendif: A time-dependent Boltzmann solver for partially ionized gases.* Computer Physics Communications, 1990. **58**: p. 127-152.

11. Penetrante, B.M., M.C. Hsiao, J.N. Bardsley, B.T. Merritt, G.E. Vogtlin, A. Kuthi, C.P. Burkhart, and J.R. Bayless, *Identification of mechanisms for decomposition of air pollutants by non-thermal plasma processing.* Plasma Sources Science and Technology, 1997. **6**: p. 251-259.

12. Winstead, C., Q. Sun, V. McKoy, J.L. Lino, and M.A. Lima, *electronic excitation of CH4 by low-energy electron impact.* Journal of Chemistry and Physics, 1993. **3**(1): p. 2132-2137.

13. Pitchford, ONeil, and Rumble, Phys. Rev, 1981. **23**: p. 294.

14. Le, H., L.L. Lobban, and R.G. Mallinson, *Some temperature effects on stability and carbon formation in low temperature ac plasma conversion of methane.* Catalysis Today, 2004. **89**: p. 15-20.

15. Tsai, P. and J.R. Anderson, *Reaction of acetylene over ZSM-5 type catalysts.* Journal of Catalysis, 1982. **80**: p. 207-214.

16. Rajanikanth, B.S. and S. Rout, *Studies on nitric oxide removal in simulated gas compositions under plasma-dielctric/catalystic discharges.* Fuel Processing Technology, 2001. **74**: p. 177-195.

17. Chang, J.S., P.A. Lawless, and T. Yamamoto, *Corona discharge processes.* IEEE Transactions on Plasma Science, 1991. **19**(6): p. 1152-1166.

18. Mizuno, A., Y. Yamazaki, S. Obama, E. Suzuki, and K. Okazaki, *Effect of voltage waveform on the partial discharge in ferroelectric pellet layer for gas cleaning.* IEEE Transactions on Industry Applications, 1993. **29**(2): p. 262-267.

19. Serway, R.A., *Physics for scientists and engineers.* Third Edition ed, ed. Saunders. 1990, Philadelphia: Saunders College Publishing.

20. West, R.C., *Handbook of chemistry and physics.* 55th Edition ed. 1974, Cleveland: CRC Press.

CHAPTER 4 – Conversion of Methane to Hydrogen and Higher Hydrocarbons Using a dc Plasma Reactor

4.1 Introduction

There are many factors that are changing and shaping the fuel and energy industries of the future. Environmental, political, economic, and availability issues are just some of these factors. With environmental regulations becoming stricter, the emission of greenhouse gases is a major concern. With the decrease in oil resources, there is a need for other sources of fuel and chemical production.

Large quantities of hydrogen are used as a feedstock in the manufacturing of ammonia, methanol, and a variety of other petroleum processes. The synthesis of methanol occurs via the following reactions:

$$CO + 2H_2 \leftrightarrow CH_3OH, \ \Delta H_{298} = -91 \text{ kJ mol}^{-1}, \qquad \text{Equation 4.1}$$

$$CO_2 + 3H_2 \leftrightarrow CH_3OH + H_2O, \ \Delta H_{298} = -50 \text{ kJ mol}^{-1} \qquad \text{Equation 4.2}$$

$$CO + H_2O \leftrightarrow CO_2 + H_2, \quad \Delta H_{298} = -41 \text{ kJ mol}^{-1} \qquad \text{Equation 4.3}$$

Synthesis gas (CO and H_2) production results in a large fraction, approximately 60%, of the cost of methanol. The synthesis gas for methanol is now almost exclusively produced by steam reforming of natural gas.

The production of hydrogen from methane has received much research interest over the last decade. There are many good reasons for the conversion of methane, the principle component of natural gas, to other products. Natural gas is a very abundant resource with reserves throughout the world. Methane, with its 4:1 hydrogen to carbon ratio is also an excellent source for hydrogen. Hydrogen is projected to play an important role as a source of energy in the years to come. There will be a large increase in hydrogen demand as it becomes a general-purpose energy source for space heating, electrical power generation, and as a transportation fuel [1].

Also, hydrogen is a clean burning fuel, which can be stored as a liquid or a gas, and is distributed by means of a pipeline [2].

Catalytic steam reforming of methane is currently the primary means of hydrogen production. About 50% of all hydrogen is produced from methane, with 40% of that coming from the steam reforming of methane. It can be seen from Table 4.1 that the steam reforming of methane has the lowest CO_2 impact compared to other fossil fuels.

The production of hydrogen from steam methane reforming results from the following two reversible steps:

$$CH_4 + H_2O \leftrightarrow CO + 3H_2, \quad \Delta H_{298} = 206 \text{ kJ mol}^{-1} \qquad \text{Equation 4.4}$$

$$CO + H_2O \leftrightarrow CO_2 + H_2, \quad \Delta H_{298} = -41 \text{ kJ mol}^{-1} \qquad \text{Equation 4.5}$$

With the overall reaction written as follows:

$$CH_4 + 2H_2O \leftrightarrow CO_2 + 4H_2, \quad \Delta H_{298} = 165 \text{ kJ mol}^{-1} \qquad \text{Equation 4.6}$$

While the reforming step [4] does not produce any carbon dioxide, it is the water gas shift reaction [5] that produces the carbon dioxide while removing the carbon monoxide and in return yielding another hydrogen molecule. Thermodynamically, the methane steam reforming process is favorable at high operating temperatures and low

Table 4.1. Variance of CO_2 coproduction with different hydrocarbon feedstocks [3]

H_2/CO_2	Technology
4.0	Steam methane reforming
3.2	Steam pentane reforming
3.0	Partial oxidation of methane
1.7	Partial oxidation of heavy oil
1.0	Partial oxidation of coal

pressures due to the endothermic reaction and the increase in moles. The high operating temperature requires an intensive energy input to maintain these high temperatures. In addition, it is necessary to operate the system with excess steam in order to reduce the formation of carbon. This in itself is an extra cost due to the increase in equipment size.

Therefore, it is desirable to produce synthesis gas more economically. Cold plasmas or "non-equilibrium" plasmas have been shown to activate methane at temperatures as low as room temperature [4]. A cold plasma is characterized by high electron temperatures, while the bulk gas temperature can remain as low as room temperature, decreasing or eliminating the heat transfer energy requirements. It is the highly energetic electrons that allow for the conversion of methane that otherwise would not be feasible at low temperatures. In this paper, we discuss the use of our electrical discharge system to convert methane into hydrogen, acetylene, and carbon monoxide. A valuable feature of this system is the very low concentrations of carbon dioxide and water formed.

4.2 Experimental

In general, the experimental apparatus is similar to the system that has been described previously [4]. The feed gases consisted of a combination of methane, oxygen, hydrogen, and helium. Helium was only used in initial experiments and for characterization studies of the catalyst. The feed gas flowrates were controlled by Porter mass flow controllers, model 201. The feed gases flowed axially down the

reactor tube. The reactor is a quartz tube with a 9.0 mm O.D. and an I.D. of either 4.5 mm or 7.0 mm. The configuration of the reactor can be seen in Figure 2.2.

The reactor's electrode configuration consists of a point to plane geometry, meaning that the top electrode is a wire point electrode and the bottom electrode is a flat plate that also serves as a support for the catalyst. The top electrode is positioned concentrically within the reactor, and the gap between its tip and the plate is 8.0 mm. The catalyst is loaded from the top onto the flat plate electrode. A stainless steel wire cloth is placed between the electrode and catalyst in order to prevent the catalyst from falling through the holes on the electrode plate. Another stainless steel wire cloth is placed on top of the catalyst in order to prevent movement of the catalyst. Due to the electrostatic nature of the zeolites and the plasma itself, this top screen is necessary to keep the catalyst bed uniform. The preparation and characterization of these zeolites has been discussed elsewhere [5, 6]. The dc corona discharge is created using a high voltage power supply (Model 210-50R, Bertan Associates Inc.).

As mentioned before, this system operates at low temperatures. A furnace around the reactor is used to heat the system to the desired temperature. The temperature is measured by an Omega K-type thermocouple that is attached to the outside of the reactor near the catalyst bed. The temperature measured on the outside has been calibrated against the internal temperature of the reactor, and has been discussed elsewhere [5, 6]. However, when the desired operating temperature is below 373 K it is necessary to use cooling air to control the temperature since the

plasma itself does heat the gas to some extent. The system pressure varies depending on the experiment. The pressure is controlled using a GO back pressure regulator.

The product gases are passed through a dry ice/acetone bath that allows for any condensable organic liquids to be separated from the product gases. It should be noted that the dc system does not produce any liquids, including water. The effluent gases can be analyzed on-line by either a gas chromatograph or a mass spectrometer. The gas chromatograph is a CARLE series 400 AGC (EG&G) gas chromatograph equipped with a hydrogen transfer system to quantify the hydrogen; a HayeSep column to quantify carbon dioxide, ethane, ethylene, and acetylene; and a molecular sieve column to quantify oxygen, nitrogen, methane, and carbon monoxide. Also, a MKS mass spectrometer is used for on-line analysis of the products and for temperature programmed oxidation of carbon deposited on the catalyst.

4.3 Results and Discussion

4.3.1 Radial Bypassing and Oxidative Experiments

The actual streamer discharges only occupy a very small fraction of the reaction zone. However, the conversion of the system is much higher than would be expected by the visual coverage of the discharge. Therefore, the streamer discharge must be capable of driving reactions in volumes not directly exposed to the discharge. Reactors with two different cross sectional areas were employed to study bypassing of the feed gases around the plasma discharge because the streamer discharges only occupy a fraction of the reaction volume with the streamers moving around the

plasma zone. Figure 4.2 shows the effect of residence time on the conversion of methane. The conditions in these two different reactors were identical except for the inside diameter of the reactors. The depth of the catalyst bed remained constant in both reactors; 0.1 grams and 0.04 grams were used in the large and small reactors, respectively. The original reactor had a 7.0 mm I.D., while the smaller reactor had a 4.5 mm I.D.

As expected, the conversion increases as the residence time increases for both reactors. The data in Figure 4.2 show that at any residence time, the larger reactor has a lower conversion than the smaller reactor at the same residence time. This is indicative of bypassing, as the volume average rate of reaction is lower. This suggests that, in contrast to a typical homogenous reactor, there is a zone of higher reaction rate in proximity to the visible discharges and a zone of lower reaction rate, perhaps around the periphery of the reactor. However, if the added peripheral volume of the larger tube (from the difference between the cross sectional areas of the large and small tubes) were assumed to have no reaction, the conversion shown by the dashed line drawn on Figure 4.2 would result. This is in agreement with the data at the shorter residence times (high gas velocities), but the fact that the measured conversion is higher at longer residence times suggests that some level of radial mixing occurs that reduces bypassing at lower velocities. As tube size is made larger such mixing would be desirable to increase the volumetric averaged reaction rate.

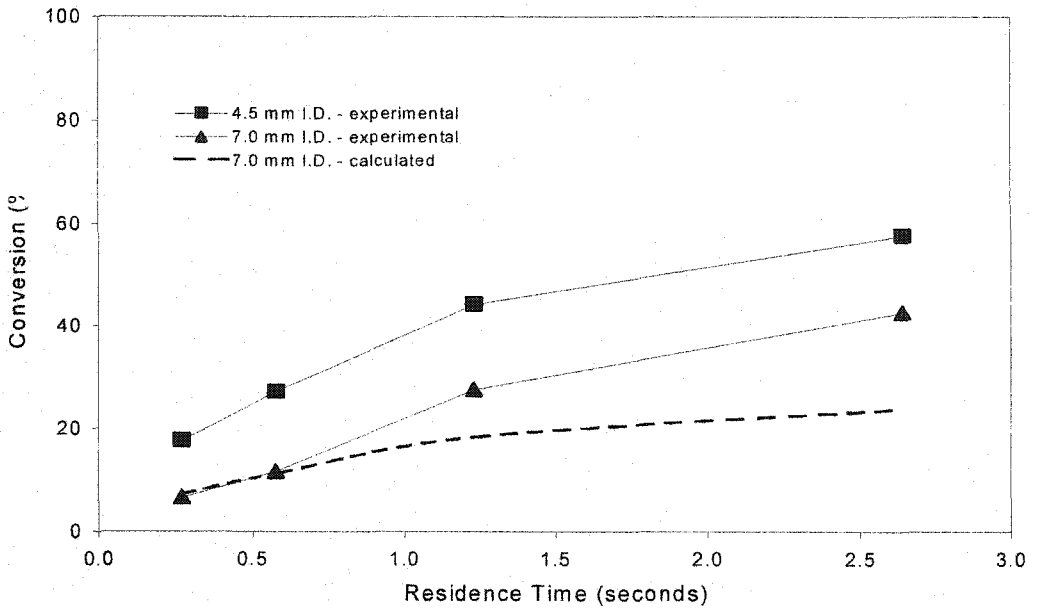

Figure 4.2. Methane conversion versus residence time in two different cross sectional area reactors. Feed composition, 4/1 CH_4/O_2; gas temperature, 298 K; power, 5.2 watts. Calculated line is for 7.0 mm reactor based on 4.5 mm reactor data.

Hydrogen, acetylene, and carbon monoxide are the primary products of the conversion of methane in the dc plasma system. In addition, small amounts of ethane, ethylene, and carbon dioxide are produced. Of the C_2 products, acetylene accounts for 90%, while ethylene and ethane comprise 6% and 4%, respectively. Carbon dioxide is less than 0.2% of the effluent gas. No measurable amount of water is produced in the system.

The selectivity and yield of hydrogen, acetylene, and carbon monoxide can be seen in Figures 4.3-4.5. The definitions of conversion, selectivity, and yield for this system are as follows:

CH_4 conversion = (moles of CH_4 consumed/moles of CH_4 introduced) x 100%

O_2 conversion = (moles of O_2 consumed/moles of O_2 introduced) x 100%

Selectivity of C_2H_6 = 2 x (moles of C_2H_6 formed/moles of CH_4 consumed) x 100%

Selectivity of C_2H_4 = 2 x (moles of C_2H_4 formed/moles of CH_4 consumed) x 100%

Selectivity of C_2H_2 = 2 x (moles of C_2H_2 formed/moles of CH_4 consumed) x 100%

Yield of C_2 hydrocarbons = CH_4 conversion x Σ(selectivities of C_2H_2, C_2H_4, C_2H_6)

Selectivity of H_2 = 0.5 x (moles of H_2 formed/moles of CH_4 consumed) x 100%

Yield of H_2 = CH_4 conversion x selectivities of H_2

Selectivity of CO = (moles of CO formed/moles of CH_4 consumed) x 100%

Yield of CO = CH_4 conversion x selectivities of CO

In general, the yields of the products follow the same trend as that of the methane conversion. The selectivities of the respective products did not vary much with either reactor size or residence time. Figure 4.3 shows that the selectivity of hydrogen has little variance between the different reactor sizes and residence times. The largest variance is 10%, with experimental uncertainty accounting for at least 2-3% of this.

The acetylene selectivity, seen in Figure 4..4, shows a trend of increased selectivity toward acetylene with residence time for both reactor geometries. In addition, the 4.5 mm reactor has a higher selectivity towards acetylene than the 7.0 mm reactor, and the difference in selectivity increases as residence time increases. Therefore, it seems that the higher the conversion, whether achieved by altering the reactor size or residence time, the higher the acetylene selectivity. Carbon monoxide selectivity, shown in Figure 4.5, goes through a maximum at the intermediate residence times.

4.3.2 Non-oxidative Studies

The above results were for a feed composition of 80% methane and 20% oxygen. The use of large quantities of oxygen in the feed has many negative consequences. Oxygen is expensive to produce, and may lead to undesired products such as carbon dioxide. In order to reduce the cost associated with oxygen as a feedstock, and to reduce the carbon monoxide impact as it may later be converted to

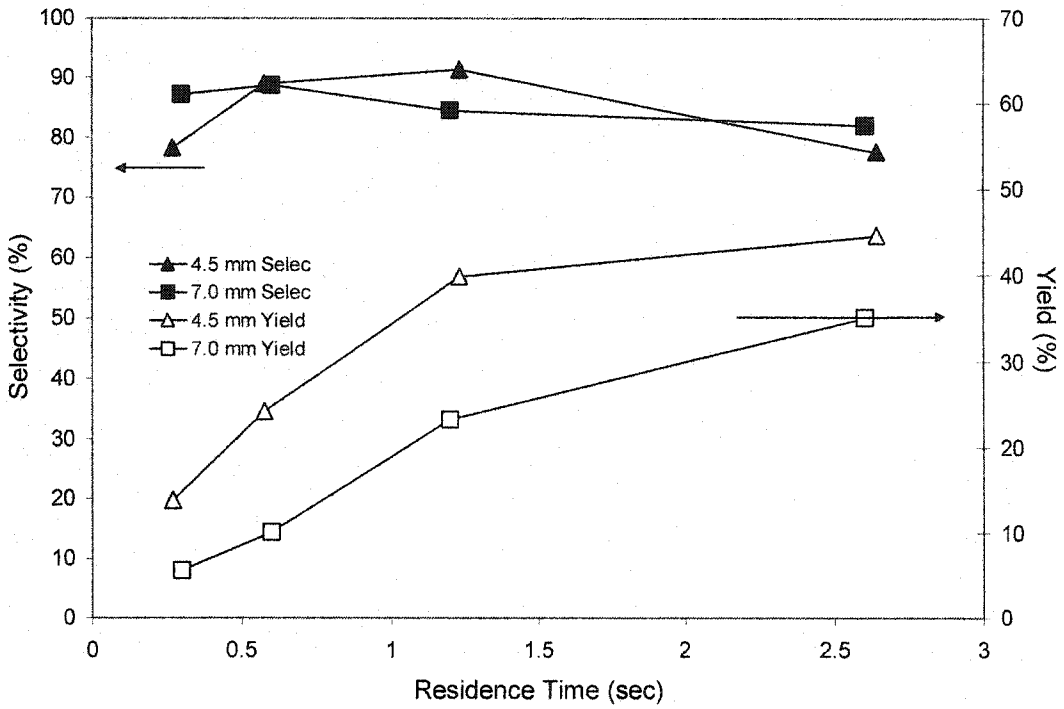

Figure 4.3. Hydrogen selectivity and yield for the two different reactor cross sectional areas at different residence times. Feed composition, 4/1 CH_4/O_2; gas temperature, 298 K; power, 5.2 watts.

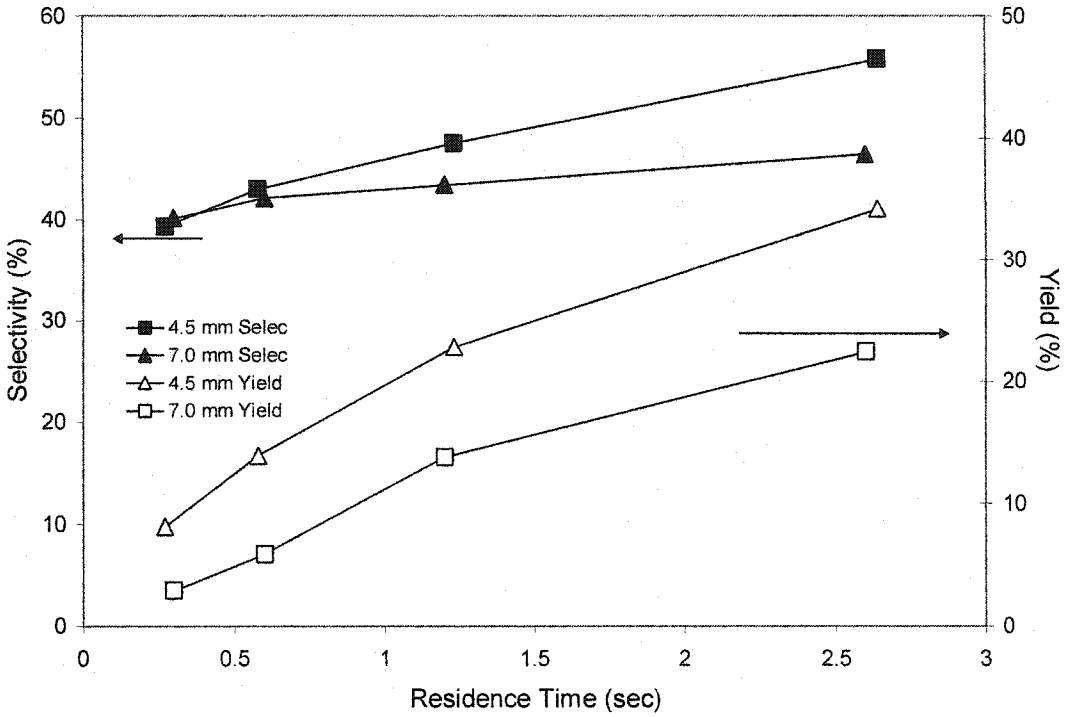

Figure 4.4. Acetylene selectivity and yield for the two different reactor cross sectional areas at different residence times. Feed composition, 4/1 CH_4/O_2; gas temperature, 298 K; power, 5.2 watts.

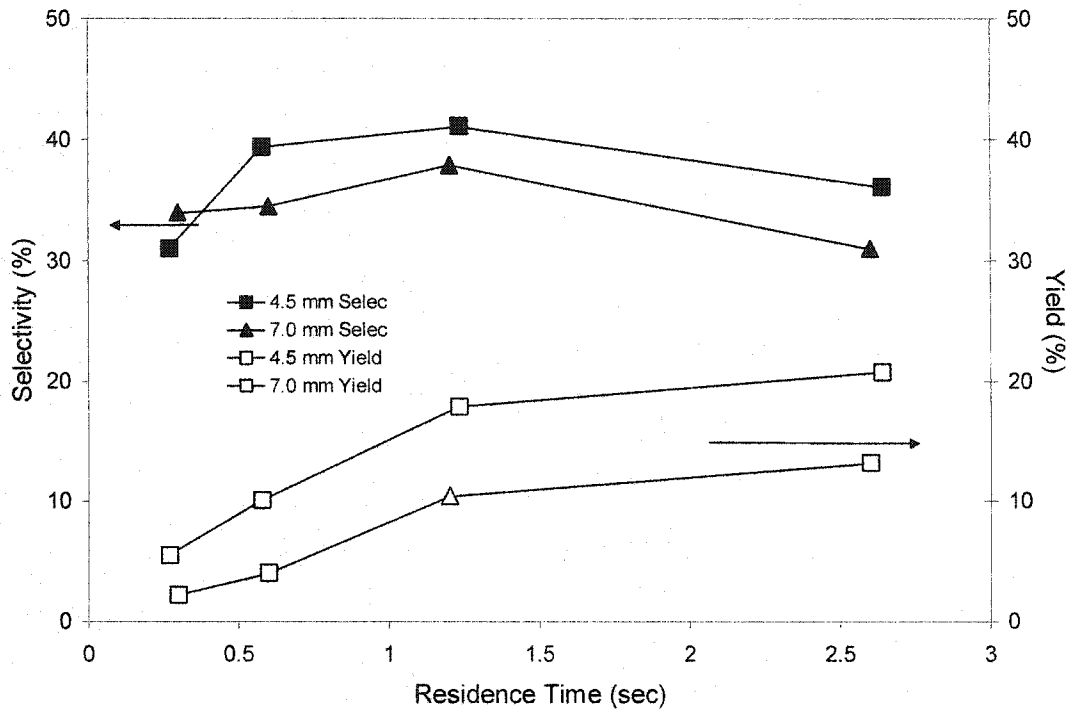

Figure 4.5. Carbon monoxide selectivity and yield for the two different reactor cross sectional areas at different residence times. Feed composition, 4/1 CH_4/O_2; gas temperature, 298 K; power, 5.2 watts.

carbon dioxide, several studies were performed to optimize the feed conditions with minimal oxygen. It has been determined from previous studies that 2-2.5% oxygen is still needed for the non-oxidative conditions [7]. Concentrations lower than 2% have instability problems, while concentrations above 2.5% yield stable discharges, but do not increase methane conversion. In addition, the concentrations of oxygen above 2.5% do lower the selectivity towards C_2's and increase the selectivity towards carbon monoxide. Thus, it was necessary to replace the removed oxygen with another gas component.

A higher methane partial pressure would be the preferred option as to not have to recycle hydrogen. Figure 4.6 shows the conversion and eV/molecule of methane converted for various methane partial pressures. All the data was obtained during a stable streamer discharge. However, the experiments with H_2/CH_4 less than unity resulted in rapid carbon formation on the reactor walls. This carbon formation provided a conductive path for the discharge which resulted in a transformation of the discharge from the streamer discharge to an arc discharge. The transformation typically occurred within the first 30 minutes, while all other experiments were stable for a minimum of 3 hours. These studies showed with little or no oxygen in the feed, it is necessary to have a H_2/CH_4 ratio above one in order to achieve a stable plasma discharge in a non-oxidative environment. It is presumed that the 20% oxygen in the first set of experiments and the hydrogen in the second set of experiments play an important role in reducing carbon formation in the reaction zone, which in return plays an important role in the stability of the streamer discharges.

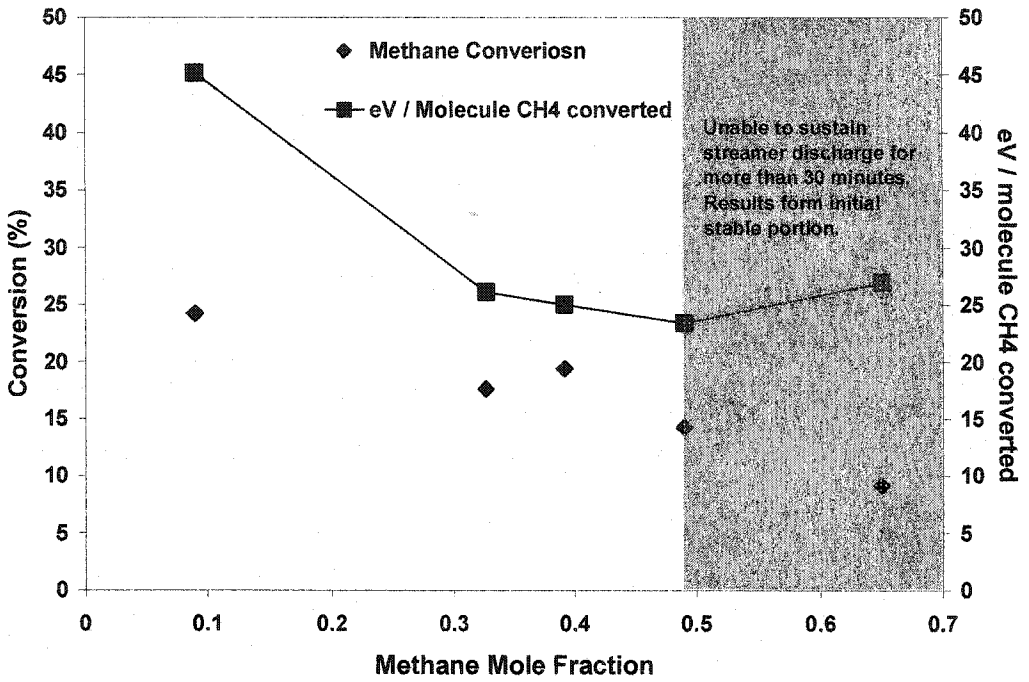

Figure 4.6. Methane conversion and electrical efficiency (eV/molecule of methane converted) versus methane partial pressure. Balance hydrogen and 2% oxygen, 32 sccm, NaOH Y zeolite

Even though the conversion is lower at the higher partial pressures of methane, it would probably be more economical to operate at the higher partial pressures. As the partial pressure decreases, the methane conversion increases, but so does the eV/molecule of methane converted. For constant power input, the reaction rate has significantly decreased at the lower methane partial pressures resulting in a higher energy cost per methane converted. The higher throughput of methane results in a more economically feasible process. The majority of the remainder of the experiments were operated at a 2/1 H_2/CH_4 ratio with 2% oxygen (66% hydrogen, 33% methane, and 2% oxygen). This allowed for the highest partial pressure of methane without constantly pushing the boundary which results in excessive carbon formation. The first step was to compare the oxidative and non-oxidative systems at various residence times.

The effect of the feed composition on the fractional conversion is shown in Figure 4.7. The feed composition was the only parameter changed between the two systems. The fractional methane conversion is higher for the 2% oxygen system than for the 20% oxygen system. However, the methane reaction rate, not shown, is higher for the 20% oxygen system due to the higher throughput of methane in the system. The conversion in both conditions increases with an increase in residence time.

Figures 4.8-4.10 show the effect of residence time on the selectivity and yield of the two different feed compositions Hydrogen, acetylene, and carbon monoxide are still the major products of both systems, while carbon dioxide is still very low and

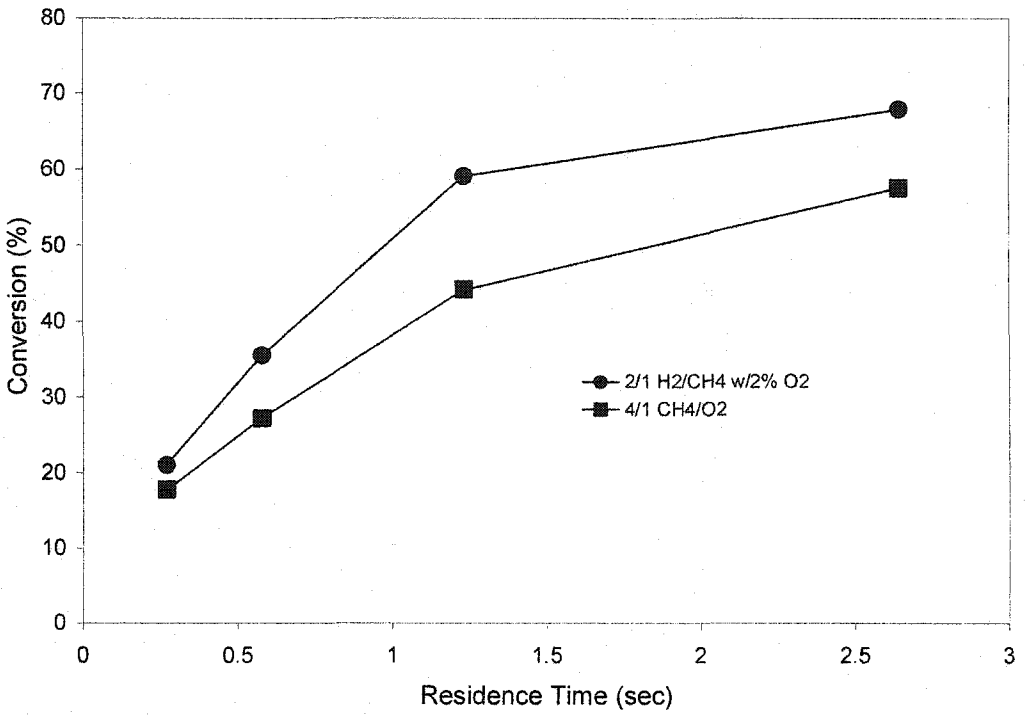

Figure 4.7. Comparison of methane conversion versus residence time for two different systems: feed compositions of 2/1 H_2/CH_4 with 2% oxygen, and 4/1 CH_4/O_2.Gas temperature, 298 K; power, 5.2 watts.

water is negligible for both systems. However, the selectivity of the major products is different in the two systems. Acetylene still makes up 90% of the C_2's in both cases with ethylene and ethane around 6% and 4%, respectively.

. The yield basis for hydrogen includes only the net hydrogen produced from the reacted methane. The selectivity towards hydrogen, shown in Figure 4.8, is lower for the system that contains hydrogen in the feed. However, the methane conversion is higher in that system resulting in a hydrogen yield that is essentially the same in both systems at each residence time. With the lower oxygen concentration, the 2% oxygen system shows a higher selectivity toward acetylene, Figure 4.9, and a lower selectivity toward carbon monoxide, Figure 4.10.

The high concentration of oxygen in the feed for the 20% oxygen system causes an over oxidation of the carbon species to CO, reducing the selectivity towards acetylene. This product flexibility could be useful in that it would allow for hydrogen to be produced with acetylene for higher hydrocarbons or with carbon monoxide to produce a synthesis gas feed stream. Synthesis gas production is a very costly step in many industrial processes.

4.3.3 Environmental Impact and Hydrogen Cost Analysis

The production of hydrogen from methane is important because it has a relatively low environmental impact compared to hydrogen production from other hydrocarbons. The production of hydrogen via steam reforming has a H_2/CO_2 ratio of 4 (Table 4.1), the lowest CO_2 impact of any fossil fuel source. The dc plasma system

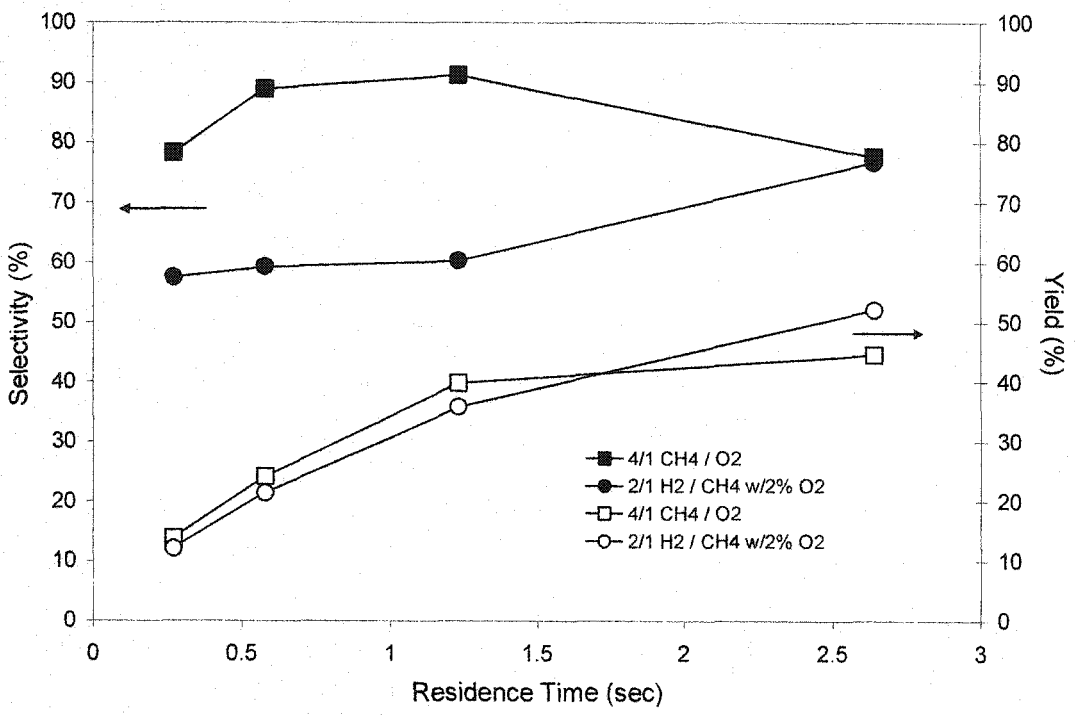

Figure 4.8. Hydrogen selectivity and yield for the two different feed compositions at different residence times. Feed compositions of 2/1 H_2/CH_4 with 2% oxygen or 4/1 CH_4/O_2; gas temperature, 298 K; power, 5.2 watts.

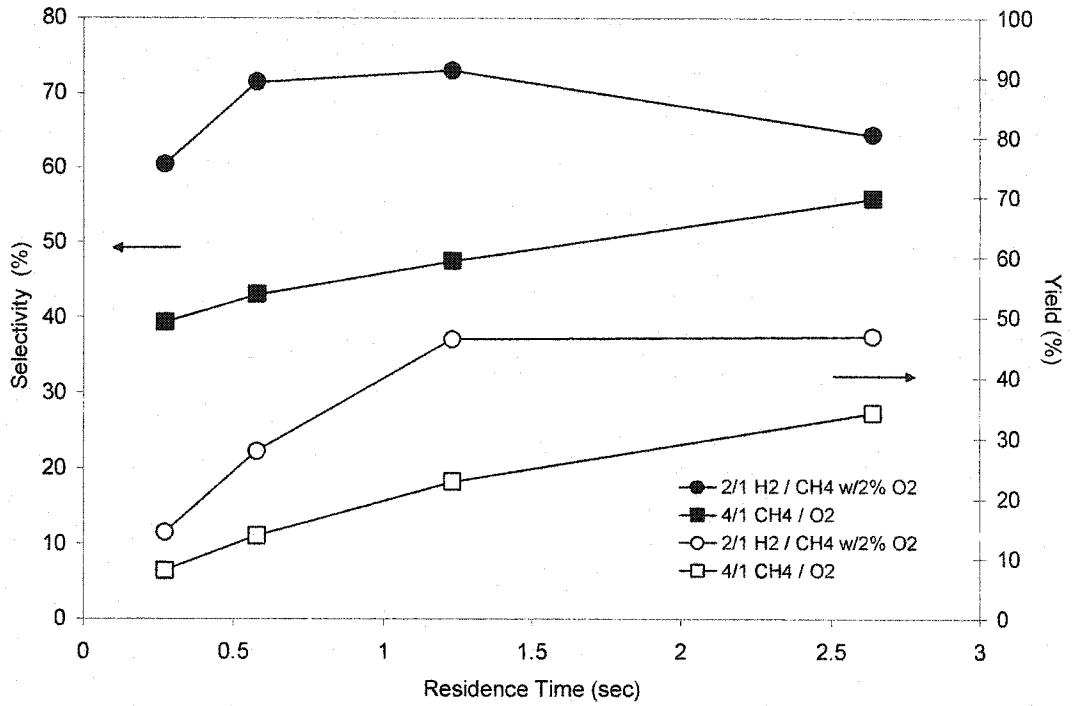

Figure 4.9. Acetylene selectivity and yield for the two different feed compositions at different residence times. Feed compositions of 2/1 H_2/CH_4 with 2% oxygen or 4/1 CH_4/O_2; gas temperature, 298 K; power, 5.2 watts.

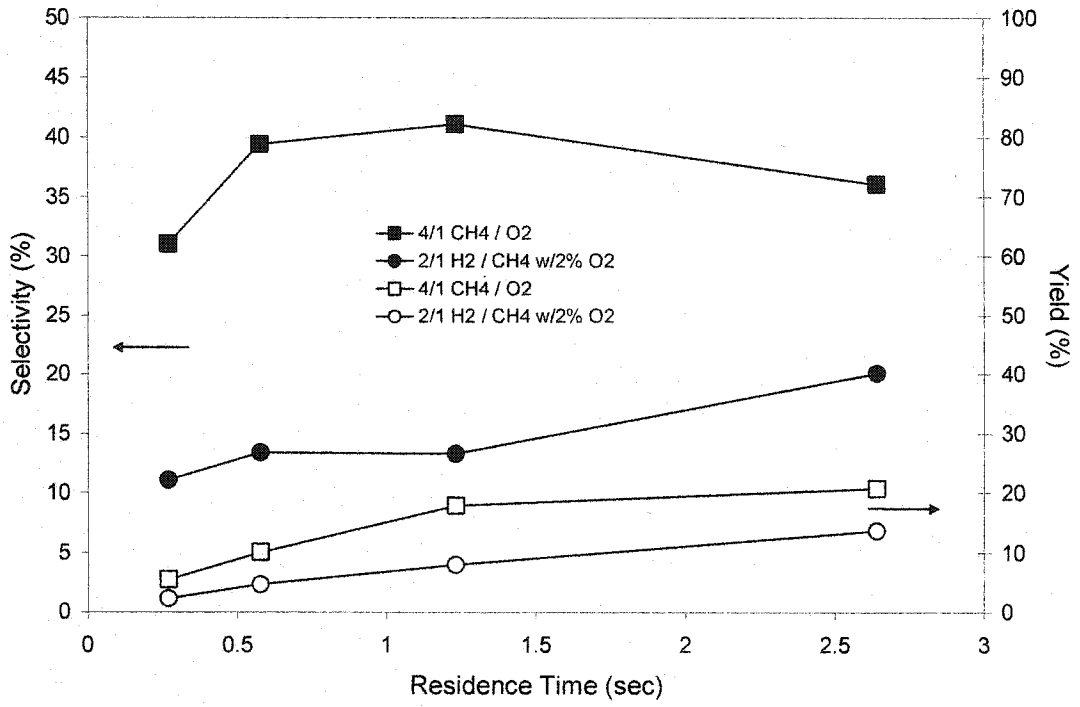

Figure 4.10. Carbon monoxide selectivity and yield for the two different feed compositions at different residence times. Feed compositions of 2/1 H_2/CH_4 with 2% oxygen or 4/1 CH_4/O_2; gas temperature, 298 K; power, 5.2 watts.

produces a H_2/CO_2 ratio of about 1000 and 300 in the effluent stream for the non-oxidative and oxidative environment, respectively, Figure 4.11. However, CO is a major product of the system. The CO may be converted to CO_2 which in return would yield another molecule of H_2 for every CO via the water-gas shift reaction. If the water-gas shift reaction were used to convert all of the produced CO into CO_2 via reaction [5], the resulting H_2/CO_2 ratio would be approximately 9 for either system (non-oxidative and oxidative). This value is still considerably better than that of other fossil fuels, including steam reforming.

Hydrogen is not the only valuable resource produced in this system. As previously mentioned, the other major products are acetylene and carbon monoxide. These products can return some value from either their heating or chemical value. The product gas stream of unreacted methane, acetylene, and carbon monoxide retains over 94% of the heating value that was put into the system via methane. The major cost of hydrogen production in this system is the energy required to obtain the plasma discharge. Currently, the production of hydrogen from methane in the catalytic dc system costs about four times the projected goal for the cost of hydrogen. However, the cost of hydrogen could be reduced if the acetylene was sold for its chemical value or even further processed to a higher value chemical.

4.3.4 Elevated Operating Pressure

As stated previously, the throughput of methane plays a large role in determining the overall energy efficiency of the system. One way to increase the

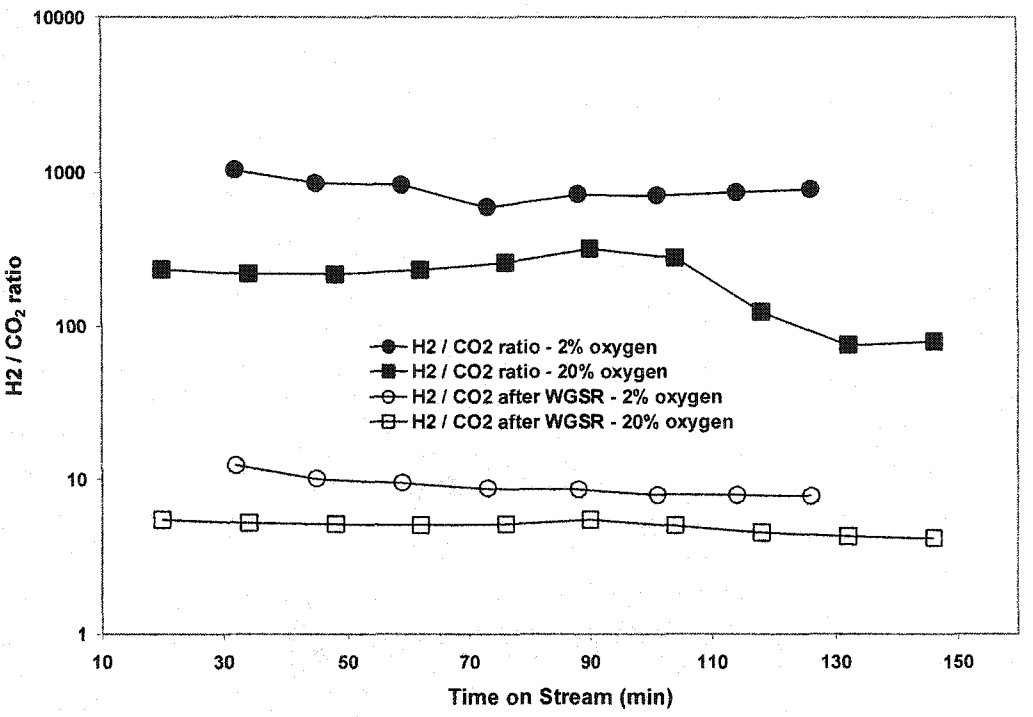

Figure 4.11. Carbon dioxide production for an oxidative and non-oxidative system, before and after water-gas shift reaction.

throughput of methane is increasing the pressure. Increasing the pressure while maintaining the same residence time allows for an increase in the methane throughput. However, the voltage necessary to sustain a discharge also increases, as does the power. Figure 4.12 shows the effect of pressure on reaction rate at various residence times. The conversion was constant from 1 atm to 2 atm; thus, the reaction rate doubled from 1 atm to 2 atm. However, there was no further increase in reaction rate from 2 to 3 atm. Laboratory equipment limitations limit current pressure studies to 3 atm.

4.4 Conclusions

The dc plasma catalytic system is very effective in the conversion of methane to hydrogen, acetylene, and carbon monoxide. Reducing the cross sectional area of the reactor decreased the gas bypassing the streamer discharges resulting in an increase in methane conversion. Single pass methane conversions as high as 68% and hydrogen, acetylene, and carbon monoxide yields of 52%, 47%, and 21%, respectively, have been achieved. The highest conversions were obtained with an oxygen concentration of 2% and a residence time of 2.6 seconds. High hydrogen yields can be achieved under different conditions. Further work needs to be done to reduce the energy cost. The projected cost of hydrogen may be met by increasing conversion and the throughput of methane while maintaining similar power requirements. This could be accomplished by further minimizing bypassing to increase the overall efficiency of the plasma zone.

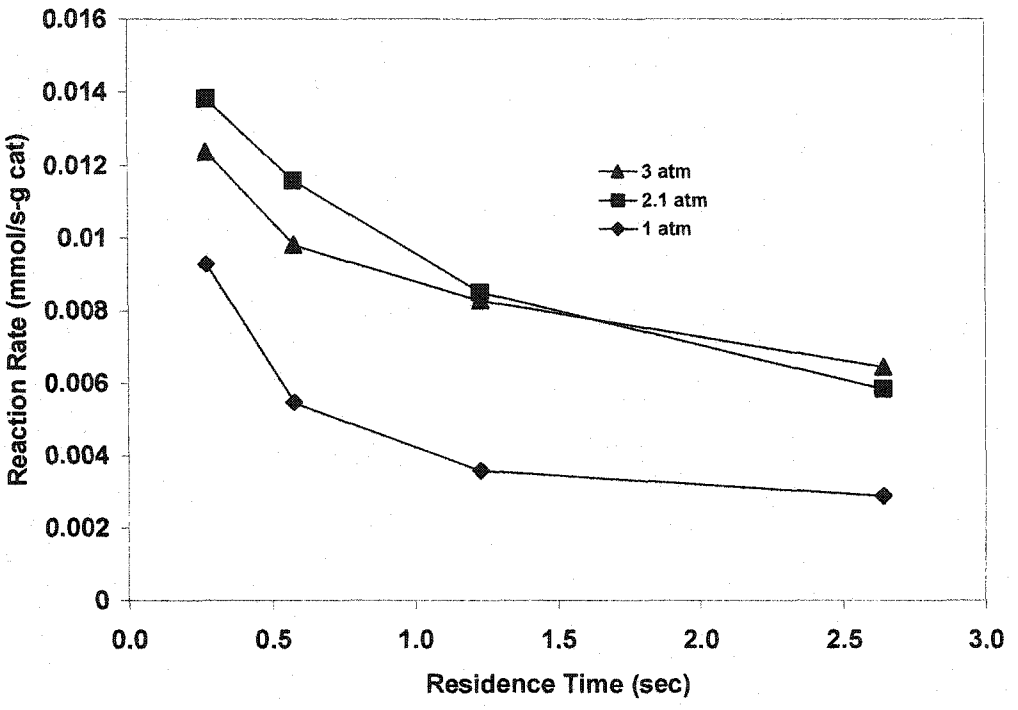

Figure 4.12 Methane reaction rate versus residence time at varying total system pressure. 2/1 H_2/CH_4 with 2% oxygen, NaOH Y zeolite

4.5 Acknowledgements

The authors would like to express their appreciation to the United States Department of Energy (Contract DE-FG21-94MC31170) and the National Science Foundation for sponsoring a Graduate Research Traineeship in Environmentally Friendly Natural Gas Technologies. Some of the experimental work was performed by Duc Le, and his help is greatly appreciated. In addition, the assistance from P. Howard, T. Caldwell, D. Larkin, H. Le, and L. Zhou is appreciated.

4.6 References

1. Balasubramanian, B., A. Lopez Ortiz, S. Kaytakoglu and D.P. Harrison, *Hydrogen from methane in a single-step process.* Chemical Engineering Science, 1999. **54**: p. 3543-3552.

2. Armor, J.N., *The multiple roles for catalysis in the production of hydrogen.* Applied Catalysis A: General, 1999. **176**: p. 159-176.

3. Scholz, W.H., *Processes for industrial production of hydrogen and associated environmental effects.* Gas separation & purification, 1993. 7(3): p. 131.

4. Liu, C.J., R.G. Mallinson and L.L. Lobban, *Nonoxidative methane conversion to acetylene over zeolite in a low temperature plasma.* Journal of catalysis, 1998. **179**: p. 326-334.

5. Liu, C.-J., A. Marafee, B.J. Hill, G. Xu, R.G. Mallinson and L.L. Lobban, *Oxidative coupling of methane with ac and dc corona discharge.* Industrial & Engineering Chemistry Research, 1996. **35**(10): p. 3295-3301.

6. Marafee, A., C.-J. Liu, G. Xu, R.G. Mallinson and L.L. Lobban, *An experimental study on the oxidative coupling of methane in a direct current corona discharge reactor over Sr/La2O3 catalyst.* Industrial & Engineering Chemistry Research, 1997. **36**: p. 632-637.

7. Howard, P.J., L.L. Lobban and R.G. Mallinson, *Methane conversion using a dc corona discharge over NaOH-treated NaX zeolite*, in *School of Chemical Engineering and Materials Science*. 1999, University of Oklahoma: Norman. p. 99.

CHAPTER 5 - Selective hydrogenation of acetylene to ethylene during the conversion of methane in a catalytic dc plasma reactor

5.1 Introduction

It is generally agreed that natural gas will become increasingly important as a petrochemical feedstock and source of liquid fuels. Natural gas reserves are abundant throughout the world. A limitation to the utilization of the reserves is the transportation of the natural gas to the desired location.

Methane can be activated by group VIII metals and oxidized to syngas [1]. Therefore, most processes being implemented/investigated involve the production of synthesis gas from methane, followed by a process that utilizes the synthesis gas in the production of fuels or chemicals, e.g. Fischer-Tropsch and methanol synthesis.

The cost of synthesis gas production can amount to about 60% of the total cost of the process. Much of this cost is for the production of oxygen. Cryogenic separation of air requires a very large scale to lower its unit production cost, but it is still expensive even at these large scales. Thus, it would desirable to convert methane directly to a more valuable product, such as C_2 hydrocarbons.

C_2 hydrocarbons consist of acetylene, ethylene, and ethane. Ethane is primarily used for the formation of ethylene by dehydrogenation, and ethylene has largely replaced acetylene as a petrochemical building block. The United States alone produces nearly 60 billion pounds of ethylene per year. Ethylene is highly reactive, due to its double bond, allowing it to be converted to a large assortment of products by addition, oxidative, and polymerization reactions. It is primarily used in the production of plastics, fibers, films, resins, adhesives, and elastomers [2], but is can also be oligimerized to liquid hydrocarbons.

Ethylene can be derived from many different feedstocks. The feedstock, and the resulting process, varies depending on the region. Table 5.1 lists different feedstocks used in the production of ethylene and their relative amounts in the United States. However, for Western Europe and Japan naphtha is the primary feedstock for the production of ethylene since natural gas is less abundant.

The thermal cracking of petroleum based naphtha with steam, known as pyrolysis, is used for over 97% of the worldwide production of ethylene. This

Table 5.1 Ethylene feedstocks in the U.S.A.

Ethane	27-30 billion pounds
Propane	8-10 billion pounds
Naphtha	10 billion pounds
Other	10 billion pounds

process uses a feed stream that is a mixture of hydrocarbons and steam. The stream is preheated to a temperature of 500-650°C, and then raised to 750-875°C in a controlled manner in a radiant tube [3]. In the radiant tube the hydrocarbons crack into the major products: ethylene, olefins, and diolefins. Due to the high temperatures required for the endothermic reaction, an intensive energy input is required to drive the process. The large amount of by-products resulting from the use of the heavy hydrocarbon feedstock also requires oversized equipment for the resulting ethylene quantity.

The production of ethylene from ethane is also done by steam cracking. Not including methane, ethane requires both the highest temperature and the longest residence time to achieve acceptable conversion [3]. A typical ethane process operates near 60 % conversion of ethane and achieves an ethylene selectivity of 85%. This process uses the burning of the unwanted by-products to provide the necessary heat for the endothermic reaction. Over 10% of the ethane is thereby converted into carbon dioxide, and nitrogen oxides are also formed by the combustion. Production of ethylene by steam cracking is a large contributor to greenhouse gases [4]. It is desired, therefore, to introduce technologies that will reduce the emission of greenhouse gases during the production of ethylene.

It is already known that the use of methane as a petrochemical feedstock can lead to environmentally friendly technologies. The production of hydrogen by means of steam reforming is the only significant use of natural gas in the petrochemical industry. Steam reforming of methane is the industry's cleanest option for the

production of hydrogen. Steam reforming of methane results in one carbon dioxide released for every four hydrogen molecules produced. On the other hand, the partial oxidation of coal results in a 1:1 production of carbon dioxide and hydrogen.

It has also been shown [5] that plasma reactors can activate methane at low temperatures. Low temperature plasmas offer the potential for efficient processes for direct conversion of methane to higher value products or the widely used intermediate, synthesis gas. The reaction is driven by highly energetic electrons that are created by applying an electric potential across the reaction volume. The low temperature plasma makes use of these excited electrons as initiators in what is predominantly a free radical pathway for conversion. The bulk gas temperature remains relatively low, allowing for unique, non-equilibrium product distributions.

In addition, the systems can run with little or no oxygen, eliminating the need for costly oxygen plants. The primary role of oxygen and hydrogen in the feed is to inhibit coke formation, which alters the discharge. There is no distinguishable change in methane conversion from 0.4% to 6% oxygen, only an increase in stability due to a reduction in carbon formation. Oxygen concentrations greater than 2% by volume allow for stable operation.

Thus, a plasma system overcomes two major obstacles needed for an economic process for methane conversion: 1) no energy intensive preheating/cooling (requiring large-scale energy integration) of the gas which may not be completely recoverable, and 2) small oxygen source needed (could be air or oxygen enriched air).

However, the main products are still gases that present a similar problem concerning remote locations and the transportation of gases.

Figure 5.1 shows a simplified flowsheet of a plasma process. The major feed components of the plasma system are the feed gases and electricity. Therefore, the plasma system might be coupled with a natural gas based power plant. The power plant could provide both power and natural gas to the system. It could be designed to run full time at a given production rate or designed to take advantage of off-peak times of the power plant. This chapter will discuss the use of a dc plasma catalytic reactor for the production of C_2 hydrocarbons and/or synthesis gas (H_2 and CO).

5.2 Experimental

The experimental apparatus is similar to the system that has been described previously [5, 6]. The feed gases consisted of a combination of methane, oxygen, hydrogen, and helium. Helium was only used in initial experiments and for characterization studies of the catalyst. The feed gas flowrates were controlled by Porter mass flow controllers, model 201. The feed gases flowed axially down the reactor tube. The reactor is a quartz tube with a 9.0 mm O.D. and an I.D. of either 4.5 mm or 7.0 mm.

A point-to-plane electrode configuration was employed, meaning that the top electrode is a wire point electrode and the bottom electrode is a flat plate that also serves as a support for the catalyst, Figure 2.2. The top electrode is positioned concentrically within the reactor, and the gap between its tip and the plate is 8.0 mm.

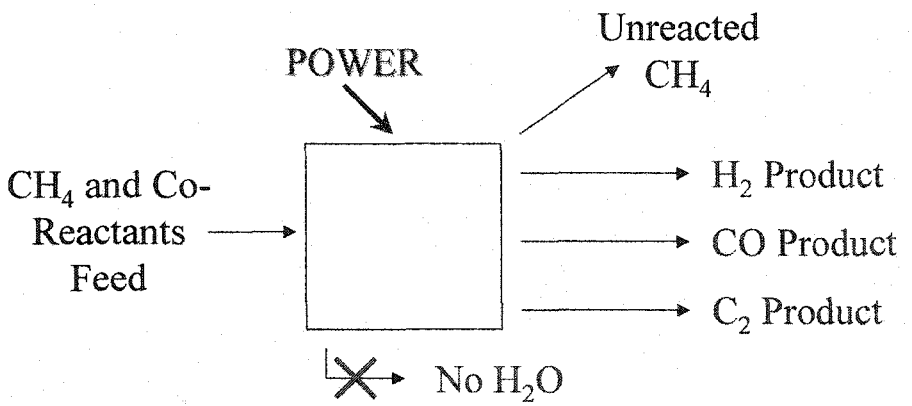

Figure 5.1 Simplified flowsheet of plasma process.

The dc corona discharge is created using a high voltage power supply (Model 210-50R, Bertan Associates Inc.).

The preparation and characterization of the NaOH treated Y zeolite has been discussed elsewhere [7, 8]. Palladium was added using chemical vapor deposition according to the following procedure. The NaOH Y zeolite was calcined at 400°C, then mixed with the appropriate amount of palladium acetylacetonate to achieve the desired Pd loading (ranging from 0.025 to 1 wt%). The mixture was then heated slowly under vacuum to a temperature of 130°C to disperse the palladium throughout the NaOH Y zeolite. This Pd on NaOH Y zeolite will henceforth be referred to as Pd-Y zeolite. The Pd-Y zeolite was then calcined for the final time to a temperature of 350°C.

Subsequent preparations of Pd-Y and Ag-Pd-Y catalysts used the incipient wetness technique. At the low loadings used, there were no distinguishable differences in the performance of the catalyst when comparing chemical vapor deposition and incipient wetness.

The incipient wetness of the Y zeolite was found by adding water to a known amount of catalyst until the catalyst could not take up any more water. A solution of tetraaminepalladium (II) nitrate was made such that for the amount of catalyst to be prepared, the amount of solution used for incipient wetness would provide the desired metal loading on the catalyst, 0.025 wt% Pd-Y zeolite. The catalyst was dried for 8 hours in a 110°C oven to remove the water. The catalyst was then subsequently calcined in air for a total of 6 hours. The catalyst was heated to 350°C over the first

two hours, then left at 350°C for 4 hours. This catalyst will be referred to as 0.025 wt% Pd-Y zeolite. The catalyst was reduced in flowing hydrogen at 350°C prior to each experiment.

The silver-palladium Y zeolite was prepared in a similar manner using the incipient wetness technique. Silver was added to the 0.025 wt% Pd-Y zeolite using silver nitrate. The incipient wetness of the catalyst was assumed to be the same as determined previously. The catalyst was dried and calcined in the same manner as the 0.025 wt% Pd-Y zeolite. Loadings of 0.01 wt%, 0.025 wt%, and 0.1 wt% Ag on 0.025 wt% Pd-Y zeolite were prepared.

The fresh catalyst is pretreated in the reactor before each experiment. The NaOH Y zeolite is heated at 250°C to remove any moisture from the catalyst. The Pd-Y zeolite is reduced in 30 ml stream of hydrogen for 4 hours. The temperature is slowly ramped to 350°C during the first two hours, then held at 350°C for the final two hours.

As mentioned before, this system operates at low temperatures. A furnace around the reactor is used to heat the system to the desired temperature. However, when the desired operating temperature is below 373 K it is necessary to use cooling air across the tube exterior to control the temperature since the plasma itself does heat the gas to some extent. The temperature measured on the outside has been calibrated against the internal temperature of the reactor, and has been discussed elsewhere [7, 8].

The product gases are passed through a dry ice/acetone bath that allows for any condensable organic liquids to be separated from the product gases. It should be noted that the dc system does not produce any measurable liquids, including water. The effluent gases can be analyzed on-line by either a gas chromatograph or a mass spectrometer.

5.3 Results and Discussion

5.3.1 In-Situ Selective Hydrogenation of Acetylene using a Pd-Y zeolite

The catalytic dc plasma reactor has shown to produce high yields of C_2 hydrocarbons, hydrogen, and carbon monoxide at reasonable methane conversions. It is desired, due to many factors, to shift the acetylene production to ethylene. Pd supported catalysts are commonly used for the selective hydrogenation of acetylene to ethylene. These catalysts usually convert acetylene at low concentrations in ethylene streams to ethylene with a very high selectivity. The Pd-Y zeolite prepared by CVD was used to study the in-situ production of ethylene from acetylene (where the acetylene comes from the conversion of methane). Figure 5.2 shows the effect of different Pd loadings on methane conversion and acetylene, ethylene, and ethane selectivity.

The methane conversion is fairly independent of Pd loading when compared to the parent Y zeolite. The C_2 selectivities vary greatly depending on the Pd loading. As the Pd loading is increased, the amount of acetylene that is hydrogenated increases

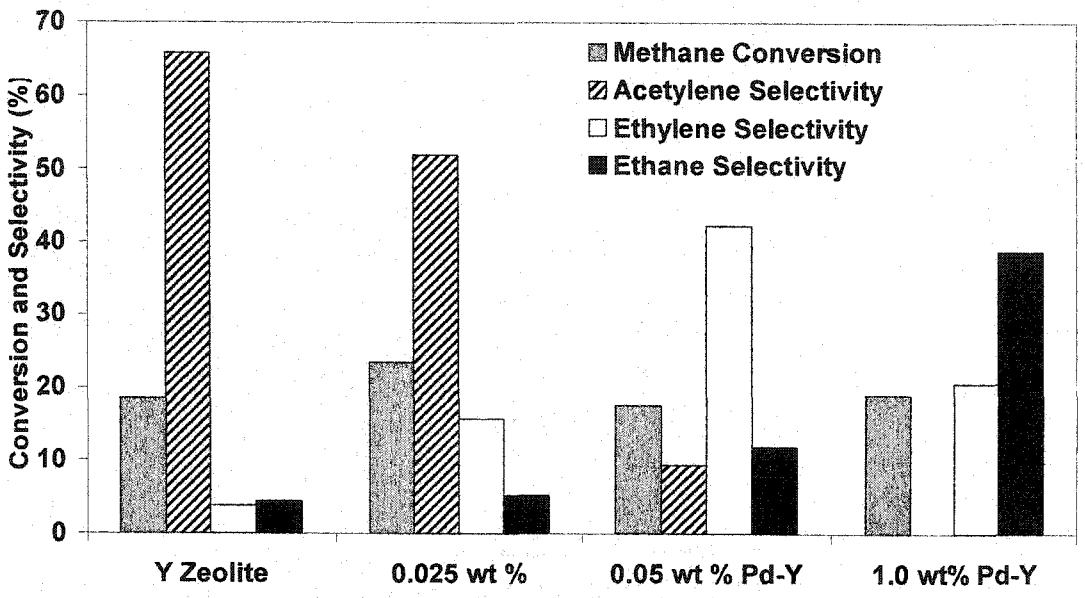

Figure 5.2 Effect of different Pd loadings on methane conversion and hydrocarbon selectivity. 2/1 H_2/CH_4 with 2% O_2, 7200 hr^{-1}, 3.9 watts, 45°C

until all of the acetylene is hydrogenated at 1.0 wt% Pd. At low Pd loadings, ethylene is the major hydrogenated product, while at the high loadings ethane predominates. This dependence is believed to be due to the amount of Pd available for hydrogenation to ethylene and ethane. It is thought that low amounts of palladium and small Pd ensembles favor the hydrogenation to ethylene, while excess Pd and large Pd clusters allow for the produced ethylene to be further hydrogenated to ethane. Acetylene's adsorption strength is higher than that of ethylene, resulting in the desorption of ethylene before it can be further hydrogenated to ethane when metal site availability is limited. However, the 1.0 wt% Pd loading has larger Pd ensembles that lead to the formation of ethane.

It was also found that oxygen plays a major role in the selectivity of the hydrogenation catalyst, probably via production of carbon monoxide. Previous researchers found that carbon monoxide reduced the hydrogenation of ethylene to ethane because of its higher adsorption strength than ethylene.[9]. In our studies we noticed a large effect on selectivity when carbon monoxide is present at low temperatures; however, it was not the usual inhibition of ethylene hydrogenation, but rather acetylene hydrogenation (Figure 5.3 and 5.4).

As seen from Figures 5.3 and 5.4, carbon monoxide affects the hydrogenation of acetylene to ethylene and ethane. When oxygen is removed from the feed, all of the acetylene is hydrogenated. Carbon monoxide seems to reduce the number of Pd sites that are available for the hydrogenation of acetylene. Similarly, when the system is operating without oxygen and carbon monoxide is injected in the system,

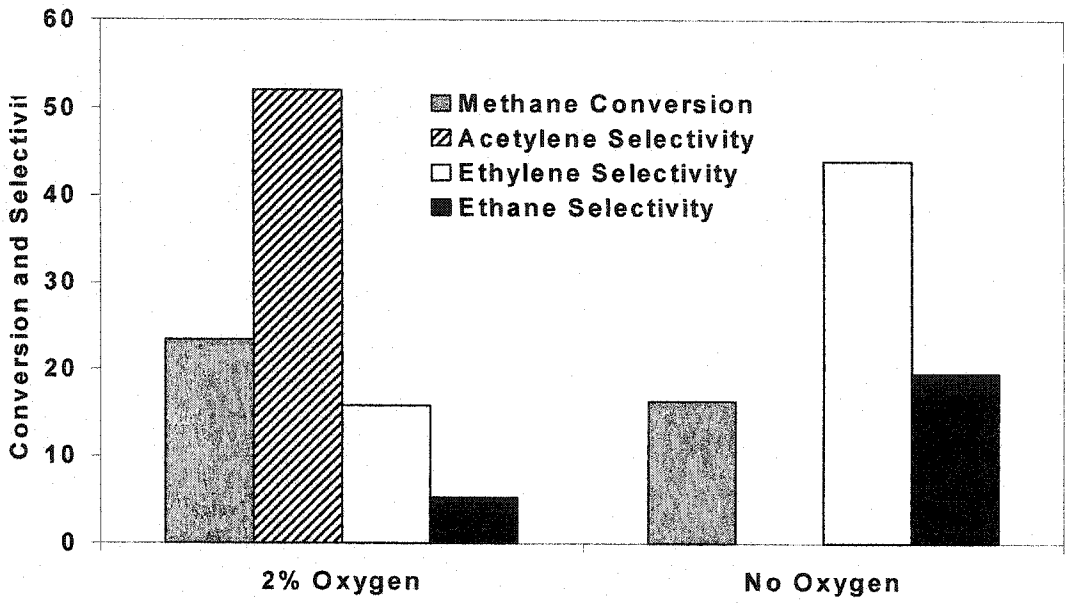

Figure 5.3 Effect of oxygen on methane conversion and hydrocarbon selectivity. 0.025 wt% Pd-Y zeolite, 2/1 H_2/CH_4 with x% O_2, 7200 hr^{-1}, 3.9 watts, 45°C

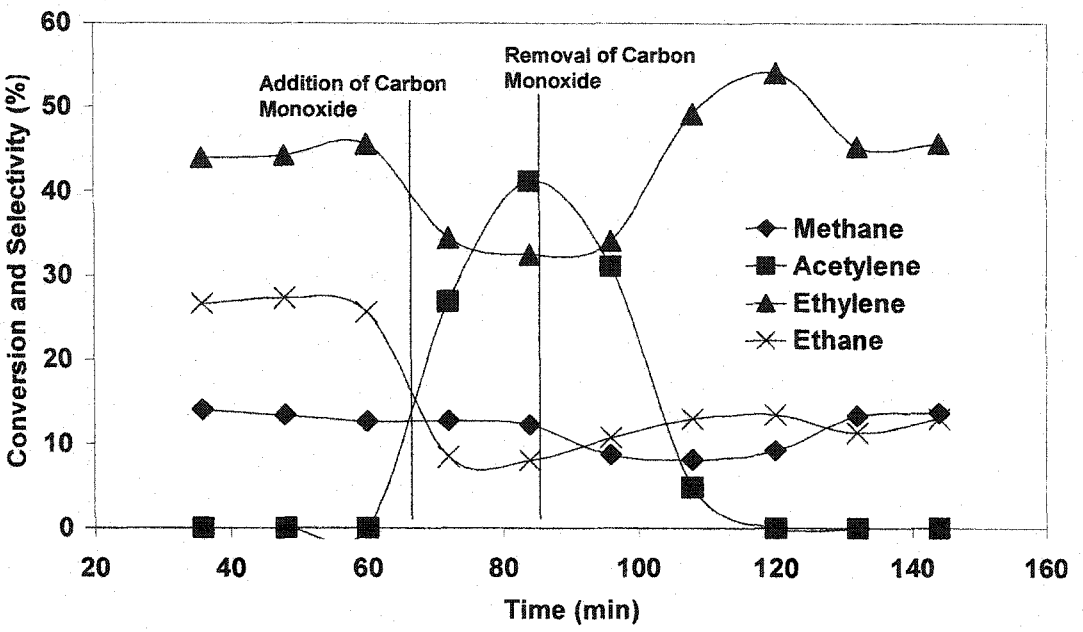

Figure 5.4 Effect of addition and removal of carbon monoxide on methane conversion and hydrocarbon selectivity. 0.025 wt% Pd-Y zeolite, 2/1 H_2/CH_4 with x% O_2, 7200 hr^{-1}, 3.9 watts, 45°C

acetylene (not present before) becomes the major product and immediately disappears upon removal of carbon monoxide.

The operating temperature plays a large role in the activity of the Pd catalyst, Figure 5.5. As the temperature is increased from room temperature to 100°C, the acetylene is completely hydrogenated to ethylene and ethane. Ethylene goes through a selectivity maximum at around 50°C. Above 50°C, the selectivity decreases due to the over hydrogenation to ethane. At temperatures above 95°C, ethane is the only C_2 hydrocarbon produced. Therefore, it is desirable to operate at low temperatures at which good conversions can still be achieved in the plasma discharge.

5.3.2 In-Situ Selective Hydrogenation of Acetylene using a Ag-Pd-Y zeolite

Work has been successful for the in-situ selective hydrogenation of the acetylene to ethylene by the addition of Pd to the parent Y zeolite [10]. Figure 5.6 shows the effect of the addition of palladium and silver to the parent Y zeolite. Methane conversion is independent of metal loading; however, C_2 selectivities are very dependent upon metal loading. The 0.025 wt% Pd-Y selectively hydrogenates the acetylene that is produced in the gas phase into ethylene and ethane. The optimum temperature for ethylene production with the 0.025 wt% Pd-Y zeolite is 45°C. The addition of 0.025 wt% Ag to the 0.025 wt% Pd-Y zeolite increases the selectivity of ethylene by reducing the over hydrogenation to ethane. In addition, silver shifts the optimum temperature for ethylene production to 85°C.

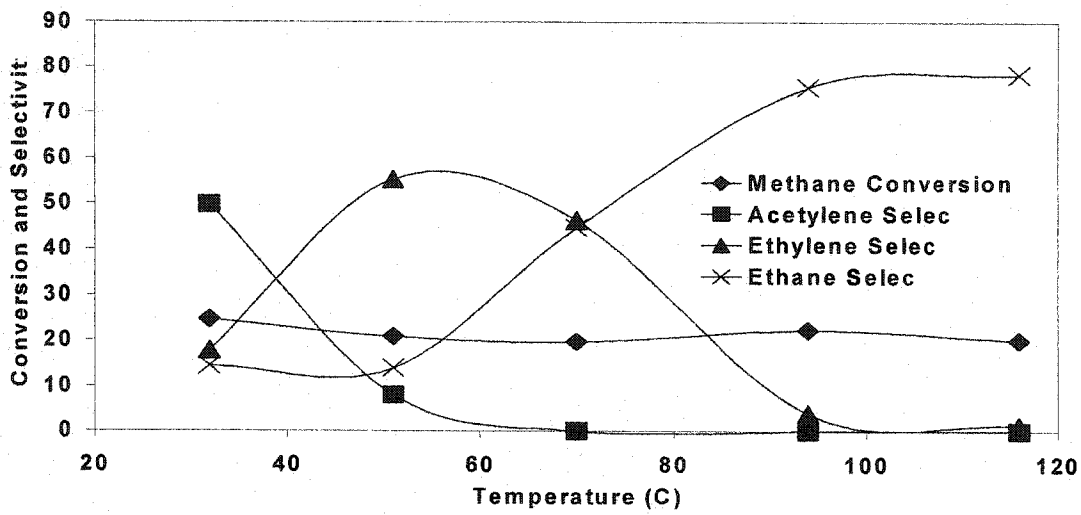

Figure 5.5 Effect of temperature on methane conversion and hydrocarbon selectivity. 0.025 wt% Pd-Y zeolite, 2/1 H_2/CH_4 with no O_2, 7200 hr^{-1}, 3.9 watts

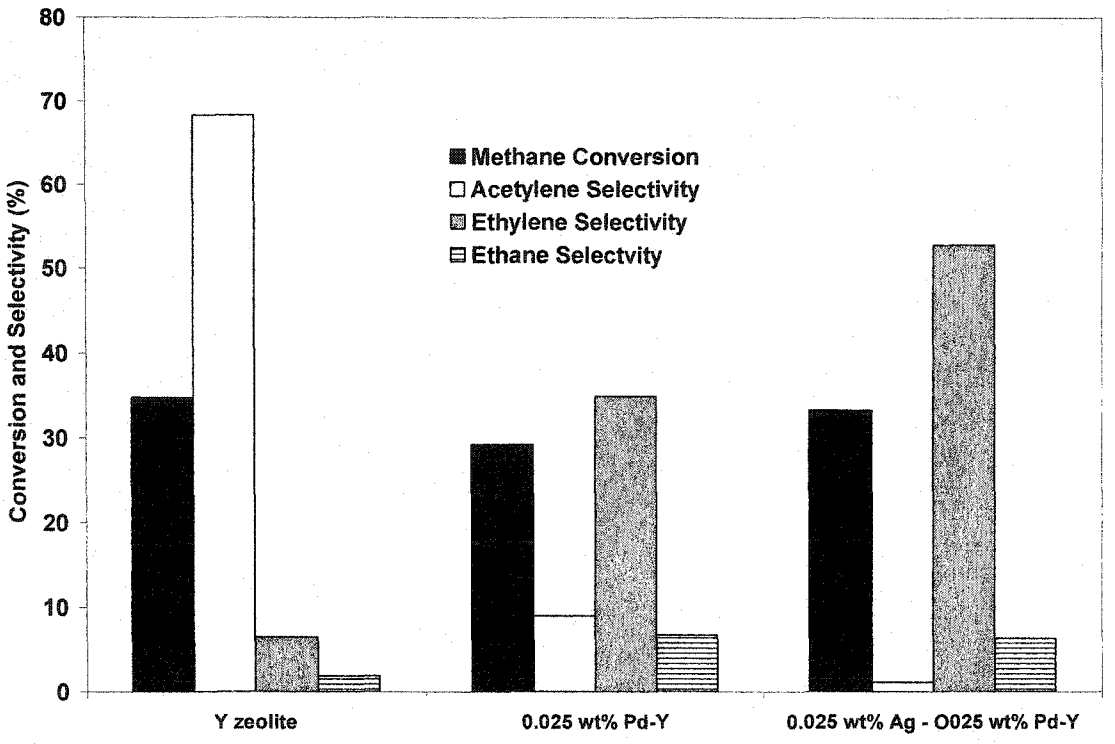

Figure 5.6 Effect of metal loading on C_2 selectivity. 1/1 H_2/CH_4 with 2% O_2, 1.2 sec residence time, 4.55 watts. 7 mm I.D., 0 psig. Temperature optimized for each catalyst to produce the highest selectivity of C_2H_4

5.3.3 Effect of residence time

It is desired to produce a high yield of ethylene. This can be achieved by having high methane conversions and maintaining high selectivities. A characteristic of the plasma process is that the product selectivities vary only slightly as the methane conversion increases or decreases. Figure 5.7 shows that as the residence time is increased the methane conversion increases without any effect on overall C_2 selectivity. Thus, the C_2 yield increased from 10% to 30% over the residence time variation of 0.54 to 2.6 seconds. However, there is an increase in the energy consumption (eV per molecule of CH_4 converted). This is a measure of the amount of power that is input as compared to the number of methane molecules converted.

5.3.4 Higher Methane Partial Pressures and Energy Efficiency

It is the decrease in the methane throughput that results in the increase in eV per molecule shown in Figure 5.7. One way to increase the methane throughput is to increase the methane fraction in the feed. Figure 5.8 shows the results of varying the feed composition. The methane fractional conversion does not vary significantly, but the increase in the feed partial pressure of methane results in a decrease in eV per molecule of methane converted (the power input is constant). In addition, there is an increase in the overall C_2 selectivity resulting in an increase in C_2

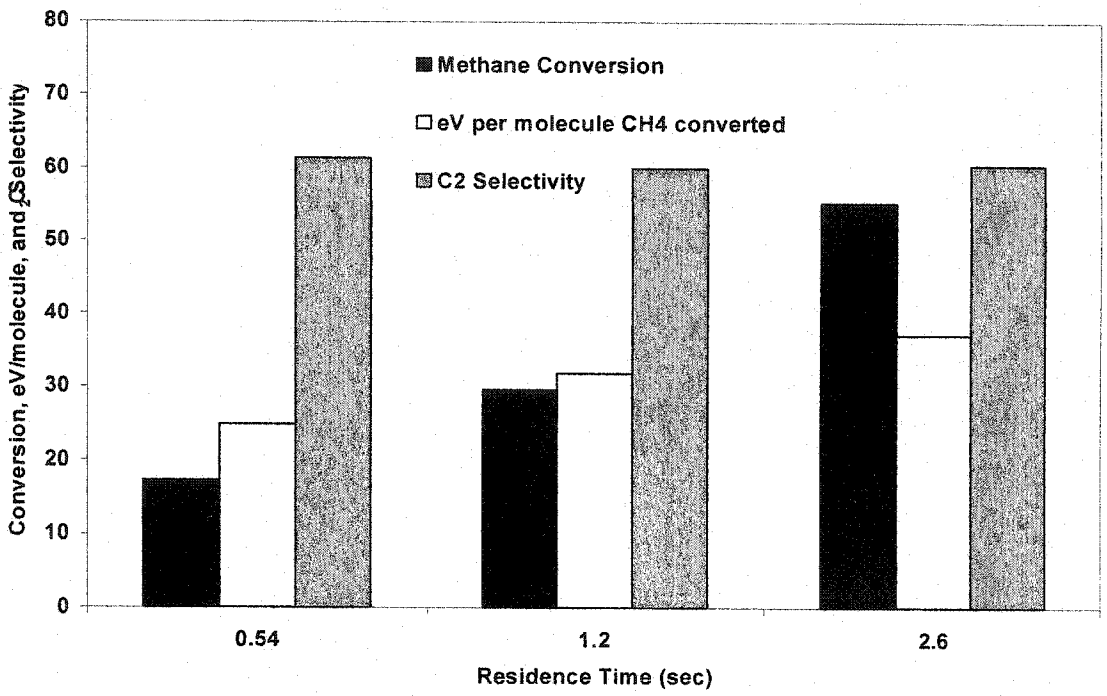

Figure 5.7 Effect of residence time on methane conversion, power consumption, and overall C_2 selectivity. 0.025 wt% Ag – 0.025 wt% Pd-Y zeolite, 1/1 H_2/CH_4 with 2% O_2, 4.55 watts. 7 mm I.D., 0 psig.

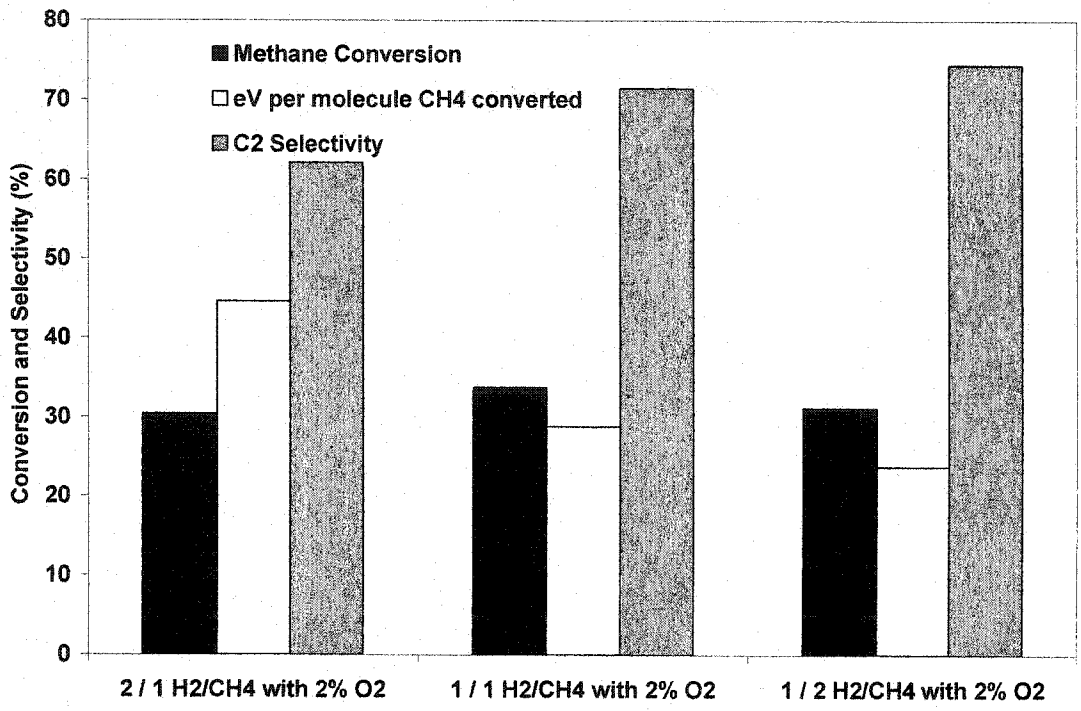

Figure 5.8 Effect of feed composition on methane conversion, power consumption, and overall C2 selectivity, 0.025 wt% Pd-Y zeolite, 4.55 watts. 7 mm I.D., 0 psig.

yield. Without the addition of metals to the catalyst, the maximum CH_4/H_2 ratio that allowed for stable operation was 1. Anything with more methane than hydrogen resulted in excess coke formation, which in return resulted in an unstable discharge. However, with Ag and Pd metals on the Y zeolite, the discharge is stable with methane fractions as high as 98%, though 2% oxygen is needed in all cases, Figure 5.9. The feed containing 98% methane has yielded the lowest eV/molecule of methane converted to date, 10eV/molecule. The higher partial pressure of methane seems to increase the reaction rate allowing for similar overall fractional conversion. Thus, with a constant power input, the energy requirements per methane converted (eV / molecule CH_4 converted) decreases. Moreover, removing hydrogen from the feed, reduces the cost of separating large fractions of hydrogen out of the product stream.

In addition, another way to reduce the energy consumption would be to maintain the conversion with decreased input power. Right now the power is assumed to be constant over time. However, several studies have led to the discovery that the discharge actually pulsates, though the pulsation is not visible to the naked eye. If the system is modeled as a pulse dc power discharge, the power input could be significantly reduced. Thus, the power would only be input in the small time frames, instead of the assumption of constant power. This would reduce the eV/molecule CH_4 converted in each case by up to 80%. Figure 5.10 shows the oscilloscope printout of the dc discharge with an applied voltage of 10 kV and a stable discharge appearance.

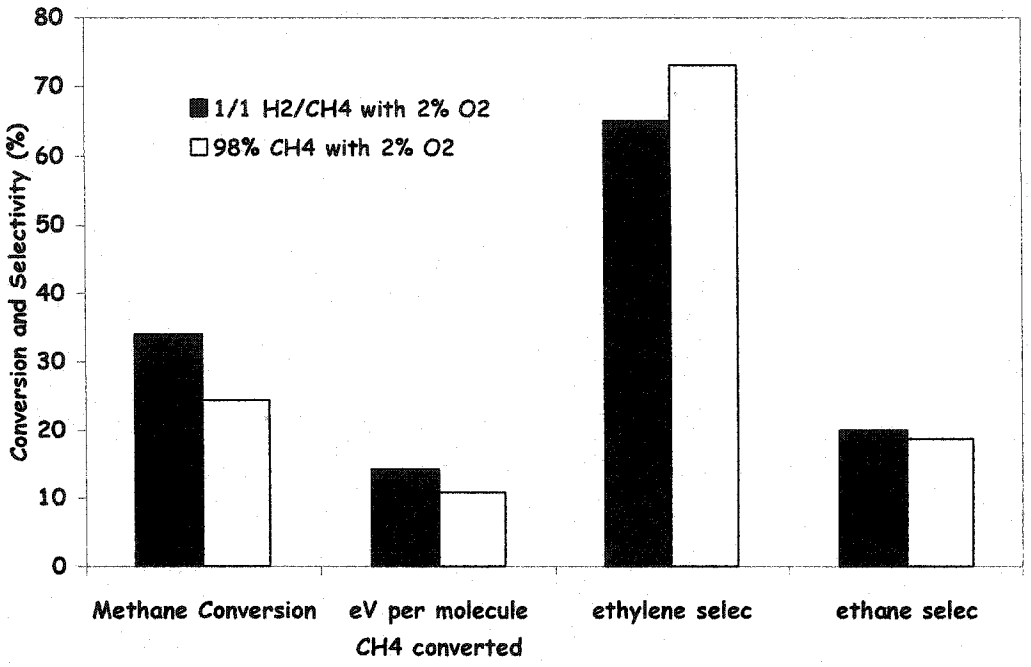

Figure 5.9 Effect of higher methane partial pressures on conversion, selectivity and energy efficiency. 10 kV, 0 psig, 0.025 wt% Ag- 0.025 wt% Pd-Y zeolite.

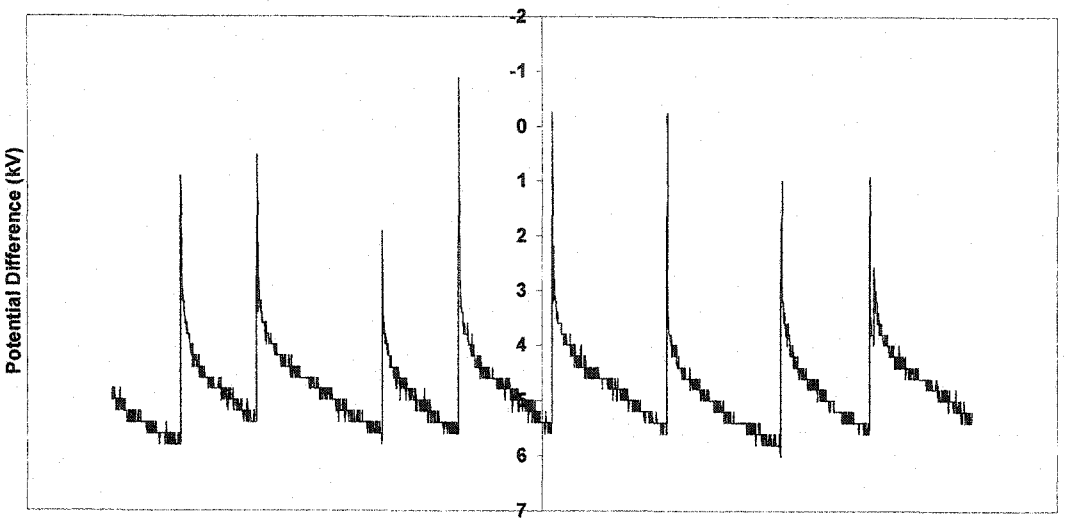

Figure 5.10 Oscilloscope output of the dc plasma discharge voltage during a stable streamer discharge.

5.3.5 Economic Analysis

To put the current results into context, a number of economic scenarios may be formulated to assist in determining the direction for optimization of a process. A simplified initial economic analysis similar to the analysis outlined by Douglas [11] is presented. The first step is determining the economic potential of the process. The economic potential is defined as the difference between the product values and the raw material costs. In this case, electricity is considered as a raw material (this could be considered as the natural gas required to generate the power). A co-production (electricity and chemicals) process can be envisioned if the plasma conversion process were to be incorporated with a natural gas based peaking power plant. Low temperature plasmas can be started up and shut down quite rapidly, and operation only during off peak power hours is possible. It is assumed that the cost of the electricity would be no greater than the off-peak price. The natural gas cost would be associated with the contract price of the power plant; however, the excess gas during off-peak could come at a substantially reduced cost. Table 5.2 shows the energy costs of the process for different conversions based on a power consumption for the conversion of 10 eV/molecule. It is assumed that the valuable products, ethylene and hydrogen, are separated out of the product stream and the remaining stream may be fed directly to the power generation plant. Thus, the only cost of the feed natural gas is for the converted portion of methane. An off-peak electricity cost of $0.025/kWh and natural gas costs of $0.50 and $2.50/MMBtu were assumed for the analysis.

Table 5.2 Energy Cost of Plasma Process

100 kg* of CH_4 feed	Electricity Cost** $0.025/kWh	Natural Gas Feed Cost*** $0.50/mmBtu	$2.50/mmBtu
10% Conversion	$0.84	$0.05	$0.25
25% Conversion	$2.09	$0.13	$0.63
50% Conversion	$4.19	$0.25	$1.27

*20 kg CH_4 = 44.5 lb CH_4 = 1264 g moles = 1000 ft^3 CH_4 = 1 mmBtu

**Based on power consumption of 10 eV/molecule of methane converted

***Reactor feed

The valuable products consist of C_2 hydrocarbons and hydrogen. For the product values, ethylene has a value of \$0.015/mole, and the Department of Energy has projected a production goal for hydrogen of \$0.002/mole [12]. Table 5.3 shows a summary of the value of the product stream from the plasma process. For a given feed composition and reactor condition, the product selectivities are independent of methane conversion. Hydrogen and ethylene selectivities of 75% and 65%, respectively, were used for this analysis.

Table 5.4 shows that it is necessary to get the natural gas at a reduced cost to produce a profit at this power consumption level. Economic potential is calculated as the difference between the value of the products (ethylene, hydrogen and ethane) and the cost of the electricity and the consumed methane. The electrical cost is the major portion of the energy cost (>90%); therefore, if the electrical costs can be reduced then the economic potential will increase dramatically. Figure 5.11 shows the effect of electrical cost (eV/molecule of methane converted) on profit margin, with the other factors held constant.

The conversion results presented in this paper have electrical consumptions higher than 20 eV/molecule. However, the dc system and an ac system [13] have significantly lower power consumptions under different conditions. To date, the dc systems lowest power is 13 eV/molecule converted. There has not yet been any investigation into the optimization of the dc power supply, which could reduce the

Table 5.3 Product values

100 kg of CH_4 feed	Value of Products	
	Hydrogen	Ethylene
10% Conversion	$0.38	$0.61
25% Conversion	$0.94	$1.52
50% Conversion	$1.87	$3.05

Table 5.4 Economic Potential

100 kg of CH_4 feed	Product Value – Energy Cost	
	\$0.50 / MMBtu	\$2.50 /MMBtu
10% Conversion	\$0.10	-\$0.10
25% Conversion	\$0.24	-\$0.26
50% Conversion	\$0.48	-\$0.54

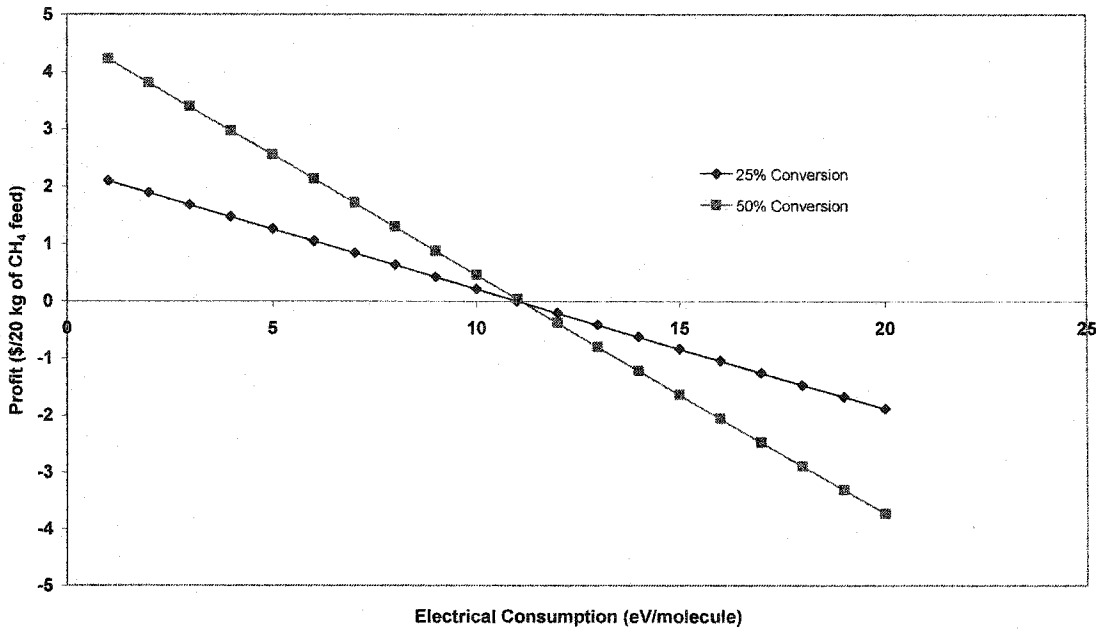

Figure 5.11 Effect of electrical consumption on profit. Hydrogen selectivity, 75%; ethylene selectivity, 65%; ethylene, $0.015/mole; hydrogen, $0.002/mole; electricity, $0.025/kWh; natural gas, $0.50/mmBtu

power consumption of the process. The ac system has achieved electrical consumptions as low as 2.5 eV/molecule, thus producing hydrogen at a cost of $0.002/mole (at the DOE target). Again, there has been no effort to optimize the power supply and transformer associated with the ac plasma process.

5.4 Conclusions

The addition of palladium to the Y zeolite used in the catalytic dc plasma reactor allows for the hydrogenation of acetylene to ethylene and ethane. Currently, operating around 50°C and with low levels of oxygen allows for greater selectivity control to the desired ethylene. Further studies and characterization should allow for improvements in the selectivity of ethylene via acetylene hydrogenation.

The catalytic dc plasma reactor can achieve high methane conversions while also maintaining high selectivities. One niche market might be to synergistically incorporate with a natural gas-based power plant. The electrical power requirements have not yet been optimized; doing so would improve the economics. If hydrogen production is not the primary objective, the initial acetylene that is produced in the gas phase can be selectively hydrogenated in-situ to ethylene by the use of palladium on the parent Y-zeolite. Also, further increases in selectivity and operating temperature are achieved by the addition of silver. The system has achieved ethylene yields as high as 30%, with similar hydrogen yields and little production of

combustion products CO_2 and H_2O. It is expected that the C_2 yield can be further improved with optimization.

5.5 Acknowledgements

The authors would like to express their appreciation to ChevronTexaco Inc., the United States Department of Energy (Contract DE-FG21-94MC31170), and the National Science Foundation for sponsoring a Graduate Research Traineeship in Environmentally Friendly Natural Gas Technologies. Duc Le's help on the experimental work is greatly appreciated.

5.6 Literature Cited

1. Rostrup-Nielsen, J.R., *Catalysis and large-scale conversion of natural gas.* Catalysis Today, 1994. **21**: p. 257-267.

2. McKetta, J.J., ed. *Encyclopedia of Chemical Processing and Design.* . Vol. 20. 1986, Marcel Dekker: 1984. 88-159.

3. Gerhartz, W., *Ullman's Encyclopedia of Industrial Chemistry.* Vol. A10. 1987, Weinheim: VCH. 45.

4. Jacoby, M., *New ethylene process is environmentally-friendly*, in *C&EN*. 1999. p. 6.

5. Liu, C.J., R.G. Mallinson and L.L. Lobban, *Nonoxidative methane conversion to acetylene over zeolite in a low temperature plasma.* Journal of catalysis, 1998. **179**: p. 326-334.

6. Gordon, C.L., L.L. Lobban and R.G. Mallinson, *The production of hydrogen from methane using tubular plasma reactors*, in *Advances in hydrogen energy*, C. Gregoire-Padro, Editor. 2000, Kulmer.

7. Liu, C.-J., A. Marafee, B.J. Hill, G. Xu, R.G. Mallinson and L.L. Lobban, *Oxidative coupling of methane with ac and dc corona discharge.* Industrial & Engineering Chemistry Research, 1996. **35**(10): p. 3295-3301.

8. Marafee, A., C.-J. Liu, G. Xu, R.G. Mallinson and L.L. Lobban, *An experimental study on the oxidative coupling of methane in a direct current corona discharge reactor over Sr/La2O3 catalyst.* Industrial & Engineering Chemistry Research, 1997. **36**: p. 632-637.

9. Price, G.L. and Y.H. Park, *Deuterium tracer study on the effect of CO on the selective hydrogenation of acetylene over Pd/AL2O3.* Industrial Engineering and Chemical Research, 1991. **30**: p. 1693-1699.

10. Gordon, C.L., L.L. Lobban and R.G. Mallinson, *Selective hydrogenation of acetylene to ethylene during the conversion of methane in a catalytic dc plasma reactor*, in *Natural Gas Conversion VI*, J.J. Spivey, E. Iglesia, and T.H. Fleisch, Editors. 2001, Elsevier Science: Amsterdam. p. 271-276.

11. Douglas, J.M., *Conceptual design of chemical processes*. Chemical Engineering Series, ed. B.J. Clark. 1988: McGraw Hill. 601.

12. DOE, *Strategic Plan for DOE Hydrogen*, . 1998, www.doe.gov.

13. Caldwell, T.A., H. Le, L.L. Lobban and R.G. Mallinson, *Partial oxidation of methane to form synthesis gas in a tubular AC plasma reactor*, in *Natural Gas Conversion VI*, J.J. Spivey, E. Iglesia, and T.H. Fleisch, Editors. 2001, Elsevier Science: Amsterdam. p. 265-270.

CHAPTER 6 - In-Situ Selective Hydrogenation of High Concentrations of Acetylene over a Pd and Ag-Pd Y-Zeolite Catalyst in a DC Plasma Reactor

6.1 Introduction

The production of acetylene as a chemical or feedstock has decreased over the last few decades. However, there are still many processes that produce acetylene as a product or as a by-product in significant quantities. These processes include electrical discharge processes (Huels and current research), flame or partial oxidation processes, and pyrolysis processes [1]. High yields of acetylene have been achieved by the non-oxidative conversion of methane in a dc plasma reactor [2]. In addition, the pyrolysis of methane results in the production of acetylene. An advantage of the

pyrolysis of methane over heavier hydrocarbon feedstocks is that there are fewer products and intermediate species involved in methane pyrolysis [3].

Since few chemical processes utilize acetylene as a chemical feedstock, there is a need for the direct conversion of acetylene to a more valuable product. One solution is uses the basis of a developed process: the selective hydrogenation of acetylene to ethylene by a Pd based catalyst. This process has been used to reduce the acetylene concentrations in a polymer grade ethylene stream to 5-20 ppm in order to prevent the poisoning of the polymerization catalyst. However, the acetylene concentrations encountered are usually quite low, 500 - 0.5% acetylene.

The amount of acetylene in this study is considerably higher than a normal feed concentration in a front-end hydrogenation unit. A normal front-end hydrogenation unit is responsible for the removal of up to 0.5% acetylene, while the present catalyst selectivity hydrogenates upwards of 5% acetylene concentrations. The addition of silver to the Pd-Y zeolite results in improved selectivity to ethylene and minimizes effects of feed stream variances. Also, the addition of Ag to the Pd-Y zeolite allows for more selective control of the hydrogenation, resulting in less ethane production [4]. In addition, this conversion of acetylene to ethylene results in a product that has a much higher chemical value.

Ethylene is one of the most significant chemicals produced in terms of volume, sales, and useful end products. The United States alone produces around 28 million tons per year of ethylene. It is primarily used for the production of poly-olefins for plastics, fibers, films, resins, adhesives, and elastomers, but is can also be

oligimerized to liquid hydrocarbons [1]. The double bond allows for its high reactivity and ease of conversion to useful products.

Ethylene is produced by the cracking of hydrocarbons, such as ethane, propane, and naphtha. The thermal cracking of petroleum hydrocarbons with steam, known as pyrolysis, constitutes over 97% of the worldwide production of ethylene. The hydrocarbons crack into the major products: ethylene, other olefins, and diolefins[5]. A disadvantage of this process is the by-products resulting from the use of the heavy hydrocarbon feedstock can constitute a large fraction of the resulting product stream. In addition, the high temperatures required for the endothermic reaction requires intensive energy input in direct fired furnaces to drive the process. Also, polymer grade ethylene requires the removal of acetylene also produced in the process of cracking.

For a front-end selective catalytic hydrogenation reactor, ethylene fractions are around 35% and hydrogen concentration can be anywhere from 10-35% [6]. Depending on location and production methods, acetylene concentrations can range from 0.5% to 500 ppm in the feed to the hydrogenation units. The acetylene concentration needs to be reduced to 20 ppm in the feed to the polymerization reactors in order to prevent poisoning of the catalyst. Initially, nickel catalysts were used for the selective hydrogenation of acetylene to ethylene; however, recent technologies using palladium and doped metals on palladium-supported catalysts have dramatically improved the selectivity toward ethylene.

In addition, acetylene hydrogenation catalysts need to be able to handle a wide variety of feed conditions that include varying feed concentrations and poisons. The activity of the catalysts depends on the availability of palladium sites. Based on heat of adsorption, the relative strengths of adsorption of gases on palladium are:

CO > C_2H_2 >> conjugated diolefins >= alkyl acetylene > diolefins >> olefins[6].

Carbon monoxide can be used as a method for controlling the activity of the catalyst. At low concentrations, carbon monoxide and acetylene compete for adsorption on the palladium metal. This can be beneficial in that it limits ethylene adsorption on the catalyst at low acetylene concentrations; conversely, it lowers the amount of acetylene that can adsorb on the catalyst, reducing the activity of the catalyst. This study shows the catalyst developed has improved selectivity toward ethylene, while limiting over-hydrogenation to ethane. In addition, the catalyst remains selective to ward the production of ethylene, even at high acetylene concentrations where typically extreme over-hydrogenation occurs

Plasmas have shown to be an effective method of converting methane to valuable chemicals such as C_2 hydrocarbons, hydrogen and carbon monoxide. A plasma is an ionized gas that is generated by electrical discharges. The types of discharges used in this study can be termed cold or non-equilibrium plasmas. Cold plasmas are characterized by highly energetic electrons that exist at a very high

temperature, while the bulk gas temperature remains low. The highly energetic electrons initiate radical reactions that kinetically and thermodynamically would not occur at the low bulk gas temperatures. This is advantageous because the feed gas does not have to be preheated to the extreme temperatures normally required for methane conversion.

The major products under these conditions are acetylene, hydrogen, and carbon monoxide. The dc plasma system has achieved high methane conversions (~70%) and extremely high acetylene selectivities (~70%). Acetylene and hydrogen yields as high as 50% have been obtained. However, acetylene is not the most desirable product. Acetylene's product value has decreased tremendously over the last decades as ethylene has replaced it as a desirable petro-chemical feedstock for the production of higher value products such as plastics. In addition, acetylene has inherent safety issues that are undesirable. Thus, recent efforts have focused on the in-situ conversion of acetylene to ethylene. Previous results show that with the addition of Pd to the parent Y zeolite, the acetylene produced in the gas phase by the plasma can be hydrogenated to ethylene and ethane [4, 7]. The parent Y zeolite within the reactor is used as a method of stabilizing the plasma discharge system. The plasma reactor operates at around 95°C, which is a typical operating range for the selective hydrogenation catalysts.

6.2 Experimental

6.2.1 Experimental Apparatus

The general experimental apparatus is similar to the system that has been described previously [2, 8]. The reactor is set up in a point to plane configuration, meaning that the top electrode is positioned concentrically within the reactor while the bottom electrode is a flat plate that also serves as a support for the catalyst. The distance between the two electrodes is 8 mm. The dc corona discharge is initiated by creating a potential difference between the two electrodes using a high voltage power supply (Model 210-50R, Bertan Associates Inc.).

The preparation and characterization of the NaOH treated Y zeolite has been discussed elsewhere [9, 10]. The preparation of the Pd-Y zeolite (CVD method) used in the initial experiments studying the effect of palladium metal on the selective hydrogenation of acetylene also has been described previously [7]. Palladium was added using chemical vapor deposition according to the following procedure. The NaOH Y zeolite was calcined at 400°C, and then mixed with the appropriate amount of palladium acetylacetonate to achieve the desired Pd loading (ranging from 0.025 to 1%). The mixture was then heated slowly under vacuum to a temperature of 130°C to disperse the palladium throughout the NaOH Y zeolite. The Pd-Y zeolite was then calcined for the final time to a temperature of 350°C. Subsequent preparations of Pd-Y and Ag-Pd-Y catalysts used the incipient wetness technique.

The incipient wetness of the Y zeolite was found by adding water to a known amount of catalyst until the catalyst could not take up any more water. A solution of tetraaminepalladium (II) nitrate was made such that for the amount of catalyst to be prepared, the amount of solution used for incipient wetness would provide the desired

metal loading on the catalyst. A loading of 0.025 wt% Pd-Y was chosen as it had shown to be the most selective catalyst to date for the hydrogenation of acetylene. The catalyst was then dried in air for 8 hours in a 110°C oven to remove the water. The catalyst was then subsequently calcined in air for a total of 6 hours. The catalyst was heated to 350°C over the first two hours, and then left at 350°C for the remaining 4 hours. This catalyst will be referred to as 0.025 wt% Pd-Y zeolite. The catalyst was reduced in hydrogen flow at 350°C prior to each experiment.

The silver-palladium Y zeolite was prepared in a similar manner using the incipient wetness technique. The silver was added to the 0.025 wt% Pd-Y zeolite using silver nitrate. The incipient wetness of the catalyst was assumed to be the same as determined previously. The catalyst was dried and calcined in the same manner as the 0.025 wt% Pd-Y zeolite. Loadings of 0.01 wt% Ag, 0.025 wt% Ag, and 0.100 wt% Ag on 0.025 wt% Pd-Y zeolite were prepared.

A furnace connected to a temperature controller is used to heat and maintain the reactor at the desired temperature. High methane conversions can be achieved at temperatures as low as room temperature; therefore, when the desired operating temperature is below 100°C it is necessary to blow cooling air across the tube exterior in order to reduce the temperature since the plasma itself does heat the gas to some extent.

6.2.2 ICP Results

Two samples of the 0.025 wt%Ag-0.025 wt% Pd Y zeolite were sent to Galbraith Laboratories for ICP analysis to confirm that the actual loading of metal on the catalyst was close to what was desired. The catalyst was selected as it had the lowest loading of palladium used (presumed to be the hardest to prepare accurately), and an intermediate silver loading. The results can be seen in Table 6.1.

As can be seen, the palladium loading was very consistent with the intended loading. A loading of 250 ppm corresponds with 0.025 wt% Pd. However, the silver loading was off, and appears the actual loading of silver was in the neighborhood of 0.02%. The best catalyst to date is the 0.1wt% Ag- 0.025wt% Pd Y zeolite, and it is believed that the accuracy of the prepared loading would improve with an increase in the loading.

6.2.3 TEM

A transmission electron microscope, TEM, was used to help clarify the dispersion and particle size of the various hydrogenation catalysts being used. Four different catalysts were studied: NaOH Y zeolite, 0.025wt% Ag – 0.025wt% Pd Y zeolite, 0.05wt% Pd Y zeolite, and 1.0wt% Pd Y zeolite. A JOEL 2000 was used for the characterization.

The NaOH Y zeolite sample, shown in Figure 6.1, revealed that the zeolite structure has not been harmed during the catalyst preparation. The two-dimensional channels could be seen on the monitor, and at least one of the channel structures can be seen in the figure. The channel width on a Y zeolite crystal is 7.4 Å, which is very

Table 6.1 ICP Results

	Palladium (ppm)	Silver (ppm)
Sample 1	249	202
Sample 2	256	197



Figure 6.1. TEM image of NaOH Y zeolite

close to the estimated channel width of 10 Å using the TEM monitor, which allows for an even higher resolution of the image. It is important to know that the structure of the catalyst has not been altered or damaged during the preparation and calcinations of the catalyst. This is also true for the further incipient wetness preparations of the metal loaded catalyst. The zeolite structure and nature is very similar to that found in the parent Y zeolite.

The 1.0 wt% Pd Y zeolite sample, Figure 6.2, showed significantly larger particle ensembles than the other samples. This is to be expected, as the loading of this catalyst was 20x higher than the next catalyst. The particle size of the palladium ensembles appears to be in the 5-8 nm range. Table 6.2 shows that the most typical size is about 5 nm.

The Y zeolite is fairly unstable under the intense beam, thus low resolution was needed to find the particles. In addition, the technique to capture the picture had to be extremely quick in order to capture a clear image. This became more difficult as the metal loading decreased. The dispersion seems to be random throughout the catalyst sample. The palladium particles were difficult to locate, then when located usually appeared in bunches, even though the particle sizes were still extremely small.

The 0.05wt% Pd-Y zeolite, Figure 6.3, showed a significant reduction in the particle size. The particle sizes appear to be in the range of 2-3 nm in diameter. Figure 6.4, the 0.025 Ag – 0.025 Pd Y zeolite appears to have a very high dispersion, as locating the particles on the TEM was extremely tedious. It appears the 0.025Ag-Pd sample had particle sizes on the order of less than 2 nm.

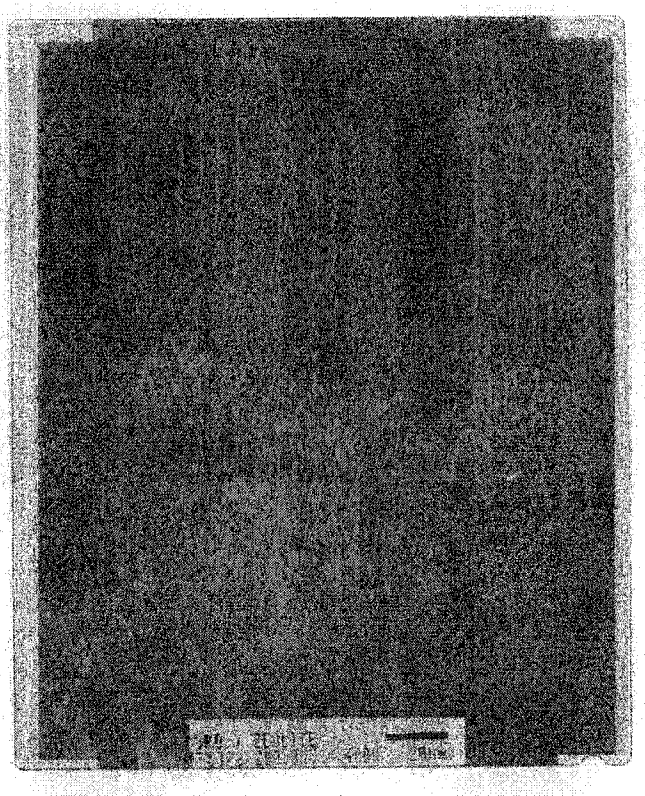

Figure 6.2. TEM image of 1.0 wt % Pd-Y zeolite

Table 6.2 Catalyst particle size and dispersion.

	Dispersion	Average Particle Size
0.025wt%Ag-0.025wt% Pd- Y zeolite	0.37	< 2 nm
0.05 wt% Pd-Y zeolite	0.31	2-3 nm
1.0 wt% Y zeolite	0.12	5 – 8 nm



Figure 6.3. TEM image of 0.05 wt% Pd-Y zeolite

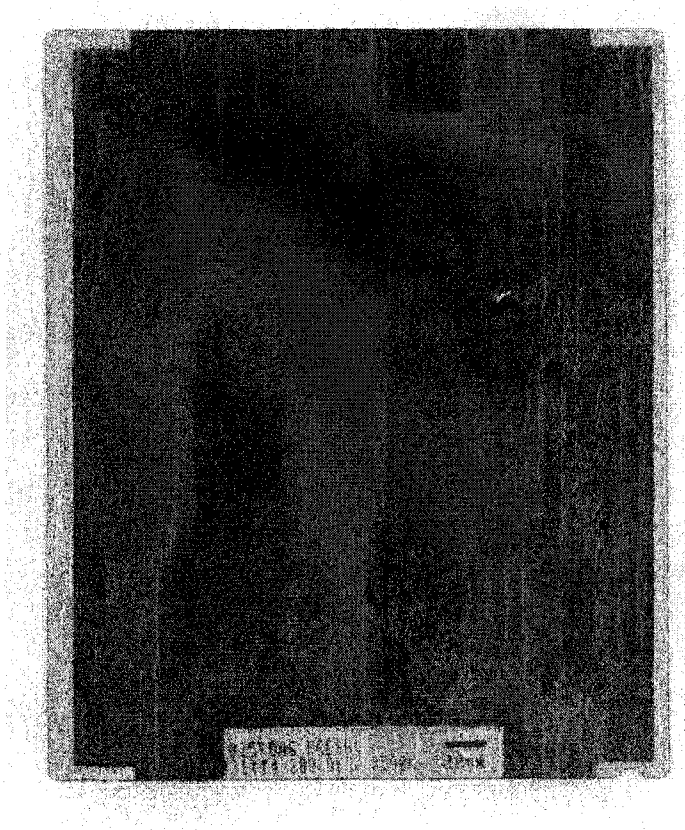

Figure 6.4. TEM image of 0.025 wt% Ag- 0.025 wt% Pd Y zeolite

All of the TEM data helps to prove what was believed to be the case with the catalyst samples: that the lower loadings of metal had much higher dispersions, as well as, much smaller particle size. This data supports the theory that the particle size plays a major role in the selective hydrogenation of acetylene to ethylene, and a larger role in the over hydrogenation of ethylene to ethane.

In order to try to experimentally determine the dispersion of the catalyst, reaction rate studies were carried out involving the CO oxidation to CO_2. The rate of conversion of CO to CO2 was determined experimentally. Then using a turnover frequency of 0.012 molecules / Pd surface atom – sec, obtained from Libuda [11] et al., the number of active sites (Pd surface atoms) was determined. The ratio of the active sites to total number of Pd sites in the system yielded the dispersion. The results of dispersion and/or particle size can be found in Table 6.2. It was found the best catalyst, the 0.025 wt% Ag - 0.025 wt% Pd Y catalyst, had the highest dispersion of 0.37. The next catalyst tested was the 0.05 wt% Pd Y zeolite and it had a slightly lower dispersion of 0.31. This corresponds extremely well with the average particle size of the palladium particles from the TEM samples. The two samples did not show a large difference in particle size. This data also corresponds very well with other dispersions and particle sizes of other researchers [12].

6.3 Results and Discussion

6.3.1 Selective Hydrogenation with Ag-Pd-Y zeolite

Previous results showed that the addition of Pd to the parent Y zeolite allowed for the hydrogenation of the acetylene produced in the gas phase by the plasma discharge. In addition, the addition of Ag-Pd allowed for even more selective hydrogenation of the acetylene to ethylene without the over-hydrogenation to ethane, Figure 5.6.

The addition of silver allowed for the improvement of ethylene selectivity, further work was done to find the optimal loading of silver that provides the best ethylene selectivity. Figure 6.5 shows the effect of different Ag loadings on methane conversion and C_2 selectivities. The methane conversion is nearly independent of metal loading. This correlates well with previous results [13], which indicate that the primary reactions (methane conversion and acetylene production) occur in the gas phase. The zeolite "catalyst" stabilizes the streamer discharge though it is not catalytically responsible for the production of the products. The addition of the metal to the catalyst does allow for a surface reaction, the selective hydrogenation of the acetylene formed in the gas phase.

The C_2 selectivity was affected by the amount of silver present in the catalyst. Increasing the silver loading reduced the over hydrogenation of ethylene to ethane. The ethylene:ethane ratio increased from 4:1 to 11:1 as the silver loading was increased. It is believed that multiple adjacent palladium sites lead to the adsorption of ethylene and the further hydrogenation to ethane [14-16]. The silver acts as an inhibitor of this

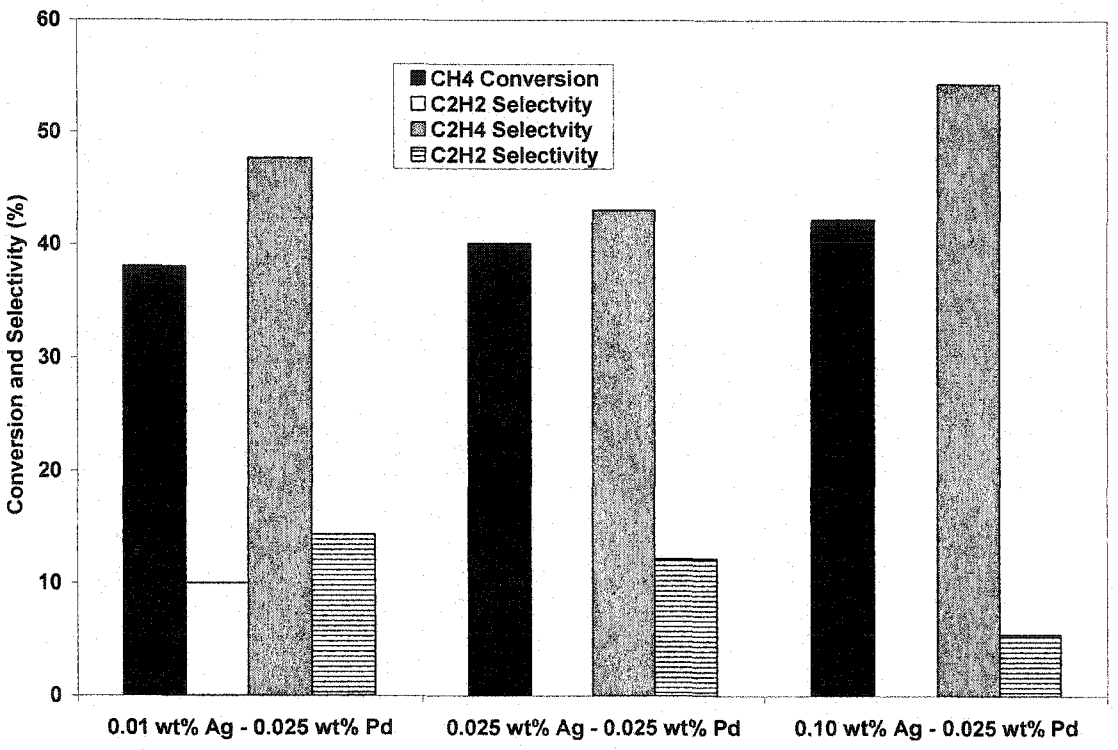

Figure 6.5. Effect of Ag loading on methane conversion and ethylene and ethane selectivity, 32 sccm, 0 psig, 0.05 grams of catalyst, 10 kV.

mechanism by covering some of the palladium. This in return reduces the number of sites for over-hydrogenation of ethylene to ethane leading to a higher ethylene/ethane ratio. Silver is also known to increase the catalysts tolerance to fluctuations in feed conditions (both temperature and poisons)[6].

In addition, the silver shifts the operating range of the process. As the silver content is increased, both the initial temperature at which hydrogenation occurs and the optimal temperature are increased. Thus, the activation energy of the reaction is increased. The profile of selectivity versus temperature for the selective hydrogenation of acetylene to ethylene is not affected by the silver concentration but the curve is shifted 20°C as the silver loading is increased from 0.0 wt% to 0.1 wt%, shown in Figure 6.6. This temperature shift has also been noted by Zhang et al[17]. The 0.01 wt% Ag and 0.025 wt% Ag, indistinguishable between themselves, did show a slight shift as compared to the 0.0 wt% Ag catalyst.

Figure 6.7, shows that for the 0.0 wt% Ag catalyst, the maximum ethylene selectivity is achieved at 98°C, while the 0.1 wt% Ag catalyst has a maximum ethylene selectivity near 130°C. Though a slight amount of silver, 0.01 wt% Ag, is capable of affecting the selectivity and mechanism of the reaction, a silver loading in excess of the Pd loading provides for higher ethylene selectivity and operating temperature. The 0.1 wt % Ag – 0.025 wt % Pd Y zeolite provided complete acetylene conversion and optimum ethylene selectivity around 120 °C. Though this higher than the normal operating range of the plasma system, it is not extremely

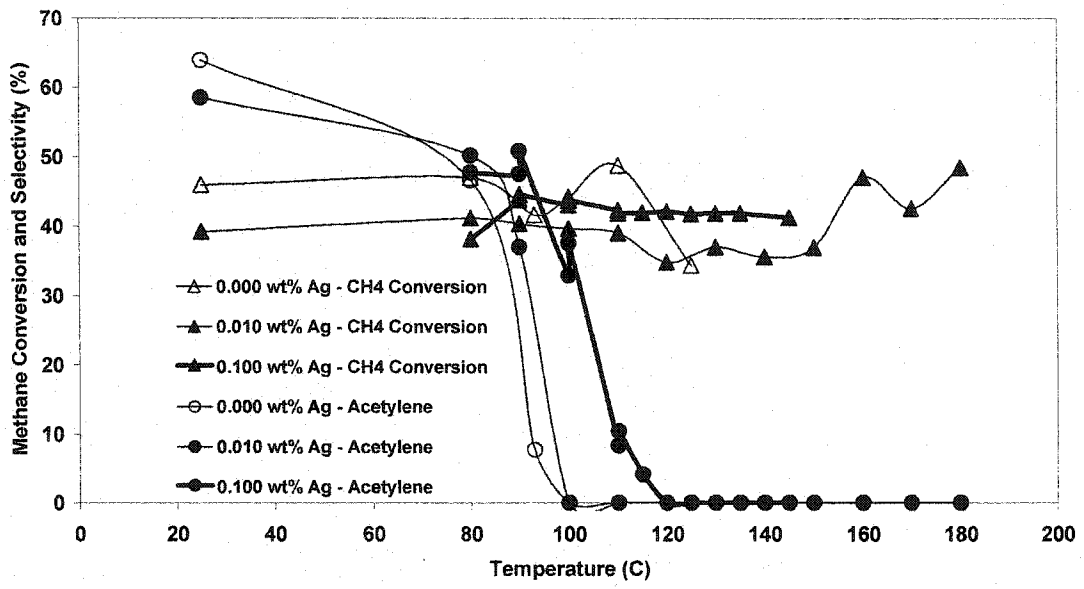

Figure 6.6. Effect of temperature on methane conversion and acetylene hydrogenation, 32 sccm, 0 psig, 0.05 grams of catalyst.

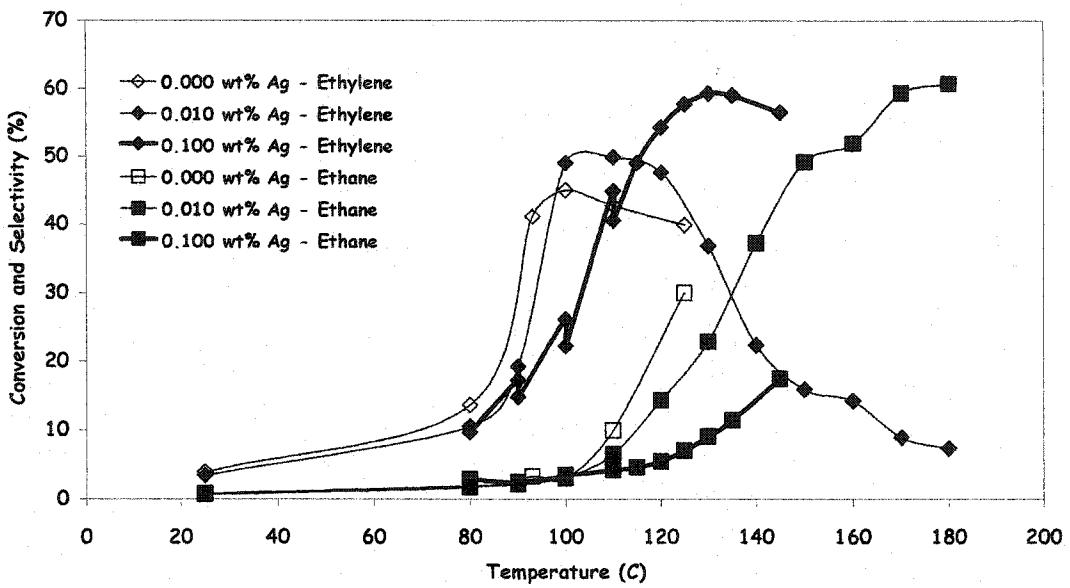

Figure 6.7. Effect of temperature on ethylene selectivity and ethane selectivity, 32 sccm, 0 psig, 0.05 grams of catalyst.

different in temperature (90°C vs. 120°C), and the temperature of the system could be raised by low heating-value waste streams.

The Ag-Pd Y zeolite catalyst has the ability to handle high concentrations of acetylene, anywhere from 10 to 100 times the amount of acetylene that would be found in a hydrogenation unit. The concentrations discussed above were near 2.5%, while acetylene concentrations in ethylene plants range from 500 ppm to 0.5% acetylene, depending on the arrangement of the plant. Since it is desired to reduce acetylene concentration to near 25 ppm, it is important to study the catalyst's selectivity at conversions near 100% when the reaction proceeds in a series, i.e. as acetylene goes to ethylene and then to ethane [18]. This is important because acetylene adsorption strength is higher than ethylene, but once the acetylene concentration is reduced at high conversions, ethylene has access to the sites and can be further hydrogenated to ethane. Several experiments were conducted to test the activity and selectivity of the catalyst at extremely high acetylene concentrations. Figure 6.8 and 6.9 show the acetylene conversion and ethylene selectivity, respectively, as the temperature is increased.

Figure 6.8 shows that the addition of silver increases the temperature at which the selective hydrogenation of acetylene to ethylene occurs, as well as the temperature at which complete conversion of the acetylene occurs. Complete conversion is achieved at 125°C and 135°C for the 0.025 wt% Pd and 0.025 wt% Ag-0.025 wt% Pd catalysts, respectively. The effect of silver loading and temperature on the over hydrogenation of ethylene to ethane is seen in Figure 6.9. It shows that the

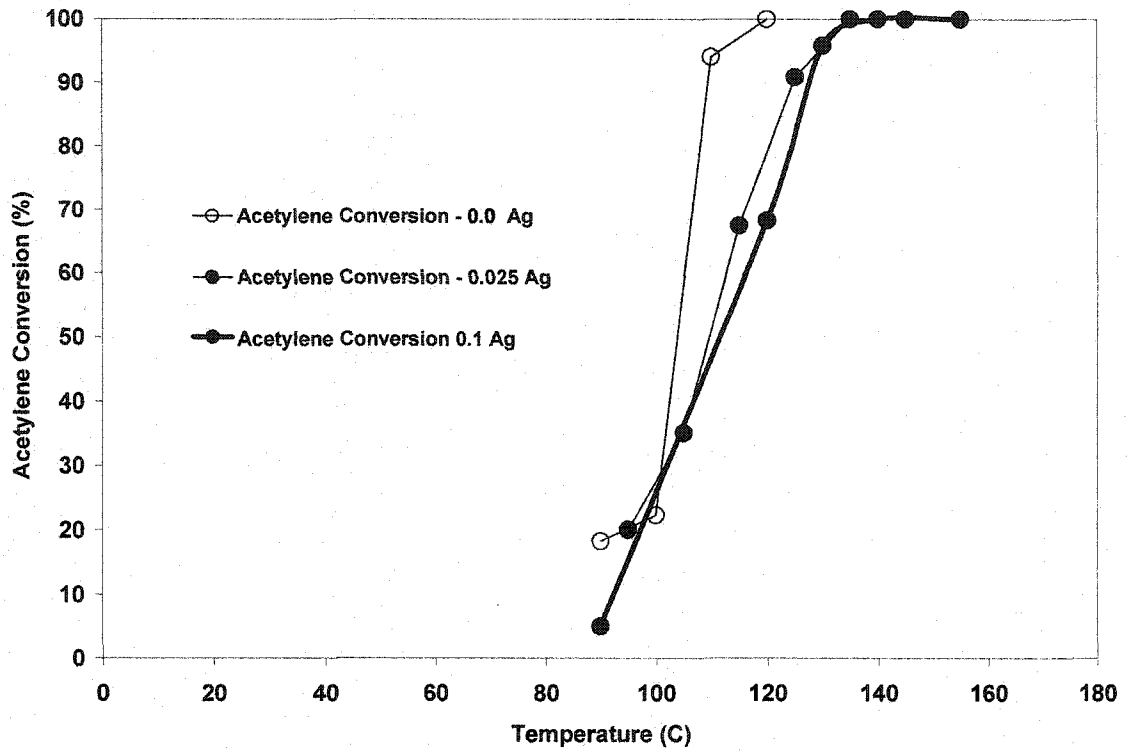

Figure 6.8. Effect of temperature on acetylene conversion at elevated acetylene concentrations, 32 sccm, 0 psig, 0.05 grams of catalyst.

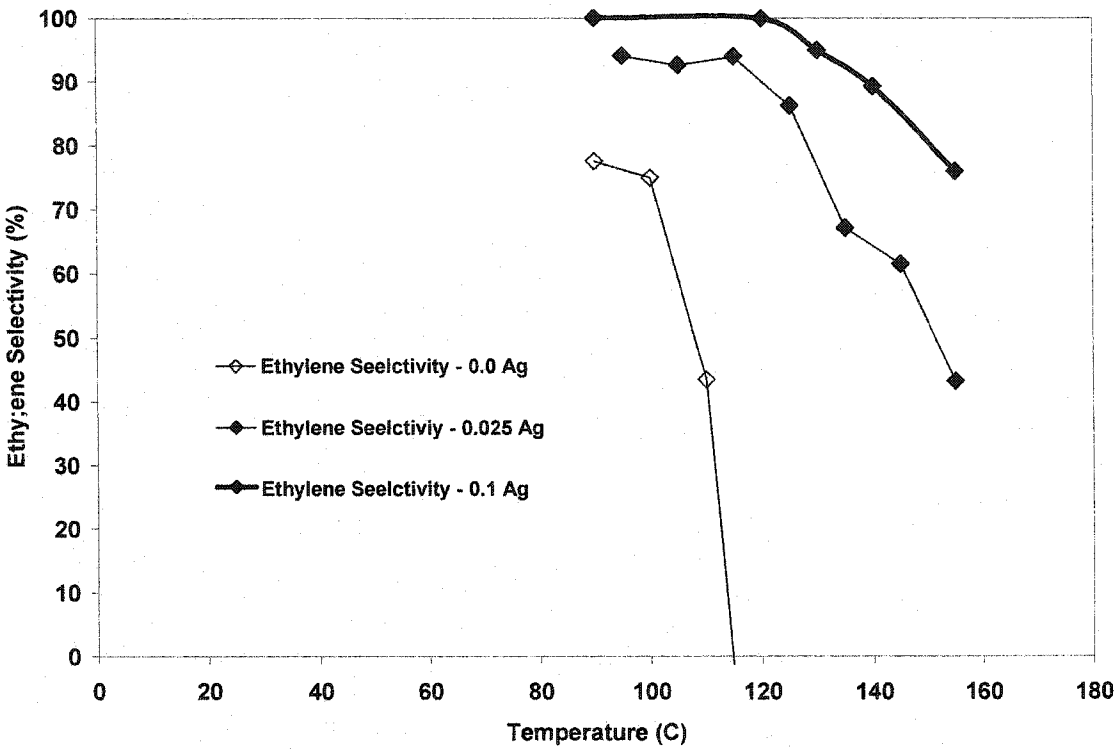

Figure 6.9. Effect of temperature on ethylene production at high acetylene concentrations and acetylene conversion. 32 sccm, 0 psig, 0.05 grams of catalyst.

higher the silver loading the less over-hydrogenation of ethylene to ethane occurs. While it is necessary to raise the temperature of the system in order to maintain the same rate of acetylene hydrogenation, the rate of over-hydrogenation decreases dramatically with the addition of silver. Even though at the higher temperatures over-hydrogenation occurs, the ethane production it is not significant. Ethane production is tolerable in the industrial systems, as long as it does not greatly affect the quality and economics of the ethylene stream. Industrial conditions consider a run away reaction to be one in which 3% of the ethylene in the feed is converted to ethane.

6.4 Conclusions

The addition of silver to the palladium catalyst has shown to be an effective method for a higher control of the selectivity of acetylene to ethylene, without the further over hydrogenation to ethane. The addition of silver increased the ethylene:ethane ratio from 4:1 without silver to 11:1 with the highest silver loading of 0.100 Wt% Ag – 0.025 wt% Pd-Y zeolite. Another feature of the catalyst is its ability to handle the conversion of high concentrations (10x that found in extreme industrial conditions) of acetylene while still maintaining acceptable limits of ethane production.

6.5 References

1. McKetta, J.J., ed. *Encyclopedia of Chemical Processing and Design.* . Vol. 20. 1986, Marcel Dekker: 1984. 88-159.

2. Gordon, C.L., L.L. Lobban and R.G. Mallinson, *The production of hydrogen from methane using tubular plasma reactors*, in *Advances in hydrogen energy*, C. Gregoire-Padro, Editor. 2000, Kulmer

3. Khan, M.S. and B.L. Crynes, *Survey of recent methane pyrolysis literature.* Industrial and Engineering Chemistry, 1970. **62**(10): p. 54-59.

4. Gordon, C.L., L.L. Lobban and R.G. Mallinson, *Ethylene production using a Pd and Ag-Pd Y-zeolite catalyst in a dc plasma reactor.* Catalysts Today, 2003. in progress.

5. Gerhartz, W., *Ullman's Encyclopedia of Industrial Chemistry*. Vol. A10. 1987, Weinheim: VCH. 45.

6. Tiedtke, D.B., T.T. Cheung, J. Leger, S.A. Zisman, J.J. Bergmeister and G.A. Delzer, *Chemicals influencing the activity of palladium-based catalysts for the selective hydrogenation of acetylene to ethylene in acetylene converters.* Ethylene Producers Conference, 2001.

7. Gordon, C.L., L.L. Lobban and R.G. Mallinson, *Selective hydrogenation of acetylene to ethylene during the conversion of methane in a catalytic dc*

plasma reactor, in *Natural Gas Conversion VI*, J.J. Spivey, E. Iglesia, and T.H. Fleisch, Editors. 2001, Elsevier Science: Amsterdam. p. 271-276.

8. Liu, C.J., R.G. Mallinson and L.L. Lobban, *Nonoxidative methane conversion to acetylene over zeolite in a low temperature plasma.* Journal of catalysis, 1998. **179**: p. 326-334.

9. Liu, C.-J., A. Marafee, B.J. Hill, G. Xu, R.G. Mallinson and L.L. Lobban, *Oxidative coupling of methane with ac and dc corona discharge.* Industrial & Engineering Chemistry Research, 1996. **35**(10): p. 3295-3301.

10. Marafee, A., C.-J. Liu, G. Xu, R.G. Mallinson and L.L. Lobban, *An experimental study on the oxidative coupling of methane in a direct current corona discharge reactor over Sr/La2O3 catalyst.* Industrial & Engineering Chemistry Research, 1997. **36**: p. 632-637.

11. Libuda, J., I. Meusal, J. Hoffman, J. Hartmann, L. Piccolo, C.R. Henry and H.J. Freund, *The CO oxidation kinetics on supported Pd model catalysts: A molecular beam/in situ time-resolved infrared reflection absorption spectroscopy study.* Journal of Chemical Physics, 2001. **14**(10): p. 4669-4684.

12. Slinko, M.M., N.V. Peskov and N.I. Jaeger, *Analysis and simulation of the dynamics of a catalyzedmodel reactions : CO oxidation on zeolite supported palladiums.* Kinetics and Catalysis, 2003. **44**(2): p. 183-197.

13. Gordon, C.L., L.L. Lobban and R.G. Mallinson, *Stability and C2 production in a dc plasma reactor.* Industial & Engineering Research, 2004. **in progress**.

14. Borodzinski, A., *Hydrogenation of acetylene-ehtylene mixtures on a commercial palladium catalyst.* Catalysis Letters, 1999. **63**: p. 35-42.

15. Borodzinski, A., *The effect of palladium particle size on the kinetics of hydrogenation of acetylene-ethylene mixtures over Pd/SiO2 catalysts.* Catalysis Letters, 2001. **71**(3-4): p. 169-175.

16. Duca, D., F. Frusteri, A. Parmaliana and G. Deganello, *Selective hydrogenation of acetylene in ethylene feedstocks on Pd catalysts.* Applied Catalysis A: General, 1996. **146**: p. 269-284.

17. Zhang, Q., J. Li, X. Liu and Q. Zhu, *Synergetic effect of Pd and Ag dispersed on Al2O3 in the selective hydrogenation of acetylene.* Applied Catalysis A: General, 2000. **197**: p. 221-228.

18. Jin, Y., A.K. Datye, E. Rightor, R. Gulotty, W. Waterman, M. Smith, M. Holbrook, J. Maj and J. Blackson, *The influence of catalyst restructuring on the selective hydrogenation of acetylene to ethylene.* Journal to Catalysis, 2001. **203**: p. 292-306.

CHAPTER 7 : Conclusions and Future Work

7.1 Conclusions

The dc plasma system has shown to be an effective method for the conversion of methane. The plasma has the ability to covert methane to more valuable products at temperatures less than 100°C. These reactions would not be feasible at such low temperatures, without the highly energetic electrons that exist within the plasma. It is the creation of the plasma discharge that provides the energetic electrons. However, the creation of a stable discharge required several criteria in order to exist.

In order to establish a stable streamer discharge, the system uses a material to assist in the breakdown of the gas. The material allows for the creation of the discharge at voltages lower than what would occur without the presence of the material. This reduction in voltage is caused by the material acting as a dielectric

material. A dielectric material becomes polarized in an electric field. This polarization creates an electric field opposite of the applied electric field. Thus, the summation of the electric fields results in an overall reduced electric field within the system. This reduces the operating voltage of the system. In addition, the high electric fields around the particles provide a localized spot for the creation of a discharge.

By reducing the voltage, the amount of energy that is input into the system is also reduced. This lowers the overall temperature within the system. The temperature variance between operating at 7kV and 13kV, material and non-material operation respectively, can be as much as 50°C. The volume occupied by actual streamer discharge is extremely small in comparison to the overall reactor volume. Thus, the temperature increase of the electrons must be significant in order to increase the bulk gas temperature. The lower temperature reduces the tendency to form carbon via acetylene dehydrogenation.

The primary problem with the carbon formation (besides it being an undesired by-product) is that the presence of carbon alters the discharge. Carbon deposited on the reactor walls provides a location for the discharge to occur and the carbon provides a conductive path to the bottom electrode. This decreases the discharge gap which in return increases the reduced electric field (E/P). Increasing E/P results in increased electron energy deposition in methane dissociation and correlates with increased ethane selectivity. Decreasing E/P results in increased energy deposition in methane excitation and correlates with increased acetylene selectivity.

To assist in preventing the formation of coke, hydrogen and small quantities of oxygen are used in the feed stream. It is necessary to have at least 2% of oxygen in the feed stream to assist in the scavenging of carbon molecules. The hydrogen also serves to inhibit carbon formation.

In the dc plasma system, selectivity of the main products is independent of residence time and conversion. Acetylene and hydrogen, the two main products, achieved yields as high as 50% at long residence times. Carbon monoxide is also produced from the low concentrations of oxygen, resulting in a low selectivity. The high yields of acetylene prompted for a method for the in-situ conversion to a more desirable product.

The addition of Pd to the parent Y zeolite catalyzes the hydrogenation of the acetylene. The Pd alone hydrogenates non-selectively. Whereas, addition of Ag to the Pd-Y zeolite catalyzes the selective hydrogenation of acetylene. The 0.10 wt% Ag- 0.025 wt% Pd-y zeolite allowed for the highest selectivity of ethylene. The ethylene:ethane ratio was 11:1 with the Ag-Pd catalyst, as compared to 4:1 with the Pd-Y zeolite.

In addition, the addition of the metal to the base material allowed for the stable operation of the discharge at higher methane partial pressures, probably by reducing the partial pressure of acetylene. The higher partial pressures of methane also provided a much higher throughput of methane which resulted in an overall reduction in the energy requirements (or eV / molecule of methane converted).

7.2 Future Work

This research has provided a greater understanding of the dc plasma system. However, the system still has several areas that could use an improved understanding or analysis to assist in progressing towards an economically feasible process for an industrial application. Some of these areas include:

1.) Determination of the reaction mechanism and modeling of the rates

2.) Optimization of the power supply to increase overall energy efficiency

3.) Scale-up issues, and alternative reactor designs

4.) Economic analysis for industrial application

The effect of the reduced electric field on the product distribution should be utilized to assist in optimizing the different reactors. The study of the amount of energy that direct toward various inelastic processes should assist in determining the product distribution of various feeds and operating conditions. In general, the reactor with the lowest reduced field has provided the best energy efficiency within the laboratory. This along with the different feed conditions should provide an opportunity to produce the highest yields of a desired product at the highest energy efficiency.

The power supply used for all experiments is an off-the-shelf dc power supply. It is known, through use of an oscilloscope and PLIF studies, that the discharge is pulsed in nature even though the discharge appears continuous to the naked eye. If a power supply could be designed that allowed for a reproduction of the energy that is currently being input as pulses, this could reduce the power

consumption as high as 75%. In addition, the cost of such a power supply could be used to assist in the economic analysis of the dc plasma system.

Scale-up is another obstacle of the dc plasma system. Currently, the reactor has an I.D. of 7mm which results in a low throughput of methane. For an industrial scale process, the throughput of methane would have to be increased dramatically. The reactor could consist of a honeycomb series of reactors or a smaller number of larger reactors that consist of several pairs of electrodes within each reactor. The choice of these and other options will greatly depend on the power supply capabilities and design.

Once some of the above options have been analyzed, an overall economic study of the process should be performed. In this analysis, different markets and associated gas prices should be studied, as well as the various prices of products that could be produced. If producing a gas product, the gas will probably need to be produced near its end-use to minimize additional costs of transportation.

APPENDIX A – GC Calibrations

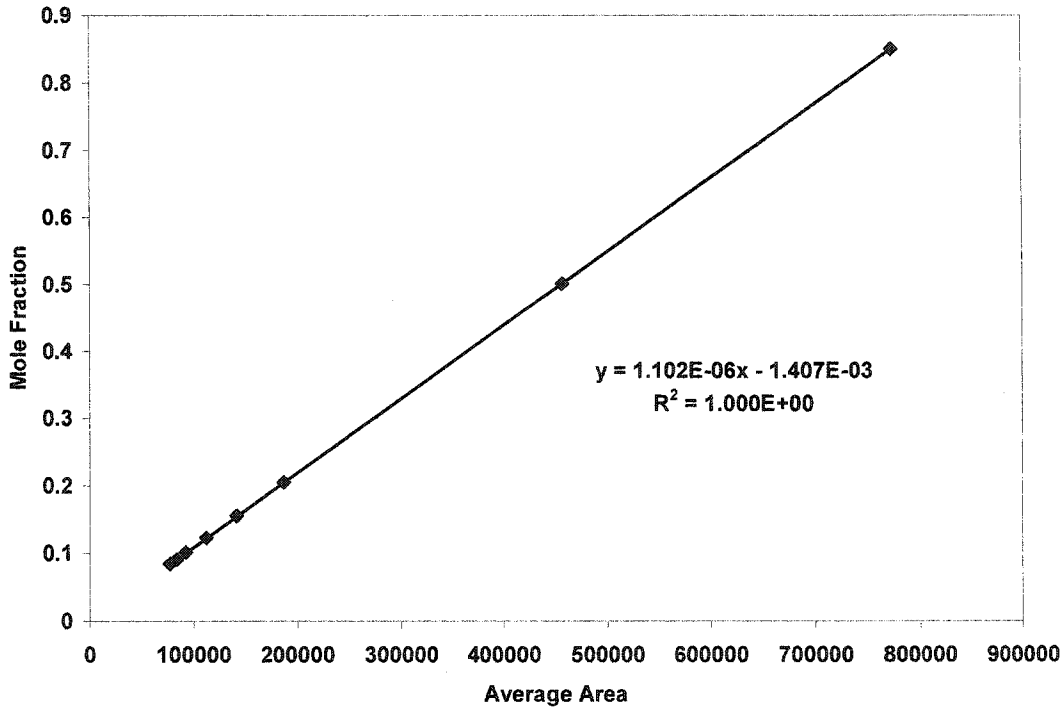

Figure A.1 Methane calibration, Carle EG&G Gas Chromatograph

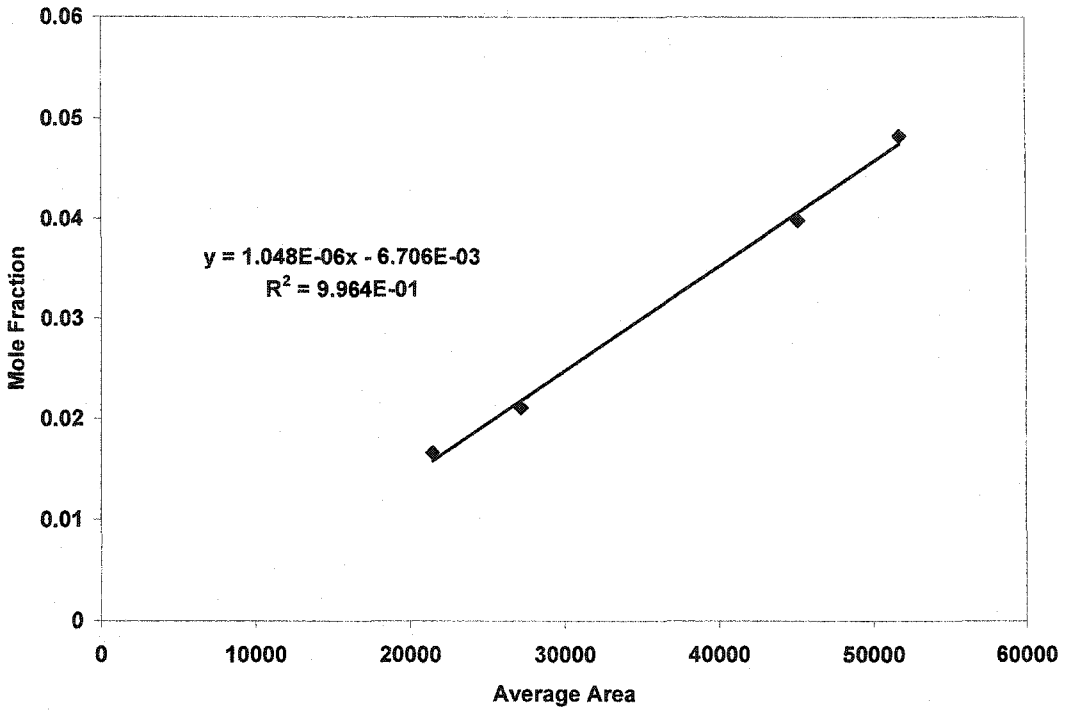

Figure A.2 Oxygen calibration, Carle EG&G Gas Chromatograph

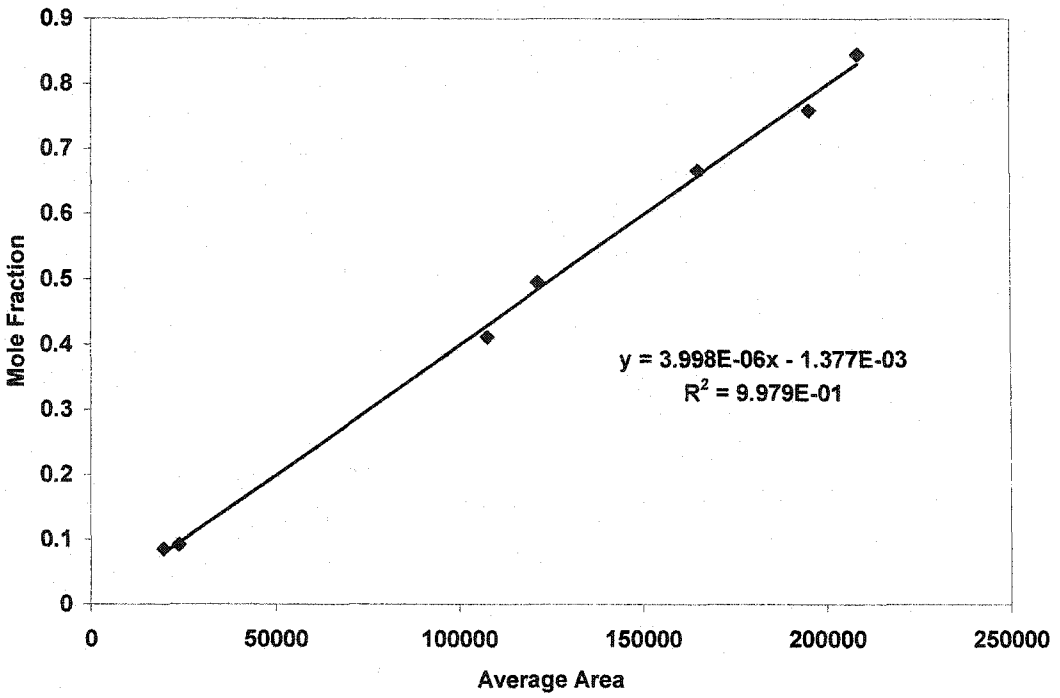

Figure A.3 Hydrogen calibration, Carle EG&G Gas Chromatograph

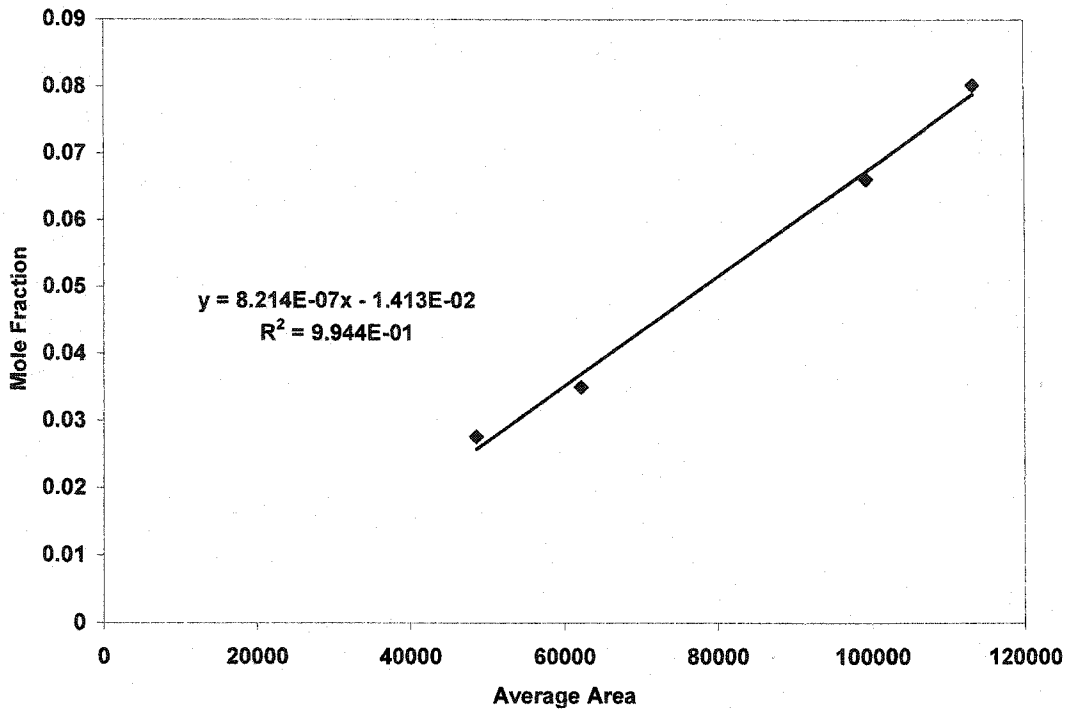

Figure A.4 Acetylene calibration, Carle EG&G Gas Chromatograph

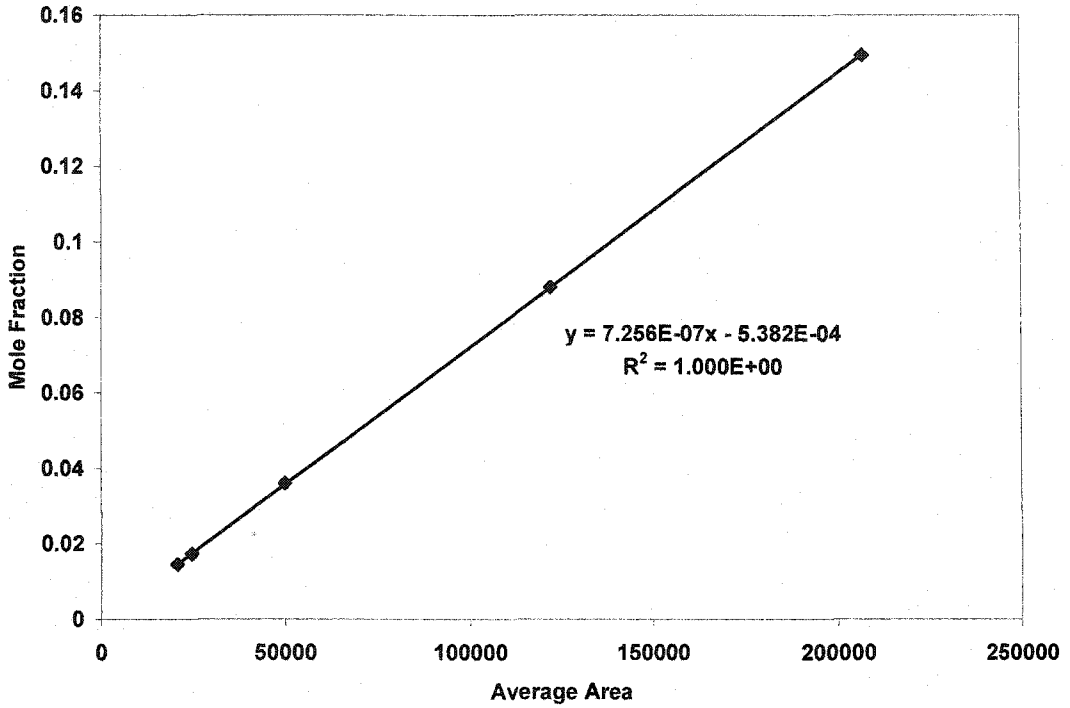

Figure A.5 Ethylene calibration, Carle EG&G Gas Chromatograph

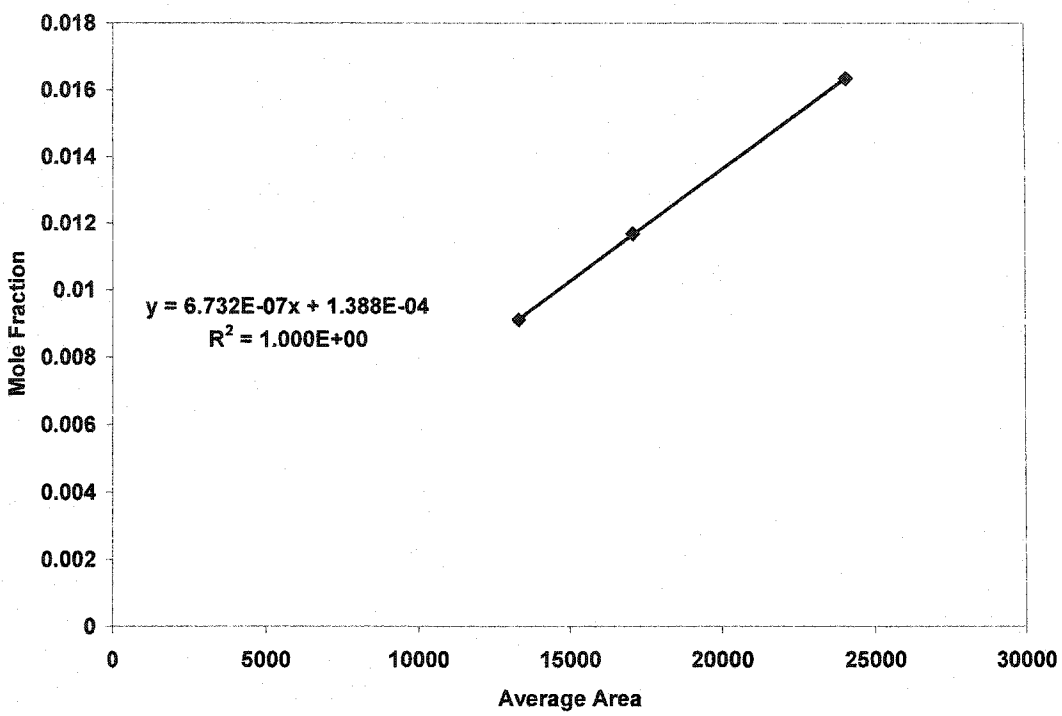

Figure A.6 Ethane calibration, Carle EG&G Gas Chromatograph

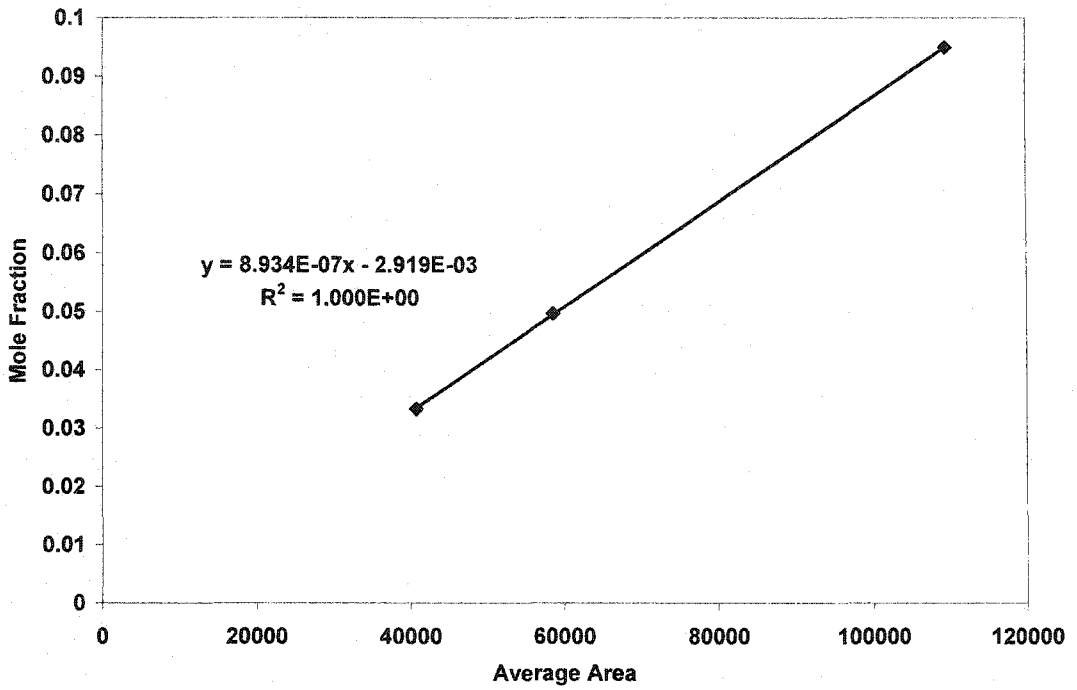

Figure A.7 Carbon Monoxide calibration, Carle EG&G Gas Chromatograph

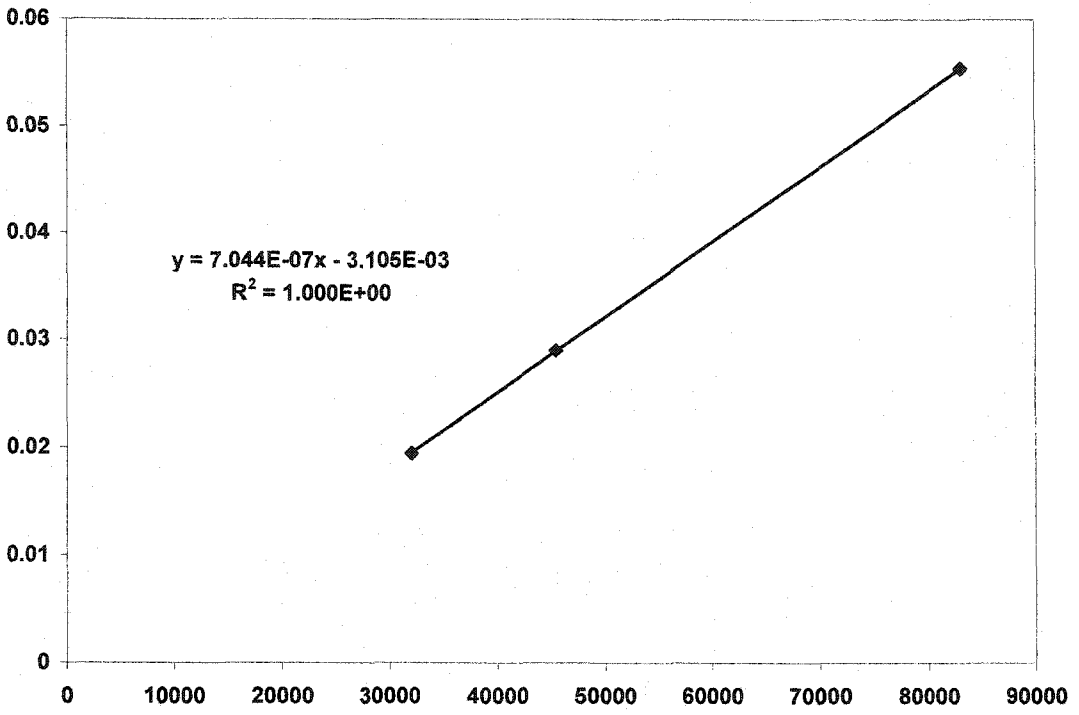

Figure A.8 Carbon Dioxide calibration, Carle EG&G Gas Chromatograph

APPENDIX B – Propagation of Error

Errors Calculated for the Various Calculations in the Experiment Results

	Value	Error	Percent Error
CH_4 Conversion	18.96%	2.51%	13.2%
O_2 Conversion	59.25%	5.3%	8.9%
H_2 Selectivity	74.70%	3.2%	4.3%
C_2H_6 Selectivity	5.21%	1.1%	21.1%
C_2H_4 Selectivity	4.39%	1.2%	27.3%
C_2H_2 Selectivity	67.89%	3.7%	5.4%
CO Selectivity	6.29%	1.0%	15.9%
eV / molecule CH_4 converted	40.06 eV	3 eV	7.5%

Assumed Errors within the experiments used during Propagation of Error

	Value	Assumed Error	Percent Error
Volume of bubble flowmeter	10 cc	0.05 cc	0.5%
Time	19.03 sec	0.1 sec	0.5%
Temperature	298 K	5 K	1.6%
Pressure	1 atm	0.012 atm	1.2%
Methane GC Area	300900 area count	900 area count	0.3%

Calculated Errors by Propagation of Error

	Value	Error	Percent Error
Volumetric Flowrate	31.53 sccm	0.22 sccm	0.7%
Number of Moles in Feed	0.001289 moles	0.0000279 moles	2.1%
Mole Fraction of Methane in Feed	0.32910	0.000992	0.3%
Number of Moles of Methane in Feed	0.0004243 moles	0.00000927 moles	2.1%
Number of Moles in Effluent	0.00134 moles	0.0000289 moles	2.1%
Mole Fraction of Methane in Effluent	0.2573	0.000992	0.3%
Number of Moles of Methane in Effluent	0.000344 moles	0.00000755 moles	2.2%
CH_4 Conversion	18.96%	2.51%	13.2%

Propagation of error for the calculation of methane conversion:

$$CH_4\ Converison = \left[\frac{molar\ \ flow\ in - molar\ \ flow\ out}{molar\ \ flow\ in}\right] * 100\%$$

Need to find the error in the calculation of the number of moles.

Total number of moles is given by:

$$n = \frac{P*V}{R*T}$$

where the Volumetric flowrate (V) is calculated.

$$V = \frac{Volume\ of\ \ bubble\ \ flowmeter * 60}{time}$$ for volumetric flowrate in sccm/min

The error associated with the above equation is assumed as flows:

Error of Volume of bubble flowmeter = 10 cc ± 0.05 cc or 0.5% (w_{vb} = **0.05)**

Error of Time with stopwatch = 19.03 sec ± 0.1 sec or 0.5% (w_t = **0.1)**

Taking the derivatives:

$$\frac{\partial V}{\partial V_b} = \frac{60}{t} = \frac{60}{19.03} = 3.153$$

$$\frac{\partial V}{\partial t} = -\frac{V*60}{t^2} = -\frac{10*60}{19.03^2} = -1.65$$

$$\omega_V = \left[\left(\frac{\partial V}{\partial V_b}\right)^2 (\omega_V)^2 + \left(\frac{\partial V}{\partial t}\right)^2 (\omega_t)^2\right]^{1/2} = \left[(3.153)^2(0.05)^2 + (-1.65)^2(0.1)^2\right] = 0.22$$

Thus, the error in the calculation of the volumetric flowrate is 31.53 ± 0.22 sccm or 0.7%

Back to calculating the number of moles of methane in the feed:

$$n = \frac{P * V}{R * T}$$

where R = 82.06

and the following constants have the associated error of:

Temperature = 298K ± 5K or 1.6%

Pressure = 1 ± 0.012 atm or 1.2%

$$\frac{\partial n}{\partial P} = \frac{V}{R * T} = \frac{31.53}{82.06 * 298} = 0.00128$$

$$\frac{\partial n}{\partial V} = \frac{P}{R * T} = \frac{1}{82.06 * 298} = 0.0000408$$

$$\frac{\partial n}{\partial T} = -\frac{P * V}{R * T^2} = -\frac{1 * 31.53}{82.06 * 298^2} = -0.0000043$$

$$\omega_n = \left[\left(\frac{\partial n}{\partial P} \right)^2 (\omega_P)^2 + \left(\frac{\partial n}{\partial V} \right)^2 (\omega_V)^2 + \left(\frac{\partial n}{\partial T} \right)^2 (\omega_T)^2 \right]^{1/2}$$

$$= \left[(0.00128)^2 (0.012)^2 + (0.0000408)^2 (0.22)^2 + (-0.0000043)^2 (5.0)^2 \right] = 2.79 \, x \, 10^{-5}$$

Thus, the number of moles in the feed is:

n = 0.001289 ± 0.0000279 or 2.1%

Next, to error within the methane calibration.

$$y = m * x + b$$

which is:

$$mole\ fraction = Slope * Area + Intercept$$

where for methane:

Slope = 1.1017×10^{-6}

Intercept = -1.4073 x 10^{-3}

The assumed error on the Area given by the GC is:

Methane Area = 300900 ± 900 or 0.3%

$$mole\ fraction = Slope * Area + Intercept$$

$$\frac{\partial MF}{\partial A} = 1.1017\ x10^{-6}$$

$$\omega_{MF} = \left[\left(\frac{\partial MF}{\partial A}\right)^2 (\omega_{MF})^2\right]^{1/2} = \left[(1.1017e-6)^2 (900)^2\right] = 9.92\ x10^{-4} = 0.000992$$

Thus, the error in the mole fraction calculation is:

Mole fraction of methane in feed= 0.32910 ± 0.000992 or 0.3%

Calculating the number of moles of methane:

Number of moles of methane = total number of moles * mole fraction

$$\frac{\partial mm}{\partial mf} = total\ number\ of\ moles = 0.001289$$

$$\frac{\partial mm}{\partial nm} = mole\ fraction = 0.32910$$

$$\omega_V = \left[\left(\frac{\partial mm}{\partial mf}\right)^2 (\omega_{mf})^2 + \left(\frac{\partial mm}{\partial nm}\right)^2 (\omega_{nm})^2\right]^{1/2}$$

$$= \left[(0.001289)^2 (0.000992)^2 + (0.32910)^2 (0.0000279)^2\right]$$

$$= 9.27\ x10^{-6}$$

Number of moles of methane in the feed = 0.0004243 ± 0.00000927 moles

Calculation of the number of moles in the product gas.

Product flowrate = 32.76 ± 0.24

$$n = \frac{P*V}{R*T}$$

$$\frac{\partial n}{\partial P} = \frac{V}{R*T} = \frac{32.76}{82.06*298} = 0.00134$$

$$\frac{\partial n}{\partial V} = \frac{P}{R*T} = \frac{1}{82.06*298} = 0.0000408$$

$$\frac{\partial n}{\partial T} = -\frac{P*V}{R*T^2} = -\frac{1*32.76}{82.06*298^2} = -0.0000044$$

$$\omega_n = \left[\left(\frac{\partial n}{\partial P}\right)^2(\omega_P)^2 + \left(\frac{\partial n}{\partial V}\right)^2(\omega_V)^2 + \left(\frac{\partial n}{\partial T}\right)^2(\omega_T)^2\right]^{1/2}$$

$$= \left[(0.00134)^2(0.012)^2 + (0.0000408)^2(0.24)^2 + (-0.0000044)^2(5.0)^2\right] = 2.89\,x\,10^{-5}$$

Thus, the number of moles in the effluent is:

n = 0.00134 ± 0.0000289 moles

Calculating the mole fraction of the effluent stream

$mole\ fraction = Slope * Area + Intercept$

$$\frac{\partial MF}{\partial A} = 1.1017\,x\,10^{-6}$$

$$\omega_{MF} = \left[\left(\frac{\partial MF}{\partial A}\right)^2(\omega_{MF})^2\right]^{1/2} = \left[(1.1017e-6)^2(900)^2\right] = 9.92\,x\,10^{-4} = 0.000992$$

Thus, the error in the mole fraction calculation is:

Mole fraction of methane in effluent stream= 0.2573 ± 0.000992 or 0.3%

Calculating the number of moles of methane in the effluent stream:

Number of moles of methane = total number of moles * mole fraction

$$\frac{\partial mm}{\partial mf} = total\ number\ of\ moles = 0.00134$$

$$\frac{\partial mm}{\partial nm} = mole\ fraction = 0.2573$$

$$\omega_V = \left[\left(\frac{\partial mm}{\partial mf}\right)^2 (\omega_{mf})^2 + \left(\frac{\partial mm}{\partial nm}\right)^2 (\omega_{nm})^2\right]^{1/2}$$
$$= \left[(0.00134)^2 (0.00092)^2 + (0.2573)^2 (0.0000289)^2\right]$$
$$= 7.55\ x\ 10^{-6}$$

Number of moles of methane in the feed = 0.000344 ± 0.00000755 moles

Finally, to calculate the conversion of methane:

$$CH_4\ Converison = \left[\frac{molar\ flow\ in - molar\ flow\ out}{molar\ flow\ in}\right] * 100\%$$

$$CH_4\ Converison = \left[1 - \frac{molar\ flow\ out}{molar\ flow\ in}\right] * 100\% = 100 - 100 * \frac{E}{F}$$

$$\frac{\partial CH_4}{\partial E} = -100 * \frac{1}{F} = -100 \frac{1}{0.0004243} = -235682$$

$$\frac{\partial CH_4}{\partial F} = 100 * \frac{E}{F^2} = 100 \frac{0.000344}{0.0004243^2} = 191078$$

$$\omega_{CH_4} = \left[\left(\frac{\partial CH_4}{\partial E}\right)^2 (\omega_E)^2 + \left(\frac{\partial CH_4}{\partial F}\right)^2 (\omega_F)^2\right]^{1/2}$$
$$= \left[(-235682)^2 (0.00000755)^2 + (191078)^2 (0.00000927)^2\right] = 2.5\%$$

The error in the conversion of methane is:

CH_4 Conversion = 18.96 ± 2.51%

APPENDIX C - Capacitor Derivation

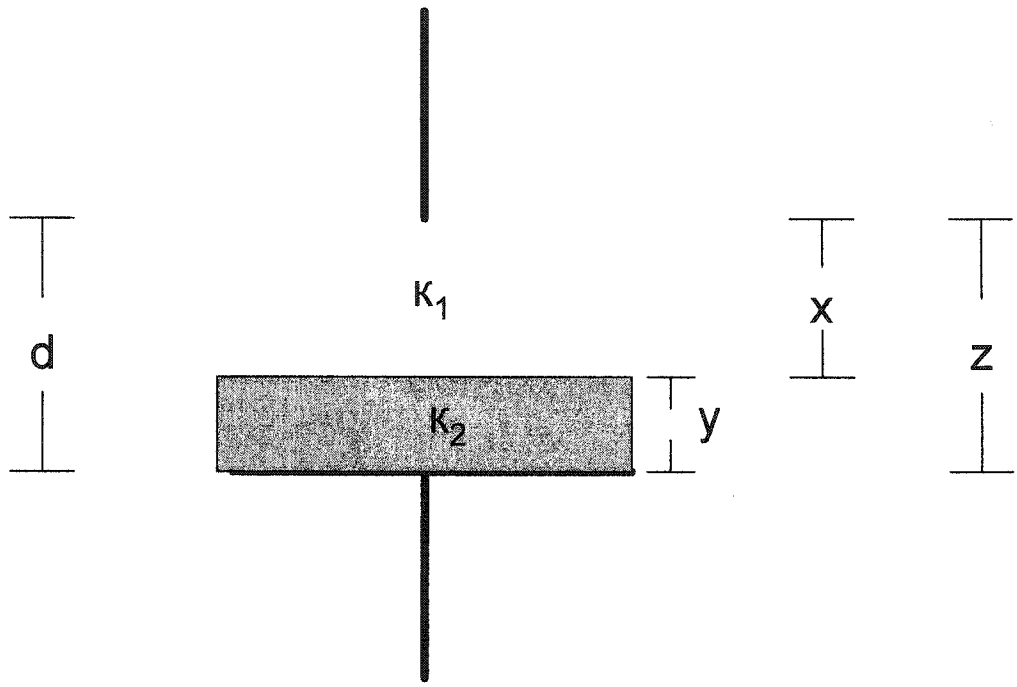

The equivalent capacitance of two capacitors in series is given by:

$$\frac{1}{C_{eq}} = \frac{1}{C_1} + \frac{1}{C_2}$$

where:

$$C_1 = \frac{\kappa_1 \varepsilon_o A}{\left(x/z\right) d}$$

$$C_2 = \frac{\kappa_2 \varepsilon_o A}{\left(y/z\right) d}$$

Therefore,

$$\frac{1}{C_{eq}} = \frac{\left(x/z\right)d}{\kappa_1 \varepsilon_o A} + \frac{\left(y/z\right)d}{\kappa_2 \varepsilon_o A}$$

Factoring out like terms from the two groups on the right side of the equation yields:

$$\frac{1}{C_{eq}} = \frac{\left(d/z\right)}{\varepsilon_o A}\left[\frac{x}{\kappa_1} + \frac{y}{\kappa_2}\right]$$

Since the dielectric constant of air is one, the dielectric constant of the gas gap will be assumed to be the same (κ_1=1).

$$\frac{1}{C_{eq}} = \frac{\left(d/z\right)}{\varepsilon_o A}\left[x + \frac{y}{\kappa_2}\right]$$

Obtaining a common denominator,

$$\frac{1}{C_{eq}} = \frac{\left(d/z\right)}{\varepsilon_o A}\left[\frac{x\,\kappa_2 + y}{\kappa_2}\right]$$

Further simplifying,

$$C_{eq} = \frac{\varepsilon_o A}{\left(d/z\right)}\left[\frac{\kappa_2}{x\,\kappa_2 + y}\right]$$

and

$$C_{eq} = \frac{\varepsilon_o A}{d}\left[\frac{z\,\kappa_2}{x\,\kappa_2 + y}\right]$$

Finally, since the definition of a capacitance and the effect of a capacitance are given by (respectively):

$$C = \frac{\varepsilon_o A}{d}$$
$$C_{eq} = \kappa\, C_o$$

The dielectric constant for the entire circuit (two capacitors in series with varying dielectric constants can be defined as:

$$\kappa = \left[\frac{z\,\kappa_2}{x\,\kappa_2 + y} \right]$$

where, z = x + y

$$\kappa = \left[\frac{(x+y)\,\kappa_2}{x\,\kappa_2 + y} \right]$$ **, defined as Equation 3.7**

This is accurate, since as y→0 the equation will become κ=1 which is what the dielectric constant is for the gas gap. As x→0, the term becomes $\kappa=\kappa_2$.